Probabilistic Models for Life Cycle Management of Energy Infrastructure Systems

by

Suresh Varma Datla

A thesis
presented to the University of Waterloo
in fulfillment of the
thesis requirement for the degree of
Doctor of Philosophy
in
Civil Engineering

Waterloo, Ontario, Canada, 2007

AUTHOR'S DECLARATION

I hereby declare that I am the sole author of this thesis. This is a true copy of the thesis, including any required final revisions, as accepted by my examiners.

I understand that my thesis may be made electronically available to the public.

Abstract

The degradation of aging energy infrastructure systems has the potential to increase the risk of failure, resulting in power outage and costly unplanned maintenance work. Therefore, the development of scientific and cost-effective life cycle management (LCM) strategies has become increasingly important to maintain energy infrastructure. Since degradation of aging equipment is an uncertain process which depends on many factors, a risk-based approach is required to consider the effect of various uncertainties in LCM.

The thesis presents probabilistic models to support risk-based life cycle management of energy infrastructure systems. In addition to uncertainty in degradation process, the inspection data collected by the energy industry is often censored and truncated which make it difficult to estimate the lifetime probability distribution of the equipment. The thesis presents modern statistical techniques in quantifying uncertainties associated with inspection data and to estimate the lifetime distributions in a consistent manner.

Age-based and sequential inspection-based replacement models are proposed for maintenance of component in a large-distribution network. A probabilistic lifetime model to consider the effect of imperfect preventive maintenance of a component is developed and its impact to maintenance optimization is illustrated.

The thesis presents a stochastic model for the pitting corrosion process in steam generators (SG), which is a serious form of degradation in SG tubing of some nuclear generating stations. The model is applied to estimate the number of tubes requiring plugging and the probability of tube leakage in an operating period. The application and benefits of the model are illustrated in the context of managing the life cycle of a steam generator.

Acknowledgements

I would like to express my sincere gratitude to my supervisor Prof. Mahesh Pandey for his constant guidance and financial support throughout the course of my Graduate program. He has helped me grow professionally and gave me freedom and encouragement in my work when needed. I always admire his simplicity and clarity in expressing his thoughts which he insists strongly while preparing a technical document or presentations.

I wish to extent my thanks to the committee members Prof. Dan M. Frangopol, Prof. K. Ponnambalam, Prof. W. C. Xie, and Prof. G. Cascante for their constructive criticism and suggestions on my thesis.

I would also like to offer my thanks to Dr. Mikko Jyrkama for his helpful discussions and for providing me the data required for steam generator pitting corrosion problem. My special thanks to my friends and colleagues in waterloo, without them my stay here wouldn't be as fruitful and memorable.

I am greatly indebted to my wife, Padma for her tremendous patience, love, and support especially during the later stage of my thesis preparation. Also, special thanks to my brother for his constant help, love and encouragement.

Last but not least, I would like to dedicate this thesis to my parents and my wife who believed in me and were always a source of love and encouragement.

To my Parents and my wife

Table of Contents

List of Figures

List of Tables

Terminology

Life Expectancy

The expected or mean time to reach failure is defined as life expectancy. Failure need not be a physical failure but could also mean a failure to perform the intended function.

Maintenance

Maintenance is defined as restoring the component/system in its functional state. Restoration involves activities like replacement and repair to improve the condition of the failed component.

Risk

Risk includes the notions of probability of an unfavourable event or hazard and the consequence of the event in economic or human terms. Risk is commonly represented as Risk = (Probability of failure) × (consequence of failure). In this thesis risk is measured in terms of expected cost ($CAD).

Optimization

Optimization is the use of specific technique to determine the most cost effective solution to a problem.

Renewal Process

A renewal process is an idealized stochastic model for "events" that occur randomly in time (generically called renewals or arrivals). The basic mathematical assumption is that the times between the successive arrivals are independent and identically distributed.

List of Abbreviations and Notations

AIC	Akaike information criterion
CANDU	CANada Deuterium Uranium
CC	Chemical cleaning
CEL	Constrained expected likelihood
CL	Confidence limit
CM	Corrective maintenance
EOL	End of life
EPRI	Electric power research institute
ET	Eddy current testing
FFS	Fitness for service
GEV	Generalized extreme value
GPD	Generalized Pareto distribution
HPP	Homogeneous Poisson process
IAEA	International atomic energy agency
IEEE	Institute of electrical and electronics engineers, Inc
LCM	Life cycle management
LE	Life expectancy
ME	Measurement Error
MTTF	Mean time to failure
NDE	Non destructive examination
NDT	Non destructive testing

NHPP	Non homogeneous Poisson process
NPV	Net present value
OCB	Oil circuit breaker
PM	Preventive maintenance
RCM	Reliability centered maintenance
RMSE/D	Root mean squared error/differential
SG	Steam Generator
SI	Selective intrusive
SSC	Systems, Structures, and Components
TWD	Through wall depth
WL	Water lancing

$f_X(x)$	Probability density function of random variable X
$F_X(x)$	Cumulative distribution function of random variable X
$S_X(x)$	Survival distribution function of random variable X
$L(\Theta)$	Likelihood function of parameter Θ
$l(\Theta)$	Log-likelihood function of parameter Θ
LRS	Likelihood ratio statistic
COV	Coefficient of variation
$N(t)$	Number of events occurred up to time t (Stochastic Process)
$\lambda(t)$	Intensity function of the process
$\Lambda(t)$	Mean value function of the process

CHAPTER 1
INTRODUCTION

1.1 Background

The structure of energy infrastructure (nuclear, hydro) in North America has undergone a transition to a competitive, market-driven industry which operates as an independent business enterprise. This enterprise must be a cost-effective energy producer that maximizes economic returns for investors. The executive management at both the corporate and the plant level holds greater responsibility to provide a safe, reliable, and affordable supply of energy for consumers and prudently manage the investment of shareholders.

The power blackout in August 2003 affected 50 million people over eight states in the US and most parts of Ontario. The blackout highlighted the vulnerability of the electric grid to massive failures, giving new impetus to calls for more regulatory standards and enforcement in the power industry (US-Canada Report, 2004). The degradation of aging energy infrastructure has the potential to increase the risk of failure, resulting in power outage and costly unplanned maintenance work. The sources of uncertainty are the degree to which asset condition and performance degrade with age, economic uncertainties, and increasingly strict environmental regulations. Today, the energy infrastructure has realized that the key to enhancing asset performance, longevity, and profitability in our uncertain world is the formal implementation or enhancement of Life Cycle Management (LCM) practices.

The major advantage of LCM is that it provides decision-making tools and information in a planned, systematic, and timely way, streamlining the decision-making process in any future crises. LCM (EPRI 1998) is a process that combines the following two requirements:

- **aging management,** that is maintaining costly to replace components and structures and preventing their long term aging related degradation or failures which affect the asset performance or useful life,
- **asset management,** that is plant valuation, resource allocation, and investment strategies that account for economic, technical, regulatory, and environmental uncertainties.

LCM involves the prediction of maintenance, repair, and the associated costs far into the future and the impact of other costs on asset value. LCM creates the opportunity of reducing costs and adding value to assets through increased production and revenue. Although LCM aids in the successful operation of energy infrastructure, it also becomes crucial in a competitive environment that places emphasis on future risk and performance.

1.2 Research Motivation

Life cycle management is a framework to manage the long-term performance of ageing infrastructure systems. The success of LCM depends on the understanding of uncertainties, on quantifying them, and on developing strategies to minimize them. The degradation of aging equipment is an uncertain process which depends on many factors. A risk-based approach is therefore essential for efficient life cycle management because it accounts for various uncertainties in quantifying them.

The large uncertainty inherent in equipment degradation means that equipment lifetime is a random variable. A complete record of equipment lifetimes is rarely available from industry to estimate true lifetime distribution. It is neither practical nor economically feasible to perform frequent and intensive inspections of infrastructure systems. The inspection data collected by industry under conventional practices provide limited and indirect information about equipment lifetimes. Such inspection data complicate the estimation of equipment lifetime under real-service conditions.

The literature is deficient in information on the practical problems in developing probability models from partial inspection studies, which usually involve incomplete data for estimating life time models. This research examines such issues and attempts to develop probabilistic models based on incomplete inspection observations.

Energy infrastructure consists of a large inventory of equipment that plays a significant role in overall asset management of the infrastructure system. Maintenance of large aging infrastructures is a major problem that asset managers continue to face. The inspection of equipment in a large infrastructure network is a fairly time consuming and costly undertaking compared with overall replacement cost. Therefore, asset management models are needed for making best decisions on inspection and replacement strategies, to account for costs and risks over the life cycle of an asset.

In the nuclear industry, many aging reactors are experiencing increasing degradation. For example, steam generators (SG), which are a critical component of nuclear power plants, experience various degradation mechanisms affecting SG tubes, such as stress corrosion cracking, fretting, pitting, denting, erosion-corrosion, fatigue, wastage, wear, and thinning (IAEA, 1997). A detailed understanding of degradation mechanisms, as well as methods for assessing and mitigating degradation, is essential to ensure the structural integrity and reliable SG systems.

Various in-service inspection techniques are used to monitor the extent of degradation in SGs. The uncertainty in quantifying defect sizes using standard inspection tools affects the estimation of degradation model. The inspection data required for estimating degradation is also limited by a scarcity of data due to workplace constraints imposed by radiation exposure and poor access to components in a nuclear reactor. To obtain suitable data, engineers often pool the data from similar equipments working under similar conditions. The unobserved heterogeneity within pooled data can be quantified using frailty models (Lawless, 2003). Probabilistic modelling of degradation mechanisms considering various

uncertainties is required for a best estimate of risk-of-failure in a future operating period.

The motivation for this research comes from the need to develop better probabilistic models than currently available, to support risk-based life cycle management plans in energy infrastructure systems.

1.3 Research Objectives

The main objective of this thesis is to develop probabilistic models to support life cycle management of energy infrastructure systems. Emphasis is placed on modelling the uncertainties in inspection data collected from energy systems. The objectives of the thesis are

- To estimate lifetime distributions from incomplete lifetime observations commonly encountered in field inspections.
- To discuss applications in energy infrastructure, namely utility wood poles, oil circuit breakers, insulators, and feeder pipes; then conduct comprehensive statistical analysis and interpretation of actual inspection data collected by industry.
- To develop a probability model of asset management for making optimum maintenance decisions.
- To develop a probabilistic life cycle management model for pitting corrosion degradation in steam generators
- To develop probability models to account for detection and measurement errors associated with inspection data
- To discuss the application of pitting corrosion model to a Steam Generator in the context of Life cycle management.

1.4 Thesis Organization

The thesis is organized into seven chapters. Chapter 1 discusses the background, research motivation, and objectives of the research. Chapter 2 outlines the scope

of probabilistic modelling in the context of life cycle management (LCM). The concept of LCM in energy infrastructure is discussed along with the EPRI LCM process. The main concerns about LCM, namely aging management and asset management, are discussed along with distinctive objectives. Various maintenance practices as well as current probabilistic asset management practices are reviewed.

Chapter 3 presents comprehensive statistical techniques used in lifetime data analysis, taking into account incomplete inspection data. The chapter explores various types of incomplete data encountered from the inspection of components in power utilities. The applications discussed in this chapter focus on interpreting incomplete data and the related effects on estimating the realistic lifetime distributions. Estimating lifetime distributions from strongly censored observations is not a straightforward task. The Maximum Likelihood method can be used to estimate the lifetime distributions from various types of incomplete data. The chapter discusses the use of statistical methods in interpreting censored data usually encountered during field inspections.

The snap shot data on wood pole condition in an inspection campaign collected by the power utility is considered for lifetime analysis. The data are interpreted assuming different models on lifetimes to produce realistic estimates on pole lifetime distribution. The sensitivity of using different parametric distributions is also discussed, as are censoring models. The uncertainty among observed poles is also accounted for by using frailty models for lifetime distribution analysis.

Other applications in energy infrastructure are explored, namely oil circuit breakers, electric insulators, and feeder pipes in which the inspection data collected is limited in estimating realistic lifetime distribution.

Chapter 4 presents the application of probability models in asset management for maintenance decisions in the context of a distributed component population. The optimal age-based refurbishment policy for wood pole management is demonstrated as a function of life cycle cost. Next, a sequential condition-based

replacement policy for a distributed population is presented to show the effect of inspection interval in estimating the maintenance cost, risk, and life cycle cost. The component replacement (Corrective Replacement) policy from the renewal theory framework is demonstrated in estimating the expected future replacement costs. The use of lifetime distribution in maintenance optimization of imperfect preventive maintenance is presented. To account for imperfect preventive maintenance, a probabilistic model is proposed using the concept of virtual age. The effect of a maintenance interval under imperfect maintenance conditions is illustrated by the use of lifetime distribution of equipment.

In Chapter 5, a pitting corrosion model is proposed, based on the data obtained from the eddy current inspection of steam generator tubing in a nuclear generating station. Background information on the process of pitting corrosion and probabilistic modelling is presented. An overview of life cycle management issues in steam generators (SGs) of nuclear power plants is presented, and a need for efficient life cycle management decisions based on the current degradation of SGs is discussed.

The rate of pit generation is modeled as the non homogeneous Poisson process, which belongs to the class of stochastic birth process models. The parameters of the pit generation process are estimated by taking into account censored observations as well as non-censored observations. The pit depth distribution exceeding a threshold pit depth is modeled as the generalized Pareto distribution (GPD), which falls in the class of extreme value distribution. Details of the probabilistic model development, along with parametric estimation and the derivation of the extreme pit depth model, are discussed.

Uncertainties associated with pit depth measurements from an eddy current inspection process are discussed. The effect of measurement error and probability of detection on pit depth measurements is discussed by conducting a simulation study. The effect of sampling uncertainty from different SG inspections plans is explored. Simulation analysis is conducted to estimate the probability of tube leak

and expected number of tubes plugged in next outage, using data from different inspection plans.

In Chapter 6, the developed methodology is applied to the corrosion pit data obtained from a nuclear generating station. The application and the benefits of the model are illustrated in the context of steam generator life cycle management. Maintenance optimization on the chemical cleaning cycle for a SG pitting corrosion degradation is presented.

Chapter 7 concludes the research findings, which aim to meet the research objectives presented in Chapter 1. This chapter discusses further the research contributions towards probabilistic modelling of life cycle management. The chapter concludes with recommendations for future work.

CHAPTER 2
LITERATURE REVIEW

2.1 LCM Definition

A formal definition of LCM is "integration of operations, maintenance, engineering, regulatory, environmental and business activities that

- Manage asset condition
- Optimize operating life
- Maximize plant value while maintaining plant safety.

The two major elements of asset management are physical asset management and financial asset management. Physical asset management involves the improvement of asset condition by managing the maintenance and aging of equipment. Financial asset management involves maximizing the asset value through increasing revenues, reducing costs, and optimizing resource allocation and risk management.

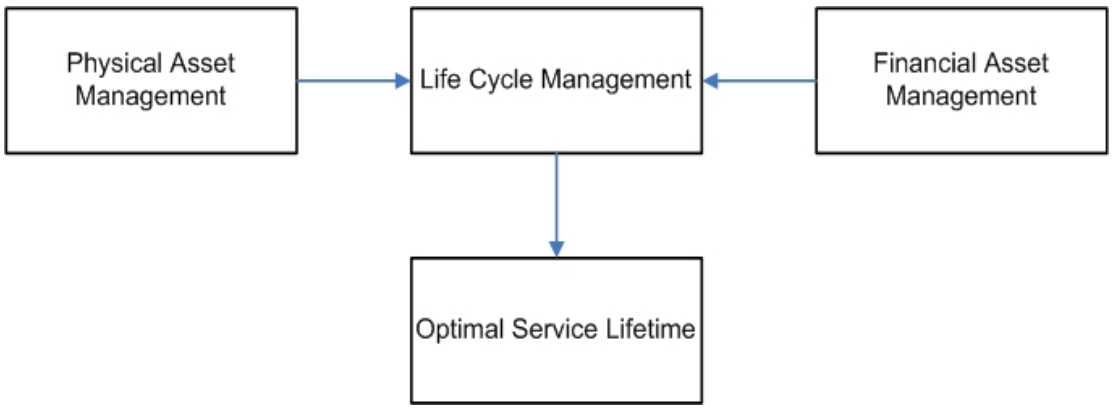

Figure 2.1: Concept of LCM Planning

The main benefits of implementing LCM are

- Increase in long-term profitability

- Reduced outages
- Improved business planning practices
- Reduced operations & maintenance costs
- Improved plant safety, reliability and availability
- Assessment of potential aging mechanisms that add to long-term risks
- Addressing obsolescence
- Improved economic forecasts

An LCM plan is a long-term strategy for preventive maintenance, replacement, and redesign of systems, structures and components (SSCs), all important to safety and reliability and to the contribution of SSCs to plant value. LCM plans generally consist of maintenance activities, and their schedule and costs over a planned plant life. LCM planning facilitates evaluation of maintenance options and what-if scenarios, assesses business risk, and considers the economic consequences of lost power.

2.2 LCM Concepts

2.2.1 EPRI LCM Process

The Electric Power Research Institute (EPRI) is an independent, non-profit, industry-wide collaborative research center that promotes public interest on energy. EPRI has developed cost-effective technology for safe and environmentally friendly electricity generation that maximizes profitable utilization of existing nuclear assets and supports promotion and development of new technology.

EPRI released implementation guides and demonstration reports on the LCM of plant SSCs, introducing advanced concepts and describing the various steps of the LCM process. The information needed to produce an LCM plan for most SSCs is provided through EPRI LCM sourcebooks. The objective of these

sourcebooks is to provide engineers with foundation information, data, sample plans, and guidance to produce long-term LCM plans for their SSCs.

The LCM planning process consists of four main stages, as shown in Figure 2.2. The first stage is the selection of SSCs important to plant safety, reliability, and economics. EPRI (2001) suggests several formal approaches in evaluating and ranking important SSCs for nuclear power plants. Once important SSCs are identified, depending on the level of criticality, LCM plans are developed for each level of SSCs. The LCM planning flow chart in Figure 2.2 shows the activities involved in each stage of the process.

Before conducting an aging assessment, the scope and functions of the SSC are defined. This information is required to plan for alternative aging management strategies to meet the scope and functions of SSC. The next step is to gather relevant technical information related to plant performance and operating history and review past and current maintenance plans. Using the technical information gathered, an aging assessment is conducted on the SSCs, and alternate LCM plans are identified. The relevant cost and failure rate data are obtained to assess the performance and costs of each alternative LCM plan. Planned and unplanned costs are taken into account to evaluate the economic value of each alternative LCM plan. Finally, an optimum SSC LCM plan is selected based on the level of safety, reliability and economics over the life of the facility. The optimum LCM approach is a function of the projected life of the facility. If the target life is not specified, then an economic analysis must be performed over a range of facility life options.

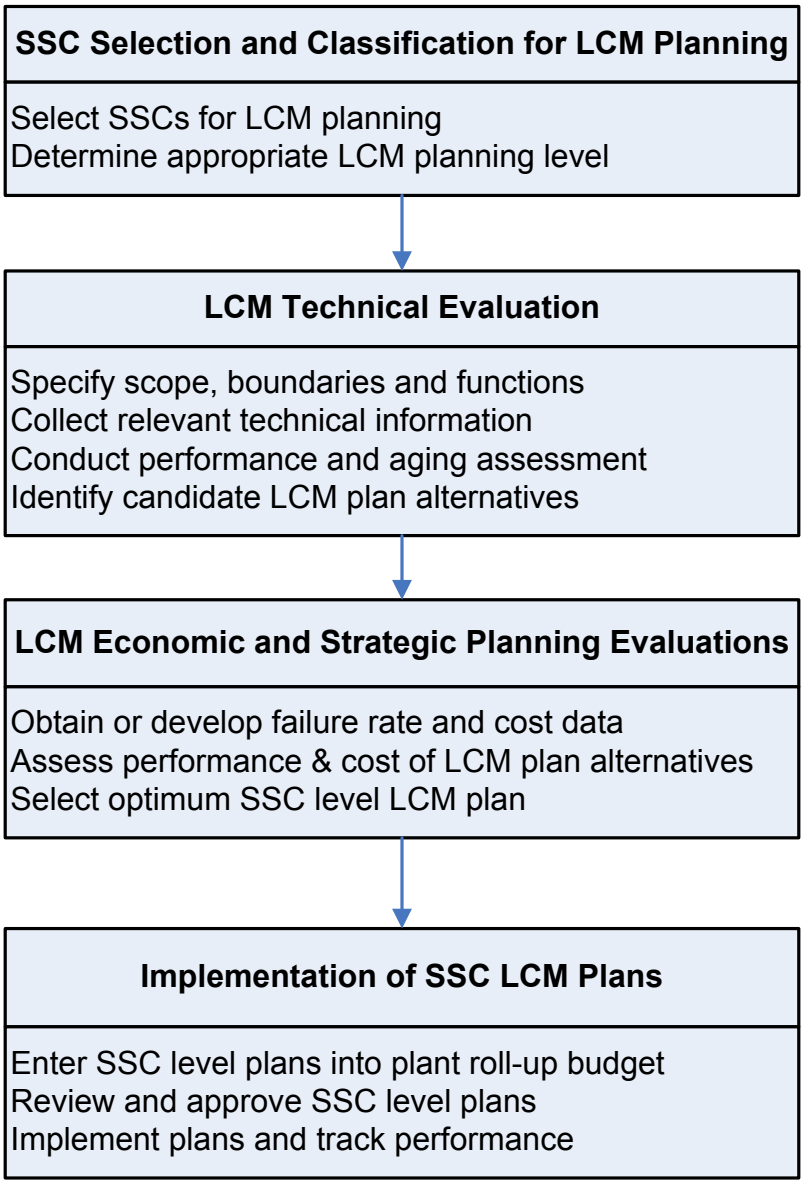

Figure 2.2: Simplified EPRI LCM planning flowchart

2.2.2 Asset Management

Asset management is a business philosophy designed to align corporate goals with asset-level spending decisions. The term asset management is derived from the financial industry, where its concepts are applied to investment portfolios containing stocks, bonds, cash, options and other financial instruments. Financial asset management techniques are used to achieve an acceptable level of risk while

maximizing expected profits. Many techniques of financial asset management are applicable to infrastructure asset management.

Today, the power industry is divided so that generation, transmission, and distribution are run as separate businesses. To resolve issues like slow load growth, aging equipment, depleting rate bases, rate freezes, and regulatory uncertainties, the power sectors are exploring ways to increase earnings, credit ratings and stock price. As the power industry is asset intensive, asset management is considered as an effective way of improving conditions in these fundamental areas.

In asset management, decisions are made to maximize profits and performance by effectively managing risks and reducing capital spending. The framework for asset management as described by Brown and Spare (2004) is a process of concern to the asset owner, asset manager and service provider. The asset owner sets the business values, corporate strategy, and corporate objective in terms of cost, performance, and risk. The asset manager identifies the best way to achieve these objectives and lays a multi-year asset plan. The service provider executes the plan efficiently, and feeds back asset and performance data into the asset management process.

Effective asset management strategies can be achieved by the prudent understanding of and accounting for various uncertainties and risks. The risk from various sources should be quantified so as to develop strategies that can reduce uncertainties. Asset management is applied to both physical components and financial components (EPRI, 1998). Physical asset management focuses on uncertainties in equipment performance, maintenance, and operations. The operations and maintenance of aging components is monitored through aging management in such a way as to maintain safety and minimize life cycle costs. The financial asset management concerns uncertainties in market prices, cost estimates, discount rates, and various regulations in order to increase revenue, reduce costs, and minimize risks.

2.2.3 Aging Management

Aging management is a part of LCM that is concerned with operations and maintenance actions to control aging of equipment and performance with the aim to maintain safety and minimize life cycle costs. Aging management involves major decisions on equipment repair, replacement, and the consequences for equipment failure or outage that results in substantial investments. To make such decisions effective, quality data on equipment condition and proper aging assessments are needed.

Maintenance is a part of the overall concept of asset management. Its goal is to increase the duration of useful component life and postpone failures that would require expensive repairs. Maintenance involves costs, and this fact is taken into account in choosing the most cost-effective policy. The costs of maintenance are balanced against the benefits from increased performance or reduced risks. Details of maintenance polices and the present polices in the electric power industry are discussed in a paper by IEEE Task Force (2001).

The importance of maintenance has been growing over the years. In this modern era of mechanization and automation, maintenance plays a vital role and is the largest department in any organization. In fact, maintenance is becoming an important part of asset management (Endrenyi, et al., 2001). The sophistication of equipment has increased the impact of unplanned downtimes caused by system failures. Today, the impact of system downtimes is unacceptably high and has to be reduced with proper maintenance planning. By performing little maintenance, system performance is reduced and may result in costly system failures. On the contrary, if maintenance is increased, system performance could increase, but the cost of maintenance will be high.

A maintenance model is a mathematical model by which both costs and benefits of maintenance are quantified and by which an optimum balance between both of them is achieved. Often norms have to be set to define failure and the benefits of maintenance, and therefore they are more difficult to quantify. In this case, one has to minimize maintenance costs in order to meet these norms. The

maintenance objectives as summarized by Dekkar (1996) are aimed at ensuring system function; ensuring system life; ensuring safety; and ensuring human well-being.

2.3 Technical Methods Needed to Support LCM

2.3.1 Overview of Maintenance Practices

The early application of maintenance management dates back to the 1950s and 60s. At that time, maintenance actions were mainly predefined activities carried out at fixed intervals called scheduled maintenance. These were meant to reduce system failures and unplanned system downtime. However, such a maintenance policy may be quite inefficient as it may be costly in the long run (Barlow and Proschan, 1965) and may not greatly extend system lifetime. In the 70s condition monitoring came forward, focusing on techniques which predict failures using information on the actual state of the equipment (predictive maintenance) (Mobley, 2002, Makis et al., 1998, Barata, et al., 2002, Jardine, et al., 1999). This approach proved to be more effective than scheduled maintenance. Detailed studies about the failure of equipment created a better understanding of failure mechanisms, resulting in better designs. But such applications are not popular in decision-making analysis (Dekkar, 1996).

The key approach popular in industry is the Reliability Centred Maintenance (RCM) (Moubray, 1997). In an RCM approach, various alternative maintenance policies can be compared and the most cost-effective for sustaining equipment reliability is selected (Vatn et al., 1996). It can be regarded as the more qualitative approach to maintenance, in which optimization models are quantitative approach. However, this approach is more heuristic and needs expert judgment at various steps. The reason various models are being proposed in the literature is to aid the maintenance scheduling, depending on the problem.

Several maintenance models are discussed in the literature (Barlow and Proschan, 1965, Dekkar, 1996, Endrenyi, 2001). The most popular maintenance models are discussed here.

2.3.1.1 Corrective Replacement

Corrective replacement is a simple and straightforward policy; when a component fails it is replaced by a new one or repaired to working condition. This technique is often called reactive maintenance or corrective maintenance (Mobley, 2002). No maintenance task is needed till the system fails, which means no money is spent on maintenance. The maintenance staff must be prepared for the any type of failure, which may be anything from replacing a few components to a complete overhaul. The major expenses associated with this type of maintenance are high inventory cost, high overtime labour cost, high machine downtime, and low production availability. However, this technique results in high maintenance costs in the long run and lower system availability.

2.3.1.2 Age Replacement and Block Replacement policy

In age replacement policy, the system is replaced either at a certain age or when it fails, whichever comes first. In block replacement policy, the system is replaced either at fixed intervals or when the system fails. These methods are extensively discussed in the literature and are still practiced. The optimal age replacement is more profitable than the optimum block replacement. But when the emergency failure costs are the same, the cost of a preventive maintenance carried out at preplanned time, as in block replacement, will be smaller than the corresponding preventive maintenance for age replacement (Gertsbakh, 2000).

2.3.1.3 Minimal Repair Policy

In the minimal repair policy technique, the system is subjected to minimal repair when the system fails, and replacements are done at fixed intervals. This method is different from block replacement, whereby the system is repaired when failure occurs (Vatn et al., 1996). It is commonly assumed that the system after preventive maintenance is either as good as new (perfect maintenance) or as bad as old (minimal maintenance). In reality, these assumptions are not particularly true, so such maintenance actions are termed imperfect maintenance (Mettas and Zhao, 2005). Minimal repair or imperfect maintenance actions restore the system

to an operating state, but there is also a risk of failure or outage in future operation. This policy may be prudent when there is a need to postpone relatively high refurbishment policy in order to extend the useful life.

2.3.1.4 Predictive maintenance

In preventive maintenance, maintenance is carried when needed. The need for maintenance is established through periodic or continuous inspection. To perform meaningful periodic inspections, diagnostic routines and techniques are required to help identify disorders that call for maintenance (Mobley, 2002). The aging mechanisms are identified from periodic or continuous inspection to understand the extent of degradation and use proper mechanistic or probabilistic models to predict the future state of degradation. This approach may suggest the right preventive maintenance action when needed. Predictive maintenance could be a cost effective alternative when it is correctly implemented. If the consequences of equipment failure are high and when the periodic inspection is feasible and less costly, predictive maintenance may result in a cost-effective alternative.

2.3.1.5 Periodic Inspection

Commonly used diagnostic methods include visual inspection, optical inspection, neutron analysis, radiography, eddy current testing, ultrasonic testing, vibration analysis, lubricant analysis, temperature analysis, magnetic flux leakage analysis, and acoustic emission monitoring. Each of these methods has advantages and limitations.

In some cases, when periodic inspection cannot reveal the actual status of the equipment or when it is not feasible to conduct periodic inspection, condition monitoring is preferred. When the cost of implementing condition monitoring is not excessive, this method proves to be more economical than maintenance based on regular inspection.

Other maintenance models discussed in the literature are total predictive maintenance (TPM) and reliability centered maintenance (RCM) (Dekkar, 1996, Mobley, 2002). TPM was developed by Deming in the late 1950s, which is meant

to improve system effectiveness. RCM is based on regular assessments of equipment condition; it involves system analysis like FMEA (Failure Mode and Effect Analysis) and an investigation on system operating needs and priorities.

Maintenance models are classified according to the deterioration model (Dekkar, 1996).

1. Deterministic Models

2. Stochastic Models

    A. Under Risk

    B. Under Uncertainty.

The deterioration process is represented by a sequence of stages of increasing wear, finally leading to system failure. Deterioration is of course a continuous process, and only for the purpose of easier modeling may it be considered in discrete steps. The difference between risk and uncertainty is that risk assumes that the probability distribution of the time to failure is available, which is not so for uncertainty. In some models, system failure can occur not only because of excessive degradation, which leads to critical state of the system, but also because of random shocks which suddenly fail the system and whose occurrence probability is degradation dependent. These models are often solved using Markov or semi-Markov models (Smilowitz and Madanat, 2000, Barata et al., 2002) and Gamma process models (Yuan et al., 2006, Frangopol et al., 2004). The probabilistic modeling of degradation mechanisms and the effects of maintenance on equipment performance and life cycle costs demand effective LCM.

2.3.2 Current Probabilistic Asset Management Practices

Traditionally, the electric power utilities employed preventive maintenance programs to keep their assets in good condition as long as the process was economical. Given the present economic constraints, an efficient maintenance program has become an important part of asset management. Various electric power organizations in different countries have begun to implement asset

management to meet the demands of the present market (Brown and Spare, 2004, Morton, 1999, Endrenyi et al., 1998, Bertling et al., 2005). This has recently led to the development of various asset management frameworks and supporting models.

In power distribution systems, two methods are developed to address the effect of maintenance on system reliability (Endrenyi et al., 2004), namely RCAM (Reliability Centered Asset Maintenance) and ASSP (Asset Sustainment Strategy Platform). Both approaches analyze the choice of a component maintenance policy in a system context. The activities involve system reliability evaluation, prioritization of component maintenance based on component criticality, effect of various component maintenance policies on system reliability, and life cycle costs. It is said that the conventional RCM (Reliability centered Maintenance) is generally not capable of showing the benefits of maintenance for system reliability and costs (Bertling et al., 2005).

2.3.2.1 RCAM (Reliability Centered Asset Maintenance)

The RCAM method is developed for asset maintenance in electric power distribution systems (Bertling et al., 2005). In this method, the failure events are assumed to occur randomly, and therefore the models are based on probability theory. A network modeling technique is applied to calculate system reliability by the minimal cut set approach. A computer code RADPOW (reliability assessment of electric distribution systems) is used to calculate system reliability and sensitivity of the components. For the components which are critical, preventive maintenance (PM) strategies are laid out, and the effects of PM and the economic analysis are modeled by another program code. These two modules interact with each other to assist in arriving at a cost-effective maintenance strategy.

The failure rate is assumed to be constant, which is an assumption reasonable for most electrical components but may not be applicable for components with continuous degradation. The effect of maintenance action is modelled by reducing the failure rate, to study its impact on overall system reliability.

2.3.2.2 ASSP Approach (for Asset Sustainment Strategy Platform)

The ASSP approach is somewhat similar to RCAM and includes several programs which interact as necessary. The reliability evaluation and sensitivity analysis is performed by programs REAL and WinAREP (Endrenyi et al., 2004); the critical components are ranked and maintenance alternatives are investigated. The effect of maintenance is carried out using programs AMP (based on Markov model which accounts for deterioration with ageing) (Endrenyi et al., 1998) and first passage times FPT (the mean times of failure from any state in the AMP model) (Anders and De Silva, 2000). To include the associated costs of maintenance, the ASSP platform includes a program called RiBAM (Risk Based Asset Management). RiBAM (Anders et al., 2001) uses the information from AMP and FPT to construct life curves and cost curves by which cost optimization can be performed.

The Markov model for deterioration is a reasonable conceptual model to determine the effect of maintenance. Collecting data periodically on a component condition is not always practical in actual field inspections. The estimation of transition probabilities in such a model is difficult from field inspection data. Hence, in such cases the transition probabilities are usually assumed to reflect the model estimates from experience and past data.

2.3.2.3 Application to Power Infrastructure Systems

The concept of asset management was introduced recently in the power industry. Most of the articles on asset management talk about the scope and advantages of the asset management approach in transmission and distribution (Brown and Spare, 2004, Butera, 2000, Morton, 1999, Chan, 2004, Wernsing and Dickens, 2004). Development of probabilistic models for the asset management of distribution network has been recently attempted by Endrenyi et al., (2004). Some results on the application of asset management techniques in power distribution systems are discussed here.

An asset management of wood pole utility structures (Gustavsen and Rolfseng, 2004) is discussed by predicting the pole replacement rate and

considering the stochastic variation in pole strength and climate loads. The paper describes the probabilistic approach for evaluating the economic impact of alternate maintenance strategies, design strategies, and compensation fees for undelivered energy. The life prediction and inspection practice for aging wood poles is also discussed (Li et al., 2004). The inspection on aging poles is based on the current condition of poles and acceptable pole replacement rate for older poles.

The feasibility of the RCAM approach for circuit breakers is discussed (Lindquist et al., 2004). From the statistics collected on circuit breaker failures and sub-components, the failure rates are estimated. A probabilistic approach based on the condition of the circuit breaker and different levels of maintenance is proposed (Natti et al., 2004). The failure, repair and maintenance sequences are described as Markov processes, and optimal maintenance intervals are discussed.

2.3.2.4 Application to Civil Infrastructure Systems

In the construction industry, operation, maintenance, repair and renewal of assets represents a major growing cost in North America (Vanier, 2001). The assets range from complex interrelated underground networks to sophisticated buildings and roadway systems. Many major asset owners in North America now recognize the importance of knowing the current and future states of their infrastructures. Asset management plays an important role in maintaining the assets to optimize expenditure and maximize the value of the asset over its lifecycle. Managers of municipal infrastructures are realizing the need for effective tools and strategies to manage the large asset base.

Application of life-cycle management in civil engineering infrastructures is used in rehabilitation/construction alternatives in pavements (Salem et al., 2003) and bridges (Kong and Frangopol, 2003).

2.4 Discussion

Most of the asset management models discussed in the literature are conceptual in nature and do not solve the practical difficulties in modeling the lifetime of the

equipment. The models described in Section 2.3.2 are prescriptive and do not consider life data obtained from field inspections.

The equipment in energy infrastructure experience degradation and the consequences of equipment failure from such degradation are high. This reality has led to the need for evaluation methods for fitness for service assessment of equipments. In the nuclear industry, the assessment of the conditional probabilities of tube failures, leak rates, and ultimately risk of core damage or of exceeding site dose limits is an approach to equipment fitness-for-service guidelines that has been used increasingly in recent years. The advantage of probabilistic analysis is that it avoids the excessive conservatism typically present in deterministic fitness-for-service guidelines (Harris et al., 1997). Probabilistic modeling of steam generator tube degradation is typically done only when the level of degradation is such that using normal deterministic fitness-for-service guidelines would result in the number of tube repairs being sufficiently large to affect the power generation capability of the affected unit.

Development of probabilistic models from inspection data recorded from plant outages will allow great confidence in assessing remaining life and in ensuring an extended operating life. The literature is deficient in information on the practical applications in developing probability models from partial inspection studies.

The rest of this thesis attempts to develop probabilistic models based on inspection data. Development of realistic probability models is crucial for making credible life cycle management decisions.

CHAPTER 3
LIFETIME DISTRIBUTION MODELS

3.1 Introduction

The estimation of lifetime distribution is essential in managing aging equipment through a systematic risk based approach. The lifetime distribution of equipment is a key input to maintenance models and life cycle cost optimizing models. These models are used to quantify the effect of various maintenance actions on the equipment performance and associated costs over equipment lifetime. The estimation of lifetime distribution hence plays a crucial role in a credible life cycle management models.

Various equipments in civil and energy infrastructures are designed with relatively high lifetime and hence the time needed to observe such high lifetimes is not practical. Continuous inspection on equipment lifetimes may not be a cost effective alternative and hence periodic or non-periodic inspections are performed and in some cases there are no inspections. Inspections are mostly affected by the safety of the equipment, economics, and accessibility. Such situations often results in incomplete observations on equipment lifetimes. Due to increasing awareness of the impact of aging equipment has alerted some utilities recently to inspect the whole population for the first time creating a snap shot situation on the population lifetimes.

Incomplete observations cannot be ignored as they provide vital information on equipment lifetimes. Such incomplete observations pose challenges in both estimating and in terms of interpreting lifetime distribution models. This chapter discusses various types of incomplete observations and statistical tools to deal with incomplete lifetimes in estimating realistic lifetime distribution models.

3.2 Types of Data

3.2.1 Background

To asses the condition of equipment in its current state and to predict its future state needs information on its operating characteristics in its service. Various inspection techniques are being used to monitor (periodically or continuously) the operating state of the equipment. The objective of inspection can vary depending upon the type of equipment and its criticality. Inspection techniques range from simple visual inspection to sophisticated Non Destructive Testing (NDT) depending on the economics and safety factors. The scope of data collection (inspection) is related to the scope of analysis to be performed on equipment over its lifetime. Depending on the scope of inspection, the observations could be lifetimes of equipment or events over lifetime.

For example in the case of wood poles, utilities have adopted the measurement of the minimum remaining shell thickness of wood pole at the ground level as an indicator of pole condition. The shell thickness can be reliably estimated using the Resistograph. Typically, a pole is considered to be at the end of service life when its minimum shell thickness is reduced to less than 2 inches (Newbill, 1993). Such a pole is referred to as a substandard pole, which has a higher risk of failure under an adverse environmental overloading. The age at which a pole reaches the substandard condition is designated as the end of life (EOL). One of the applications discussed in this chapter is based on the wood pole inspection data collected by a utility.

The condition of steam generator of a nuclear power plant is assessed by means of eddy current inspection of steam generator tubes during outages. The objective of eddy current inspection is to monitor various degradation mechanisms and characterize the defects during outages. In case of pitting corrosion degradation, the number of corrosion pits and depth of pits are observed at each outage. The extent of degradation which is characterized by the pit generation and pit depth defines the service life (lifetime) of the steam generator.

In such cases there is a need to quantify the uncertainties in observing inspection data.

Observations may be done differently depending on factors such as the time needed to observe events that define equipment state, the feasibility of following equipment over time, and the mechanism for recording relevant data on equipment condition. Such factors create situations where the observations are censored, truncated, and categorical. The information on such observations should be carefully accounted in order to reliably asses/model the equipment characteristics.

This section deals with the conceptual modeling of inspection data encountered in practices that are accounted for in the statistical modeling of lifetimes. Firstly a standard data analysis is described to estimate the lifetime distribution given a sample of complete lifetimes. Then a distinction is drawn between the standard case and the realistic case of censored inspection data collected by electrical utilities.

3.2.2 Complete Lifetime Data

Complete lifetimes of components are obtained from such follow up studies. The standard method of estimating the lifetime distribution is based on the cohort analysis technique (Elandt-Johnson and Johnson, 1999). In an ideal analysis a single cohort of in-service components is monitored regularly over a long span of time until all the components reach the end of life. As an illustration, Figure 3.1 shows components installed in a particular year (say 1970) continuously followed until the entire cohort ceases to exist. It is also referred to as a "longitudinal survey" in health sciences and demography literature (Lawless, 2003, Keyfitz, 1985). Statistical analysis of such data is quite simple which is shown in Section 3.3.3.

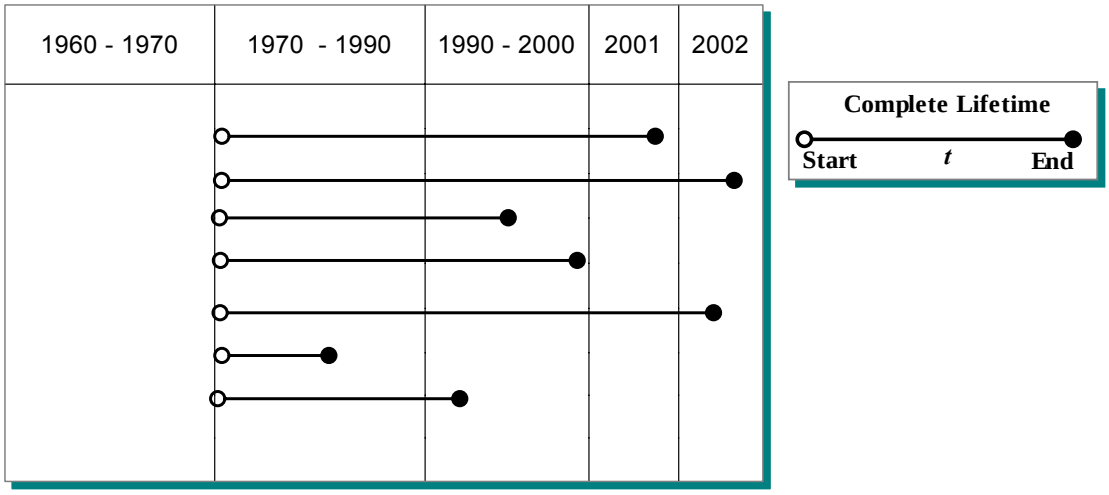

Figure 3.1: An ideal cohort data of complete service lifetimes

This approach is ideally suitable for components of low cost and short life span. However, a complete sample of lifetime data from a single cohort of wood pole is not easy to obtain. The reason is that it requires continuous follow up inspection and assessment of a large number of poles from their installation over a long service life (40 – 70 years), which is a costly and impractical undertaking. Such issues are common in most of the high lifetime components of power utilities.

3.2.3 Complete and Right Censored Lifetime Data

It is a refinement of the previous model by including in the analysis the components that were found to be under good condition. The remaining lifetime of components that are fit for service at the time of inspection is unknown; and it is referred to as right censored lifetime data.

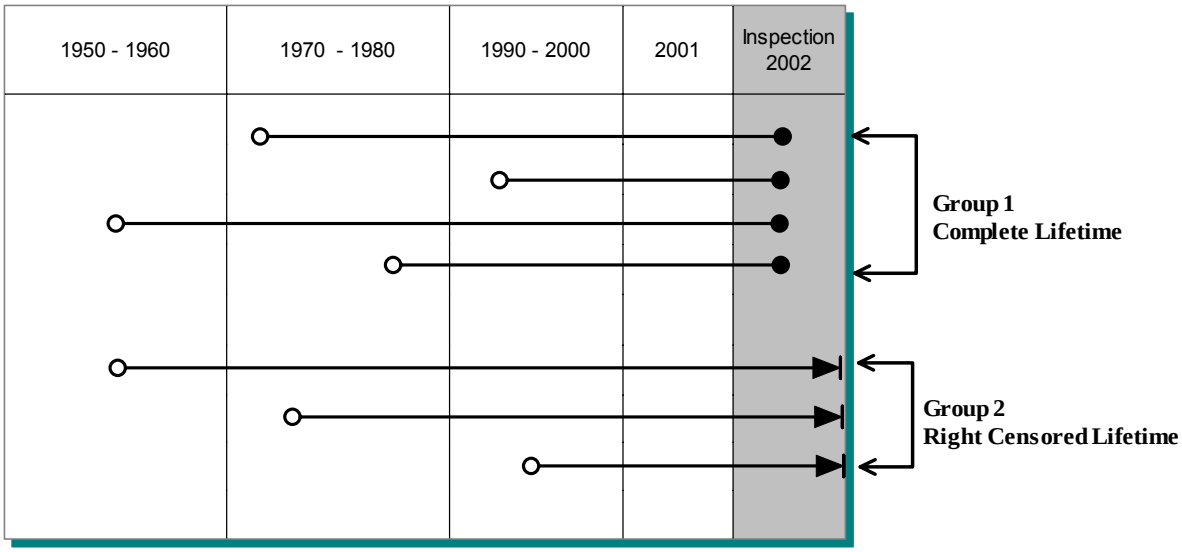

Figure 3.2: Inclusion of right censored lifetimes

Figure 3.2 shows the conceptual representation of a typical inspection data under this model. The sample can be divided into two groups of complete and right censored lifetime data. Consideration of right censored data is important for a realistic estimation, since they contain valuable information about an improved prospect of future survival. Therefore, an omission of such data from statistical analysis could lead to an underestimation of life expectancy, as shown in Section 3.4.1.

3.2.4 Interval and Right Censored

This is the most realistic model that mimics the periodic or non-periodic inspection data available from the power utility industry. In some cases the failures are not self announcing and can only be revealed from inspection. Such situations result in interval censored observations where only information between inspections is recorded. The statistical analysis of interval censored data is not straight forward but can be estimated by likelihood methods as discussed in section 3.3.4.

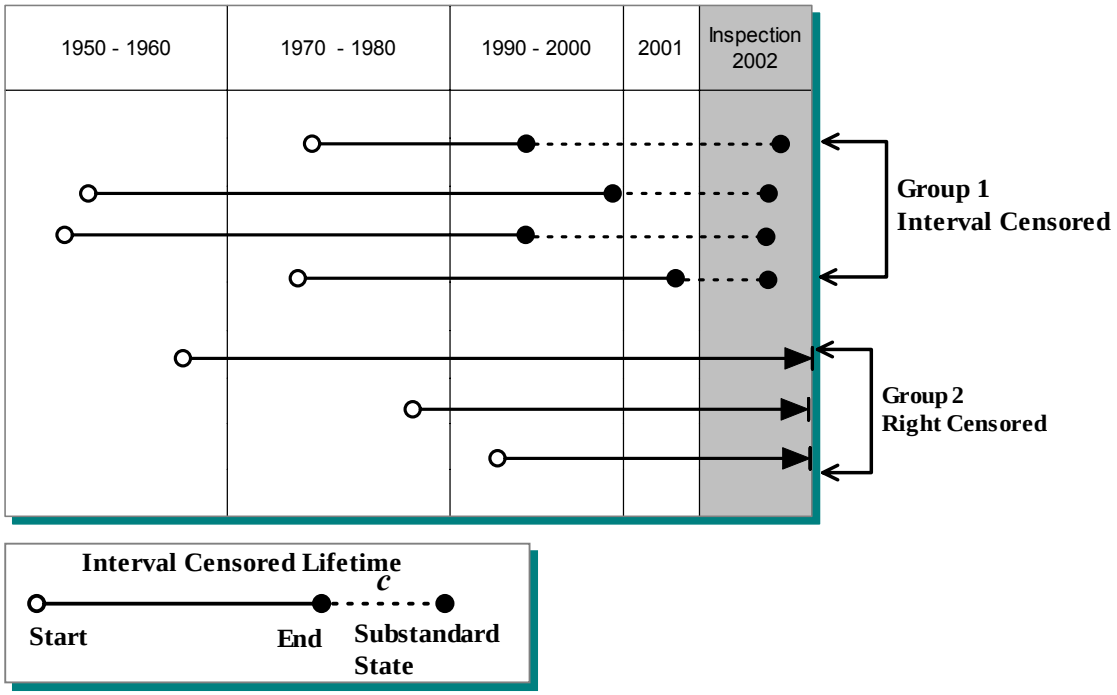

Figure 3.3: A mixed cohort data with interval censored lifetimes (c = censoring interval)

The available data on wood poles provide a single snap shot of pole population taken at the time of inspection in year 2002, as shown in Figure 3.3. The data consist of two groups: (1) right censored lifetimes, and (2) a small fraction of substandard poles, and their exact time of reaching the end of life is not known. The situation is analogous to cross-sectional surveys used in health impact assessment (Elandt-Johnson and Johnson, 1999, Lawless, 2003).

The substandard pole data is treated as interval censored lifetimes, rather than considering them as complete lifetimes. The reason for assuming interval censoring is that the wood degradation is a fairly slow and intermittent process. The fungal decay continues only under favourable environment (humidity and temperature), otherwise it remains dormant. Also, reaching the substandard state does not result in an immediate pole failure. The reason is that poles are conservatively designed and wood is subject to low stresses under normal service conditions. The pole failure is typically caused by an extreme weather event.

Therefore, substandard poles may remain in-service for many years, until detected by an inspection. Because of this, the time of detection cannot be construed as the actual end of service life.

3.2.5 Current Status Data

This is a special case of interval censored model where the censoring interval is completely unknown. The censoring interval *c* in Figure 3.3 is the age of the component, such type of observation is also referred to as left censored data. Current status observations are common from cross sectional survey of population. The component has either failed at some point of time from the start of its service or either survived at the time of inspection. Such observations introduce greater uncertainty in estimating the lifetime of the components. The statistical estimation of current status data is complicated and can be estimated by likelihood methods discussed in Section 3.3.3.4.

3.3 Lifetime Data Analysis

In order to improve or make any decisions on a system performance, the decision maker needs to have an idea on how the system behaves in its lifetime. Information on the system can be known from data on system monitoring or on system test data or on expert opinion. These lifetime data can be modelled with suitable mathematical expressions. This information is helpful in quantifying the system lifetime, which in turn helps in developing models which can improve the system performance.

The definition of lifetime includes a time scale and time origin, as well as specification of event that determines the lifetime. The commonly used models for lifetime estimation can be classified as fully parametric, non-parametric and semi parametric (Lawless, 2003, Cox and Oakes, 1984, Nelson, 1982). This section discusses the estimation techniques to model the lifetime data using illustrations from various inspection methods.

3.3.1 Terminology

3.3.1.1 Probability Distribution Function

Considering a component whose time to failure '*T*' is a continuous random variable. It means that the component can fail at any random time following a probability density function *f(t)*. The distribution function is the probability that the random variable *T* is less than time *t* which is given as

$$F(t) = \Pr(T \le t) = \int_0^t f(u)du \tag{3.1}$$

3.3.1.2 Survival Function

The survival function also called the reliability function is the probability of survival at time *t* or the probability of time to failure *T* is greater than *t*, which is given by

$$S(t) = \Pr(T > t) = 1 - F(t) \tag{3.2}$$

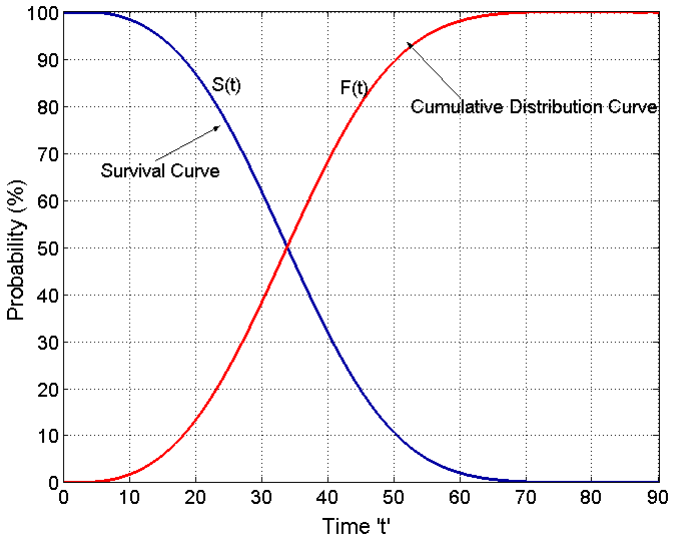

Figure 3.4 Survival and Distribution Curves

As shown in Figure 3.4, the point at which both curves meet is the median value time t_{50}. The Mean time to failure (MTTF) for the component (mean lifetime / life expectancy) is defined as

$$\mu = \int_0^\infty t.f(t).dt \tag{3.3}$$

By applying integration by parts, it can show that the MTTF can be expressed as the area under the survival curve. The expression for MTTF in terms of survival function is given as

$$\mu = \int_0^\infty S(t).dt \tag{3.4}$$

Figure 3.5 shows survival plots for two components with equal MTTF and different variance. Component 2 has lower variability than component 1 in time to failure distribution.

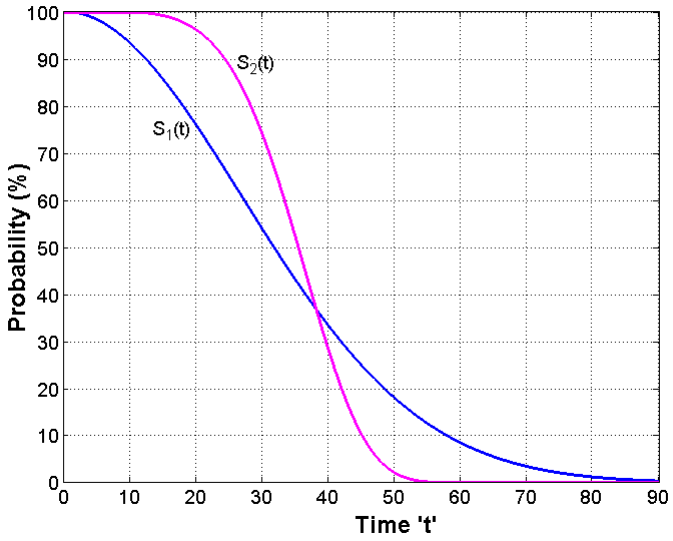

Figure 3.5 Survival curves for two components

3.3.1.3 Hazard Function

Hazard rate can be defined as the conditional failure probability of the component given that it has survived up to time *t*. The hazard rate is expressed as

$$h(t) = \lim_{\Delta t \to \infty} \frac{\Pr(t < T \le t + \Delta t / T > t)}{\Delta t} \tag{3.5}$$

The hazard rate is also called instantaneous failure rate (or age specific failure rate). By definition of density function and survival function the hazard function follows

$$h(t) = \frac{f(t)}{S(t)} \tag{3.6}$$

The cumulative hazard is integrated summation of hazard probabilities as time increases which is expressed as

$$H(t) = \int_0^t h(t).dt \tag{3.7}$$

The expressions $h(t)$, $f(t)$, $S(t)$, $H(t)$ can be derived by knowing any one of the expressions.

For example, conducting a test on the failure of N similar components and keeping track of failures with time. The survival distribution and hazard estimates can be given as

$$\hat{F}(t_i) = \frac{m_i}{N} \tag{3.8}$$

$$\hat{S}(t_i) = 1 - \hat{F}(t_i) \tag{3.9}$$

$$\hat{h}(t_i) = \frac{d(t_i)}{N(t_i)} \tag{3.10}$$

N → Total number of components
m_i → Number of components failed until time t_i
$d(t_i)$ → Number of components failed exactly at time t_i
$N(t_i)$ → Number of components survived at time t_i

The relationship between the probability functions is shown in the table below

Table 3.1 Relationship among probability functions

	$h(t)$	$f(t)$	$S(t)$	$H(t)$
$h(t)$	-/-	$h(t)=\frac{f(t)}{1-\int_0^t f(x)dx}$	$h(t)=\frac{\left(-\frac{d}{dt}S(t)\right)}{S(t)}$	$h(t)=\frac{d}{dt}H(t)$
$f(t)$	$f(t)=h(t)\exp\left[-\int_0^t h(x)dx\right]$	-/-	$f(t)=-\frac{d}{dt}S(t)$	$f(t)=\left(\frac{d}{dt}H(t)\right)\exp[-H(t)]$
$S(t)$	$S(t)=\exp\left[-\int_0^t h(x)dx\right]$	$S(t)=1-\int_0^t f(x)dx$	-/-	$S(t)=\exp[-H(t)]$
$H(t)$	$H(t)=\int_0^t h(x)dx$	$H(t)=-\log\left[1-\int_0^t f(x)dx\right]$	$H(t)=-\log[S(t)]$	-/-

There exists a variety of models which can be used in lifetime distributions, for example, exponential, Gaussian, Extreme value, Gamma etc (Lawless, 2003, Kalbfleisch and Prentice, 2002). The widely used model in engineering application is Weibull which is discussed in the next section.

3.3.2 Parametric Distributions

3.3.2.1 Weibull Distribution

The Weibull distribution is the most popular choice in the survival analysis with the survival and hazard rate functions given as

$$S_T(t)=\exp\left\{-\left(\frac{t}{\alpha}\right)^{\beta}\right\} \text{ and } h(t)=\frac{\beta}{\alpha}\left(\frac{t}{\alpha}\right)^{\beta-1} \tag{3.11}$$

where scale and shape parameters are denoted by $\alpha>0$ and $\beta>0$, respectively. The hazard decreases for $\beta<1$ and increases for $\beta>1$ whereas for $\beta=1$ Weibull distribution is an exponential with constant hazard rate. The hazard rate curves for various values of shape parameter in a sample case are shown in the Figure 3.6.

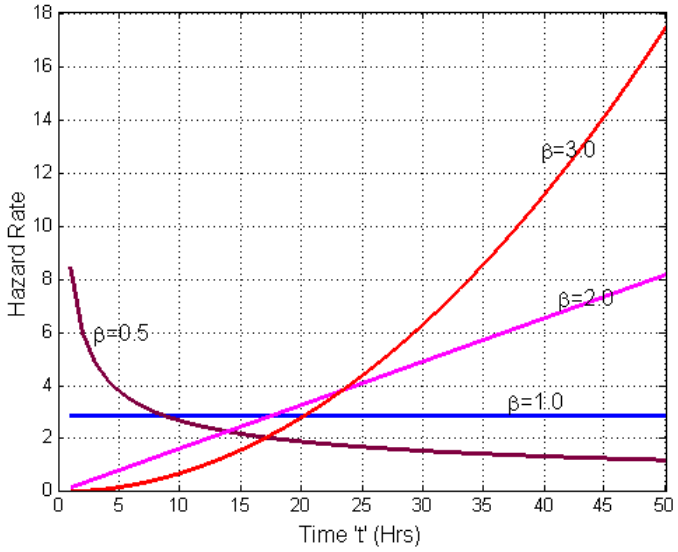

Figure 3.6 Hazard Plots with varying shape parameters

The Figure 3.6 shows that a wide variety of hazard rate behaviour can be modeled with Weibull distribution. Because of such potential and simplicity of probability functions Weibull model are popular in engineering applications. Discrete models can also be found in literature (Nakagawa and Osaki, 1975, Stein and Dattero, 1984) which is helpful in modeling particular discrete data types. In this thesis the data is modeled by a continuous Weibull distribution model.

3.3.2.2 Gompertz Distribution

The Gompertz distribution is a popular choice in the demography and its survival and hazard rate functions are given as (Keyfitz, 1985)

$$S_T(t) = \exp\left(-B(C^t - 1)/\log C\right) \text{ and } h(t) = BC^t \tag{3.12}$$

where B and C are the distribution parameters.

3.3.2.3 Log-Logistic Distribution

The log-logistic distribution is also used in the survival analysis literature (Lawless, 2003)

$$S_T(t) = \left[1 + (t/\alpha)^{\beta}\right]^{-1} \text{ and } h(t) = \frac{(\beta/\alpha)(t/\alpha)^{\beta-1}}{\left[1 + (t/\alpha)^{\beta}\right]} \tag{3.13}$$

The life expectancy is simply the area under the survival curve, i.e.,

$$m_T = \int_0^\infty S_T(x)dx \tag{3.14}$$

3.3.3 Non-Parametric Lifetime Distribution

3.3.3.1 Complete Data

In the first model as discussed in Section 3.2.2, a sample of complete lifetime data is considered for the analysis. The sample consists of d_i entries of age t_i, $i = 1, N$, and the sample likelihood is given as

$$L = \prod_{i=1}^{N} \{f_T(t_i)\}^{d_i} \tag{3.15}$$

where $f_T(t)$ is the probability density of the lifetime distribution. In other words, the sample likelihood is proportional to the probability that the data comes from the model $f_T(t)$. Assuming an analytical distribution function (e.g. Weibull distribution), its parameters can be estimation by maximizing Eq.(3.15).

An empirical (sample based) survival curve, $S_T(t)$, can be analytically derived considering that lifetimes are recorded as a discrete variable taking values $t_1 < t_2 < \ldots < t_N$. The probability density at age t_i can be estimated as $f(t_i) = S_T(t_i) - S_T(t_{i+1})$ and it is related to the hazard rate as $f(t_i) = h(t_i)S(t_i)$. Combining these relations leads to a recursive equation of survival curve.

$$f(t_i) = h(t_i)S(t_i) = S(t_i) - S(t_{i+1}) \Leftrightarrow S(t_{i+1}) = S(t_i)\{1 - h(t_i)\} \tag{3.16}$$

Finally, the discrete survival curve can be written in terms of hazard rate as

$$S_T(t_i) = \prod_{k=1}^{i-1} [1 - h(t_k)] \tag{3.17}$$

Using Eqs.(3.16) and (3.17), the likelihood function can be written in terms of the hazard rate, and maximizing the log likelihood with respect to the hazard rate, $h(t_i)$, leads to a non-parametric estimate as

$$h(t_i) = \frac{d_i}{m(t_i)} \tag{3.18}$$

where $m(t_i)$ = the cumulative number of components surviving beyond the age t_i, i.e.,

$$m(t_i) = \sum_{k=i+1}^{N} d_k \tag{3.19}$$

3.3.3.2 Complete and Right Censored Lifetime Data

This model also considers the right censored lifetimes observed in the inspection data. The censoring time corresponds to the age at the time of inspection. Considering in an age group t_i, the sample consists of d_i complete lifetimes and (n_i - d_i) right censored lifetimes, the likelihood function is given as

$$L = \prod_{i=1}^{N} \{f_T(t_i)\}^{d_i} \{S_T(t_i)\}^{n_i - d_i} \tag{3.20}$$

Again using Eqs.(3.16) and (3.17), the likelihood function is written in terms of the hazard rate, and maximizing the log likelihood leads to a non-parametric estimate of the hazard rate at age t_i similar to that given by Eq.(3.18). However, in this case the cumulative number of components surviving beyond the age t_i is estimated as

$$m(t_i) = \sum_{k=i}^{N} n_k \tag{3.21}$$

Kaplan and Meier (1958) first derived this non-parametric (or product limit) estimator of the survival function.

3.3.3.3 Interval and Right Censored Lifetime Data

In this model, the complete lifetimes are replaced with the interval censored values. The likelihood function for a sample with d_i interval censored and (n_i - d_i) right censored lifetimes in the age group t_i, is written as

$$L = \prod_{i=1}^{N} \{F_T(t_i \mid T > c)\}^{d_i} \{S_T(t_i)\}^{n_{ij} - d_i} \tag{3.22}$$

where c denotes the censoring interval and $F_T(t)$ is the cumulative lifetime (T) distribution. Note that the conditional distribution, used to account for the censoring of observed lifetimes, is given as

$$F_T[t \mid T > (t-c)] = 1 - S_T[t \mid T > (t-c)] = 1 - \frac{P(T \geq t)}{P(T \geq t-c)} = 1 - \frac{S_T(t)}{S_T(t-c)} \qquad (3.23)$$

Now the conditional survival probability in Eq.(3.23) can be written in a discrete form using Eq.(3.17) as

$$S_T[t_i \mid T > (t_i - c)] = \frac{S_T(t_i)}{S_T(t_i - c)} = \frac{\prod_{k=1}^{i-1}[1 - h(t_k)]}{\prod_{k=1}^{i-c-1}[1 - h(t_k)]} = \prod_{i-c-1 \leq k_i < i-1}[1 - h(t_k)] \qquad (3.24)$$

Although the likelihood function can be written in terms of hazard rates using Eq.(3.24), a simple analytical expression for the hazard rate estimator cannot be derived. In such cases it is convenient to use parametric distribution models to estimate survival probabilities.

3.3.3.4 Current Status Data

Estimation of non parametric estimates from current status observations as discussed in Section 3.2.5 is not a straight forward task. However, the survival function can be estimated by Maximum likelihood method as described below (Turnbull, 1976, Meeker and Escobar, 1998). Considering the case of a cross sectional study conducted on a component population in a particular year resulting in a snap shot of condition data on the population.

Consider that the component population consists of age groups $t_1, t_2, t_3, ..., t_{10}$ at the time of inspection as shown in Figure 3.7. For each age group the number of components inspected (n_i) and the number of components in failed state (d_i) is known. Consider the interval failure probabilities p_i in the population as shown in Figure 3.7 for the observed data.

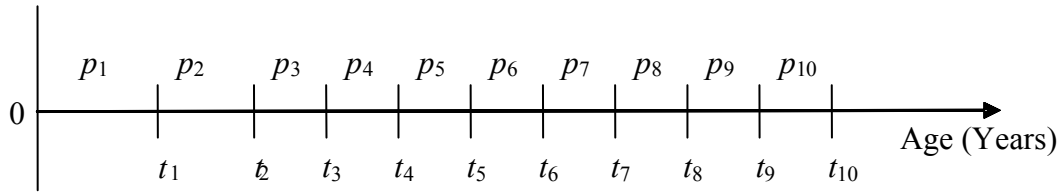

Figure 3.7: Parameters used in non-parametric MLE of current status data

The probability p_i shown in Figure 3.7 is the probability of component failure within the age interval. The cumulative probability of failure in each age group can be calculated as

$$F_T(t_i) = \sum_{j=1}^{i} p_j \tag{3.25}$$

Similarly the survival probability can be calculated as $S_T(t_i) = 1 - F_T(t_i)$. The parameters p_i in Figure 3.7 can be estimated by method of maximum likelihood. The likelihood function for the observed data on N age groups can be written as

$$L(p) = \prod_{i=1}^{N} \{F_T(t_i)\}^{d_i} \{1 - F_T(t_i)\}^{n_i - d_i} \tag{3.26}$$

where $F_T(t_i)$ is written in terms of probabilities p_i as in Eq.(3.25). The logarithm of the likelihood function in Eq.(3.26) can be maximized to obtain the maximum likelihood estimates $\hat{p}_i$. The confidence limits on the estimates can be estimated from the fisher information matrix of the likelihood function Eq.(3.26).

3.3.4 Estimation of Parametric Lifetime Distribution

3.3.4.1 Maximum Likelihood Method

The likelihood functions for various cases of complete and incomplete data sets are discussed in the previous section. In this section the application of such likelihood models is discussed for parametric estimation of the assumed distribution model. In this section the Weibull model is considered to illustrate the application of this method. Considering the case of complete data with multiple entries the likelihood function is given as

$$L = \prod_{i=1}^{n} \{f(t_i)\}^{d_i} \tag{3.27}$$

Where d_i is the number of complete observations at time t_i, n is the number of instances of lifetimes observed. Considering lifetime distribution follows Weibull model the likelihood function is given as

$$L(\boldsymbol{\theta}) = \prod_{i=1}^{n} \left\{ \frac{\beta}{\alpha} \left(\frac{t_i}{\alpha} \right)^{\beta-1} \exp\left\{ -\left(\frac{t_i}{\alpha} \right)^{\beta} \right\} \right\}^{d_i} \tag{3.28}$$

where $\boldsymbol{\theta}$ is the vector of the distribution parameters of the Weibull model. The parameters are estimated by maximizing the likelihood function. To simplify the numerical computation the natural logarithm of the likelihood is maximized to estimate the distribution parameters. The logarithm of the likelihood function is given as

$$l(\theta) = \log(L(\theta)) = \log(\beta/\phi) \sum_{i=1}^{n} d_i + (\beta - 1) \sum_{i=1}^{n} (d_i \log t_i) - \frac{1}{\phi} \sum_{i=1}^{n} d_i t_i^{\beta} \tag{3.29}$$

where ϕ is substituted for α^{β}. Standard optimization algorithm can be used to estimate the parameters by maximizing Eq.(3.29). Alternatively, the parameters are found by solving the first partial derivatives of the likelihood function Eq.(3.29) with respect to the parameter. The first partial derivatives of the log-likelihood function can be written as

$$\begin{aligned} \frac{\partial l(\theta)}{\partial \beta} &= \frac{1}{\beta} \sum_{i=1}^{n} d_i + \sum_{i=1}^{n} d_i \log t_i - \frac{1}{\phi} \sum_{i=1}^{n} d_i t_i^{\beta} \log t_i = 0 \\ \frac{\partial l(\theta)}{\partial \phi} &= -\frac{1}{\phi} \sum_{i=1}^{n} d_i + \frac{1}{\phi^2} \sum_{i=1}^{n} d_i t_i^{\beta} = 0 \end{aligned} \tag{3.30}$$

$$\phi = \frac{\sum_{i=1}^{n} d_i t_i^{\beta}}{\sum_{i=1}^{n} d_i} = \alpha^{\beta}$$

$$\frac{1}{\beta}\sum_{i=1}^{n} d_i + \sum_{i=1}^{n} d_i \log t_i - \left(\frac{\sum_{i=1}^{n} d_i}{\sum_{i=1}^{n} d_i t_i^{\beta}} \right) \sum_{i=1}^{n} d_i t_i^{\beta} \log t_i = 0 \tag{3.31}$$

Solving Eqs.(3.31), the estimates for $\hat{\beta}$ and $\hat{\alpha}$ are obtained. Likewise the parameters of the selected distribution are estimated by maximizing the log-likelihood function corresponding to the observed data.

For the case of complete and right censored, the likelihood function Eq.(3.20) takes the following form

$$L(\theta) = \prod_{i=1}^{N} \left\{ \frac{\beta}{\alpha} \left(\frac{t_i}{\alpha} \right)^{\beta-1} \exp\left\{ -\left(\frac{t_i}{\alpha} \right)^{\beta} \right\} \right\}^{d_i} \left\{ \exp\left(-\left[\frac{t_i}{\alpha} \right]^{\beta} \right) \right\}^{n_i - d_i} \tag{3.32}$$

The likelihood function applicable to Interval censored along with right censored observations is derived from Eq.(3.22) as

$$L(\theta) = \prod_{j=1}^{N} \left\{ 1 - \exp\left(\left[\frac{t_j - c}{\alpha} \right]^{\beta} - \left[\frac{t_j}{\alpha} \right]^{\beta} \right) \right\}^{d_j} \left\{ \exp\left(-\left[\frac{t_j}{\alpha} \right]^{\beta} \right) \right\}^{m_j - d_j} \tag{3.33}$$

The likelihood function for the case of current status data is similar to that given in Eq. (3.33) where censoring interval $c = 0$.

For computational purpose, the logarithm of the likelihood (Eqs. 3.28, 3.32, 3.33) is maximized with respect to the distribution parameters (α and β) using a standard MATLAB^{TM} optimization code (fminsearch and fminunc).

The Fisher information matrix is the expectation of the negative of the second derivative of the log likelihood with respect to the parameters. Fisher information is used to obtain asymptotic variance of the maximum likelihood estimator of the distribution parameters (Kalbfleisch & Prentice, 2002). The asymptotic

covariance matrix of the maximum likelihood estimators is the inverse of the Fisher information matrix.

$$\begin{pmatrix} \mathrm{var}(\hat{\beta}) & \mathrm{cov}(\hat{\beta},\hat{\alpha}) \\ \mathrm{cov}(\hat{\beta},\hat{\alpha}) & \mathrm{var}(\hat{\alpha}) \end{pmatrix} = \begin{pmatrix} -\dfrac{\partial^2 l(\theta)}{\partial \beta^2} & -\dfrac{\partial^2 l(\theta)}{\partial \beta \partial \alpha} \\ -\dfrac{\partial^2 l(\theta)}{\partial \beta \partial \alpha} & -\dfrac{\partial^2 l(\theta)}{\partial \alpha^2} \end{pmatrix}^{-1}_{\beta=\hat{\beta},\alpha=\hat{\alpha}} \tag{3.34}$$

Using the asymptotic variance of the estimated parameters the approximate confidence intervals can be obtained for the parameters estimated. A confidence interval gives an estimated range of values which is likely to include the unknown population parameter. Confidence interval is associated with confidence level which gives the probability that the true value of the parameter lies within the interval. The upper and lower bounds of the Weibull parameters are estimated as

$$\beta_L = \frac{\hat{\beta}}{\exp\left(\dfrac{k\sqrt{\mathrm{var}(\hat{\beta})}}{\hat{\beta}}\right)}; \qquad \beta_U = \hat{\beta}\exp\left(\frac{k\sqrt{\mathrm{var}(\hat{\beta})}}{\hat{\beta}}\right) \tag{3.35}$$

$$\alpha_L = \frac{\hat{\alpha}}{\exp\left(\dfrac{k\sqrt{\mathrm{var}(\hat{\alpha})}}{\hat{\alpha}}\right)}; \qquad \alpha_U = \hat{\alpha}\exp\left(\frac{k\sqrt{\mathrm{var}(\hat{\alpha})}}{\hat{\alpha}}\right) \tag{3.36}$$

The bounds are derived based on lognormal approximation with confidence level a, where $k = \Phi^{-1}(1 - a/2)$. For 95% confidence bounds (a=5%) on parameter estimates, the value of k is 1.96. The variance of a function of distribution parameters is estimated by delta method. The mean lifetime of Weibull model is given as

$$\mu_T = \alpha\Gamma\left(1 + \frac{1}{\beta}\right) \tag{3.37}$$

By delta method, the variance of mean lifetime is calculated as

$$\mathrm{var}(\mu_T) = \left(\frac{\partial \mu_T}{\partial \alpha}\right)^2 \mathrm{var}(\hat{\alpha}) + \left(\frac{\partial \mu_T}{\partial \beta}\right)^2 \mathrm{var}(\hat{\beta}) + 2\left(\frac{\partial \mu_T}{\partial \alpha}\right)\left(\frac{\partial \mu_T}{\partial \beta}\right)\mathrm{cov}(\hat{\alpha},\hat{\beta}) \tag{3.38}$$

Different types of parametric models can be applicable using likelihood functions given in Section 3.3.3. One way to check for the best fit is by comparing the parametric probability function plots with the non-parametric estimates. Besides the graphical methods statistical tests are used to check the best fit model.

3.3.4.2 Test of Goodness of Fit

Models vary in complexity and assumptions, and it is necessary to check the adequacy of the models. Although the probability plots are one of the tools to check the models, they are not just sufficient to check some of the assumptions. Hypothesis tests are most commonly used by statisticians to check the adequacy of the models. The classical procedures (Lawless, 2003) to compare the parametric models with non-parametric counterparts are Kolmogorov-Smirnov Statistic and Cramer-von Mises Statistic. Such test statistics provide evidence for or against the hypothesized model. Tests of fit for specific distributions (Lawless, 2003) like Weibull or Extreme are also available for complete and right censored data.

Likelihood Ratio Statistic (LRS) is commonly used to compare different models (Lawless, 2003, Nelson, 1982). LRS for testing null hypothesis (H_0) Vs alternative hypothesis (H_1) can be given by

$$\Lambda = 2\log L(\hat{\theta}_1) - 2\log L(\hat{\theta}_0) \tag{3.39}$$

Let the number of independent parameters in models H_1 and H_0 are m and n respectively. Then under H_0 and for large sample size Λ is approximately chi-squared distribution (χ^2_{m-n}).

3.3.4.2.1 Akaike Information Criterion (AIC)

In the absence of the true model it is difficult to compare models from tests like LRS or other tests discussed above. On the other hand Akaike (1985) has developed an information criterion (AIC) without specific reference to the true model. Hence AIC can be useful in comparing different models. AIC is based on entropy maximization principle (Akaike, 1985) which is the maximization of the

expected entropy of a true distribution with respect to the fitted predictive distribution.

It is known that the maximum likelihood method leads to biased estimates of the true parameters in case of finite sample data (Baker, 1990). Akaike derived an unbiased estimator based on an information-theoretic interpretation of the likelihood function. He proposed the following measure to test the goodness of fit of an assumed model (Akaike, 1985):

$$AIC = -2\log[L_{MAX}] + 2K \tag{3.40}$$

where K is the number of distribution parameters and L_{MAX} is maximum value of the likelihood function under an assumed model. Among all candidate distributions, the distribution that minimizes the AIC measure is considered as the best fit distribution. The mathematical proofs are further discussed by Awad (1996) and Cavanaugh (1997).

Since the AIC is on a relative scale that can range from a large negative to a large positive limit, the AIC difference is a suitable basis to evaluate the goodness of fit, which is calculated as

$$\Delta(AIC)_i = AIC_i - \min AIC \quad (i = 1 - 3) \tag{3.41}$$

where "min *AIC"* is the minimum value of the *AIC* measure among all the distributions considered. For the best fit distribution, $\Delta(AIC) = 0$.

3.3.5 Frailty Models

During lifetime data analysis among a collection of individuals it is assumed that the lifetimes are independent. But there could be some unobserved risk factors that are common between the individuals and constant over time. The frailty is the term that describes the common risks acting as a factor on the hazard function. Frailty model assume that all lifetime observations are independent given the values of the frailty. This offers an advantage in interpretation of frailty as a probability model, that is the conditional independence implies that dependence is

created by the common factors or the variation within individuals (Hougaard, 2000).

The unobserved risk within individuals is described by a random variable *Y*. The hazard conditional on *Y* has the form.

$$h(t \mid Y) = Yh_0(t) \tag{3.42}$$

The conditional survival function is found as

$$S(t \mid Y) = \exp\left\{-\int_0^t Yh_0(u)du\right\} = \exp\{-YG(t)\} \tag{3.43}$$

where $G(t) = \int_0^t h_0(u)du$. The marginal survival function can be evaluated by integrating out the unobserved distribution.

$$S(t) = \int_0^\infty S(t \mid Y) f(Y) dY = E\left[S(t \mid Y)\right] = E\left[\exp\{-YG(t)\}\right] = L(G(t)) \tag{3.44}$$

where $L()$ is the Laplace transform of the random variable *Y*.

Frailty models can be developed by choosing different parametric distributions like Exponential, Weibull, Gompertz discussed in Section 3.3.2 and distributions like Gamma and Inverse Gaussian for the frailty. In this section Gamma frailty models are considered which are popular in survival analysis.

3.3.5.1 Gamma Frailty Model

When the frailty follows gamma distribution with unit mean and finite unknown variance δ gamma frailty models are derived. The marginal survival distribution for gamma frailty models using marginal Gamma distribution is derived as

$$S(t) = \left[1 + \delta G(t)\right]^{-1/\delta} \tag{3.45}$$

If the conditional distributions are taken as Weibull the marginal survival function for Weibull gamma frailty model is given from Eq.(3.45) as

$$S(t) = \left[1 + \delta \left(\frac{t}{\alpha} \right)^{\beta} \right]^{-1/\delta} \tag{3.46}$$

When the conditional distribution is taken as Gompertz the marginal survival function for the Gompertz gamma frailty model is given from Eq.(3.45) as

$$S(t) = \left[1 + \frac{\delta B(C^t - 1)}{\log C} \right]^{-1/\delta} \tag{3.47}$$

In general gamma frailty models are parametric distribution models with an additional parameter used in modelling the lifetime distribution of components. The parameters of the gamma frailty distributions are estimated by likelihood methods discussed in Section 3.3.4.

3.3.6 Entropy and Life Expectancy

The concept of entropy discussed in this section comes from the field of demography. In general policy decisions on life saving efforts depend on the age specific mortality and life expectancy. In an effort to reduce the mortality to increase the life expectancy of the population which decade of ages would be the selected. In doing so, there is a need for better understanding of the linkage between the age specific mortality and life expectancy. Similar analogy can be derived for maintenance of engineering components. In a population of components which are distributed among various ages which age group need to be addressed for maintenance actions.

Keyfitz (1985) derived entropy of the survival function given as

$$K(0, w) = \frac{-\int_0^w S(t) \ln S(t) dt}{\int_0^w S(t) dt} \tag{3.48}$$

where w is the highest survival age, the entropy can be interpreted as a measure of heterogeneity of population with respect to mortality at different ages. If everyone dies at same age then K=0; if the hazard rate is same at all ages (Constant) then

K=1. K gives the percentage change in life expectancy produced by reducing the hazard rate at all ages by one percent. If K=0.1 then the change in life expectancy by reducing the mortality at all ages by one percent is 0.1%.

Vaupel (1986) expressed Eq. 3.48 in an alternate from which is derived as

$$\begin{aligned} K(0,w) &= \frac{\int_0^w S(t)\int_0^t h(x)dxdt}{e(0)} = \frac{\int_0^w\int_0^t S(t)h(x)dxdt}{e(0)} \\ &= \frac{\int_0^w\int_x^w S(t)h(x)dxdt}{e(0)} = \frac{\int_0^w h(x)\int_x^w S(t)dtdx}{e(0)} \\ &= \frac{\int_0^w h(x)S(x)e(x)dx}{e(0)} = \frac{\int_0^w f(x)e(x)dx}{e(0)} \end{aligned} \tag{3.49}$$

where $h()$, $f()$ are the hazard rate function and probability density function. $e(x)$ is the remaining life expectancy at age x and $e(0)$ is the life expectancy at birth (zero age). Vaupel (1986) states that this formula facilitates understanding of why K measures the percentage increase in life expectancy generated by a decrease in mortality rates of one percent. The numerator in Eq.(3.49) can be integrated within an age interval to quantify the increase in life expectancy by reducing the mortality in those ages by one percent. The case on component life expectancy is considered for illustrating the application of the entropy concept.

3.3.6.1 Illustrative case

The lifetime distribution of a component is considered with life expectancy of 67 years. Weibull distribution with shape parameter as 4.48 and scale parameter of 73.67 is considered for illustration. The entropy as calculated from Eq.(3.49) is 0.22 taking the highest age w of the component as 100 years. This shows that when the mortality is reduced by 1% among all component ages the life expectancy is increased by 0.22%. The increase in life expectancy by reducing the mortality in each component age by one percent can be shown in Figure 3.8. The Figure 3.8 shows that the change in mortality among ages near life expectancy can increase the life expectancy reasonably higher than other age groups.

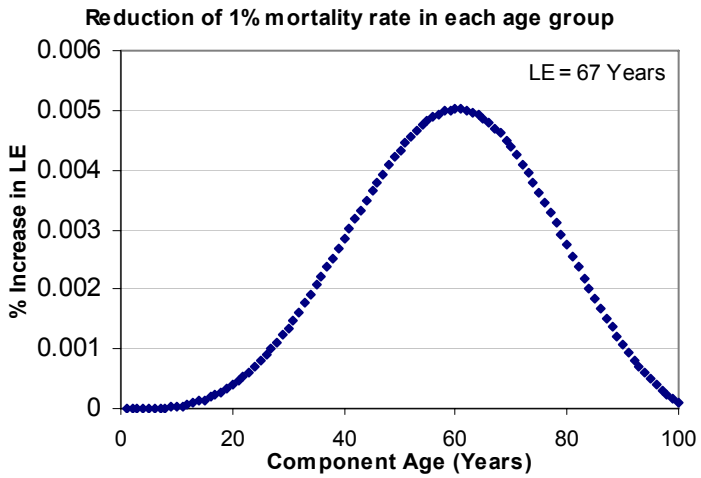

Figure 3.8: Change in life expectancy with change in mortality rate

The mortality changes in each component age can be viewed as age specific refurbishment rate. Refurbishing a fraction of components of a particular age group in a way decreases the mortality and increases the life expectancy of the population. Hence from entropy concept the change in life expectancy of the assets can be estimated from age specific refurbishment policies.

Table 3.2: Entropy among different component age groups

Component Age	Entropy
≥40 Years	0.19%
≥50 Years	0.15%
≥60 Years	0.11%

When calculating entropy for components with age ≥40 years an increase of 0.19% of life expectancy is estimated when reducing the mortality rate of components ≥40 years by one percent. Depending on population demographics of older age components, a cost benefit assessment can be made on age based refurbishment. From Table 3.2 it is evident that replacing components older than 60 years can result in around 11% increase in population life expectancy. The

estimate on benefit of increasing the life expectancy through age based refurbishment is demonstrated using the concept of entropy.

3.3.6.1.1 Remarks

The entropy of the survival function is a property of a lifetime distribution which shows the linkage between age specific mortality and life expectancy. This concept is used in demography where policy decisions are based on individual age specific mortality and life expectancy. A similar application is thought of in component refurbishment policy in a population of distributed component ages. The concept of entropy can be used in identifying which age groups to be refurbished with considerable increase in population life expectancy.

3.4 Applications in Power Industry

3.4.1 Estimation of Life Expectancy of Wood Poles

Condition assessment inspections are undertaken by power utilities to identify decayed poles and decide about their subsequent replacement depending on the degree of wood deterioration. A key input of probabilistic methodology is the lifetime distribution function of wood pole, though its estimation is often hampered by lack of data. This section presents comprehensive statistical analysis to provide estimates of life expectancy and the survival curve of typical distribution wood pole in-service in the Canadian climate (Datla and Pandey, 2006).

3.4.1.1 Summary of Data

Inspection data collected by the industry consist of classification of each inspected pole on a binary scale, i.e., whether or not the pole has reached its end of life based on its current condition at the time of inspection.

This study has reviewed a random sample of approximately 100,000 distribution wood poles (selected from a population of 2 million distribution poles in Ontario) that were assessed by inspectors of the power utilities in year 2002. The inspection program revealed that approximately 5.46% poles of different ages

were in substandard condition. The pole age was determined on the basis of the installation date stamped on each pole.

The age distribution of wood poles in the sample is shown in Figure 3.9. The average age of in-service poles is estimated as 29 years with a standard deviation of 15 years.

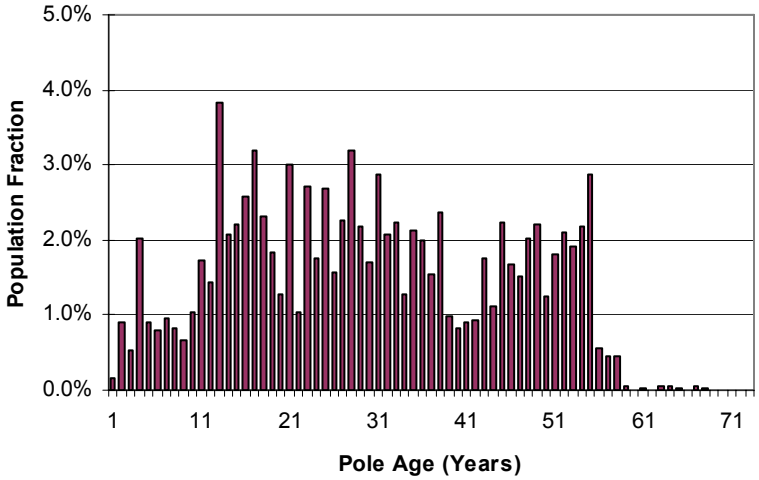

Figure 3.9: Pole age distribution estimated from inspection data

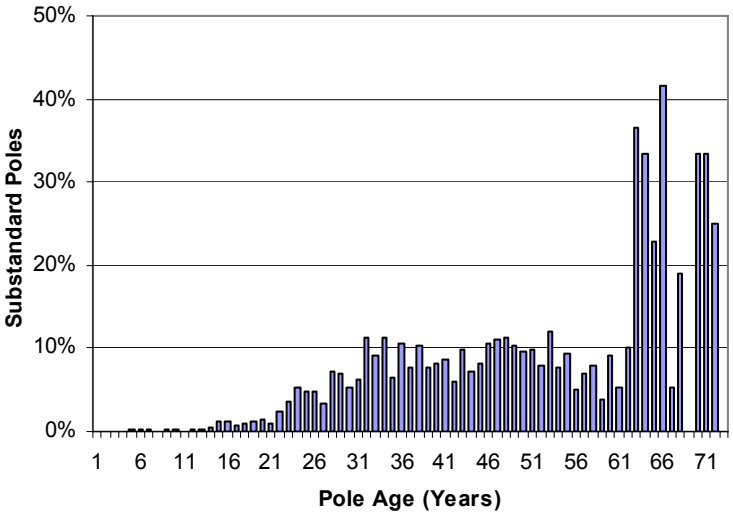

Figure 3.10: Fraction of substandard poles observed in different age groups

The fraction of substandard poles as a percentage of pole population in each age group in the sample is plotted in Figure 3.10.

The data presented in Figure 3.10 reveals the cumulative number of substandard poles in each age group. Substandard poles did not reach end of life in the year of inspection, rather it represents the number of substandard poles that were accumulated over a period of time. The reasons are that (1) there are no records a prior inspection of this sample, (2) the time of pole reaching the substandard state is not manifested by a physical pole failure and interruption in power supply, and (3) the substandard state is determined through inspection only. Because of these reasons, the estimation of lifetime distribution from inspection data is not a straightforward task.

Based on the information presented in Figure 3.9 and 3.10, estimation of the pole lifetime probability distribution is a key problem that is discussed in this section.

3.4.1.2 Numerical Results

Statistical analyses of industry's inspection data were conducted under the three models discussed in Section 3.2. In each case, the three parametric distributions were fitted to estimate the pole life expectancy and the survival curve. The effects of model assumptions and model uncertainty are discussed in this section.

Model 1: Complete Lifetime Sample

This model considers only substandard poles (5.46% of sample) assuming that they all reached the end of life in the year of inspection. The non-parametric survival curve is derived from Eqs.(3.18) and (3.19). Using the maximum likelihood method, the parameters of the Weibull, Log-Logistic and the Gompertz distributions were estimated. The numerical results presented in Table 3.3 show that the life expectancy (LE) estimates obtained from the three distributions are in close agreement. The Weibull distribution is the best fit distribution according to the AIC criterion, which estimates the LE of wood poles as 40 years.

Table 3.3: Wood pole life expectancy and lifetime distribution data – Model 1

Distribution	Parameters		Life Expectancy (years)	C.O.V (%)	AIC Differences
Weibull	β	α	40	26	0 (best fit)
	4.21	44.07			
Log-Logistic	β	α	41	34	1056
	5.75	39.22			
Gompertz	B	C	39	34	274
	0.0012	1.1032			

Model 2: Complete and Right Censored Lifetime Sample

This analysis extends Model 1 to incorporate the "right-censored" pole life times. The numerical results are presented in Table 3.4. The LE estimates vary from 62 – 79 years depending on the distribution type. The Weibull distribution is again the best fit distribution that leads to pole LE of 69 years. The Gompertz distribution is the most pessimistic with LE of 62 years.

Table 3.4: Pole life expectancy and lifetime distribution data – Model 2

Distribution	Parameters		Life Expectancy (years)	C.O.V (%)	AIC Differences
Weibull	β	α	69	25	0 (best fit)
	4.46	75.48			
Log-Logistic	β	α	79	44	104
	4.62	73.09			
Gompertz	B	C	62	23	360
	0.0001	1.1138			

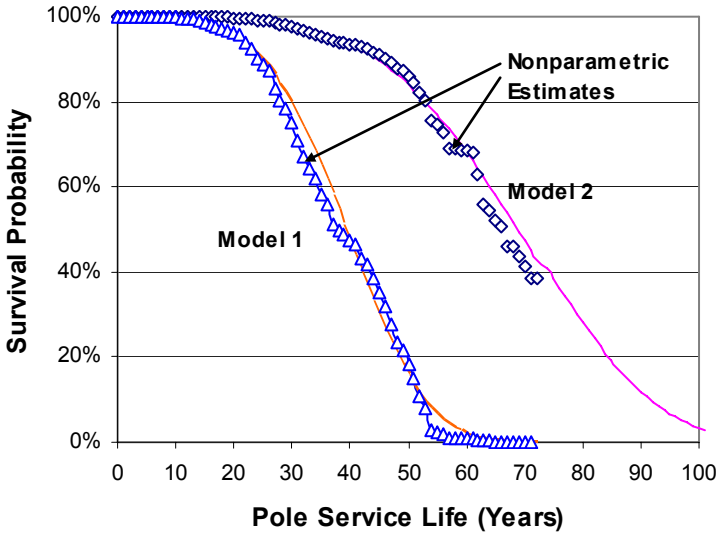

Figure 3.11: Comparison of wood pole survival curves (Model 1 vs. Model 2)

The survival curves obtained from Models 1 and 2 are compared in Figure 3.11, which plots the non-parametric estimates along with the best-fit Weibull distribution. In Model 1, an omission of right censored data results in a severe under estimation of the survival curve. The life expectancy (69 years) obtained from Model 2 is almost 75% higher than that obtained from the Model 1 (LE = 40 years). Van Noortwijk and Klatter (2004) reported a similar effect of right censored data in the analysis of bridge lifetime data.

Frailty models discussed in Section 3.3.5 are considered for the wood pole lifetime distribution analysis. The estimated parameters from Gompertz gamma frailty model are $B = 0.0001, C = 1.1195, \delta = 0.8164$. This frailty model is a better fit as compared to the Gompertz distribution model as shown in Figure 3.12.

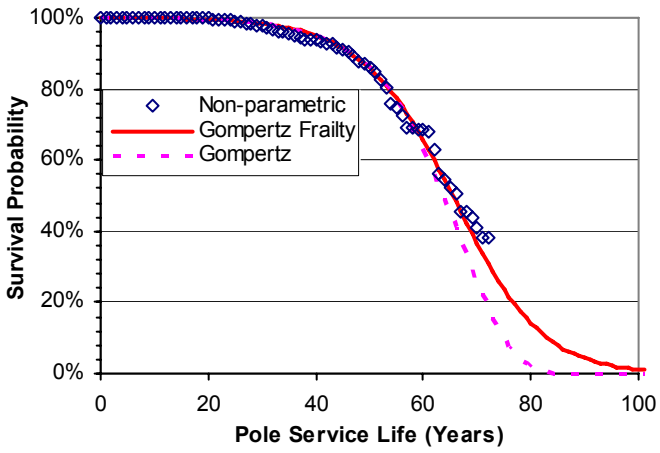

Figure 3.12: Gompertz gamma frailty survival curve

The life expectancy from the Gompertz gamma frailty model is obtained as 65 years. The maximum likelihood estimate of Weibull gamma frailty is obtained with $\delta = 0$ which is the Weibull distribution. The result suggests that Weibull model is the most suitable model for wood pole lifetime.

Model 3: Interval and Right Censored Data

In this model, an assumption of complete lifetime is relaxed by incorporating interval censoring. The censoring interval is varied from 1 – 10 years to evaluate its impact on the life expectancy estimates and results are presented in Table 3.4. From industry's experience, the average censoring interval is about 3 - 4 years. Results for 10 year censoring interval are presented to study the impact of an extreme censoring interval.

The analysis of the goodness of fit in terms of the AIC difference criterion is presented in Table 3.5, which suggests the Weibull as the best fit distribution in most cases. In comparison to Model 2, an increase in censoring interval increases the life expectancy modestly. For a 3 year interval, the Weibull LE is estimated as 70 years, which is slightly higher than that obtained from Model 2 (69 year).

Table 3.5: Pole life expectancy and lifetime distribution data – Model 3

Distribution	Censoring Interval (years)	Parameters		Life Expectancy (years)	Standard Deviation	C.O.V (%)
Weibull		**β**	**α**			
	1	4.48	73.67	67.21	16.75	25
	2	4.18	76.19	69.23	18.41	27
	3	4.05	77.47	70.26	19.25	27
	4	3.92	78.76	71.31	20.11	28
	5	3.81	80.08	72.38	20.98	29
	10	3.33	87.03	78.10	25.64	33
Gompertz		B	C			
	1	0.0001	1.1109	61.25	14.35	23
	2	0.0001	1.1073	61.71	14.67	24
	3	0.0001	1.1039	62.17	14.99	24
	4	0.0001	1.1008	62.64	15.30	24
	5	0.0001	1.0979	63.10	15.62	25
	10	0.0002	1.0853	65.48	17.19	26
Log-Logistic		**β**	**α**			
	1	4.49	72.31	78.55	35.34	45
	2	4.35	73.42	80.23	37.66	47
	3	4.21	74.55	81.95	40.09	49
	4	4.08	75.70	83.74	42.64	51
	5	3.96	76.88	85.58	45.33	53
	10	3.46	83.15	95.79	61.44	64

Table 3.6: AIC differences among parametric models

Censoring Interval (years)	Weibull	Gompertz	Log-logistic
1	0	450	90
2	0	526	66
3	0	592	46
4	0	648	30
5	0	700	18
10	24	880	0

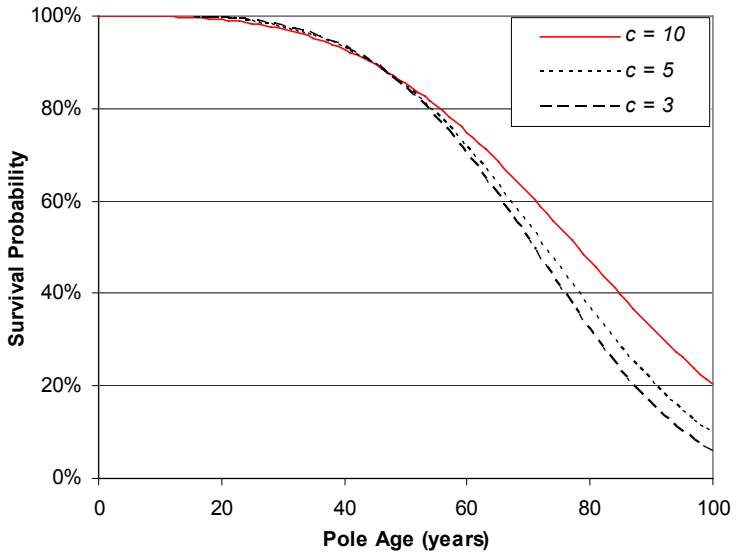

Figure 3.13: Weibull survival curves obtained for different censoring intervals (Model 3)

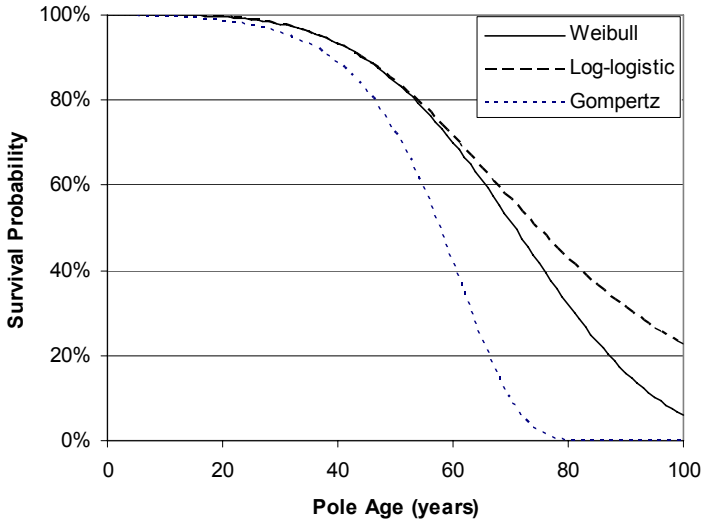

Figure 3.14: Comparison of different survival curves for censoring interval of 3 years (Model 3)

Figure 3.13 shows that the effect of 3 – 5 year censoring interval on the Weibull survival curve is quite modest. The effect of distribution type (i.e., model

uncertainty) on survival curve is illustrated in Figure 3.14 (c= 3 year). The tail of the survival curve is quite sensitive to the distribution type. The log-logistic distribution leads to an upper bound life expectancy of 82 years, whereas the Gompertz model provides a lower bound of 62 years. The reason is that the hazard rate in the Gompertz model increases with age much more rapidly than in the other two models, which leads to a low value of life expectancy. Since the survival curve is a key input to the life-cycle cost analysis, it is important to evaluate the sensitivity of model uncertainty to the cost optimization problem. This issue is discussed in Section 4.2.1.

3.4.1.3 Remarks: Model Comparison

Figure 3.15 illustrates the effect of the three modeling assumptions regarding the inspections data on estimates of the Weibull survival curve. The analysis in Model 1 is simplistic as it ignores a vast amount of information about the survival of a large fraction of the sample. Model 1 is therefore the most pessimistic model, and it provides an unrealistic lower bound estimate of pole life expectancy (LE =40 years).

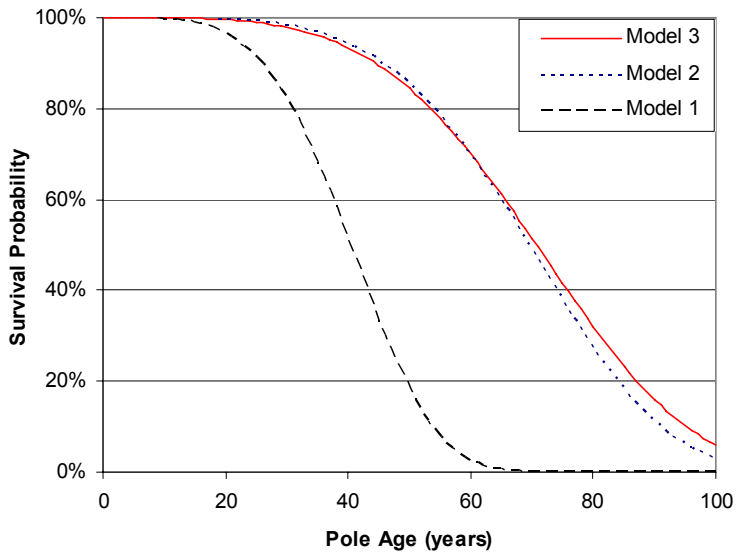

Figure 3.15: Comparison of the Weibull survival curves obtained from the three inspection models

Model 2 improves significantly the estimates of survival probabilities by consideration of the right censored data, and it leads to LE = 69 year. The survival curve of Model 3 (c=3) is in a close agreement with Model 2, and estimated LE = 70 years. The analysis illustrates that the censoring interval of 3 - 5 years has limited sensitivity to the life expectancy estimates. The reason for this insensitivity is that the interval censored data is a very small fraction (5.46%) of the sample. The effect of censoring interval on LE increases with increase in the proportion of data in the sample.

3.4.2 Lifetime Distribution of Oil Circuit Breakers

3.4.2.1 Introduction

Oil circuit breakers (OCB) are used to switch circuits and equipment in and out of a system in a substation as shown in Figure 3.16. They are oil filled to provide cooling and to prevent arcing when the switch is activated. The oil circuit breaker has number of sub-components like contacts, pushings, lifting rods etc. and all these components has to perform well in order to the circuit breaker to work.

Figure 3.16: Oil Circuit Breaker

As the oil breaker is in usage the components are subjected to operating load and environmental effects which trigger the deterioration process. Hence the oil breakers have to be subjected to periodic maintenance to ensure its smooth functioning. The maintenance packages vary from visual inspection conducted every six months to the intrusive maintenance which is the most expensive and conducted every 7 years.

3.4.2.2 Summary of Data

The data discussed in this section is obtained from a power industry which has collected maintenance data on oil circuit breaker (OCB) from 1999 to 2004. The majority of the OCBs are 27.6 kV and 44kV which consist of 752 Oil breakers that have undergone selective intrusive (SI) maintenance. For each OCB under selective intrusive maintenance has 5-6 individual tasks to access the condition of the oil-breaker and each is given a condition rating of CR1(good)-CR4(bad). SI maintenance package consists of the tasks as shown in Table 3.7.

Table 3.7: Description of SI maintenance tasks

SI Task	Description
T2	Check insulation condition.
T3	Inspect contacts and interrupters.
T4	Measure resistance/resistors.
T5	Contact wipe measurement (analyzer rod).
T6	Inspect internal components and tank

Data on Task T1 is not provided and hence will not be discussed here. Each task aims at specific degradation mechanism for various components of OCB. The condition rating of an OCB in each task is ranked as shown in Table 3.8

Table 3.8: Description of condition rating in each task

Condition Rating	Description
CR1	Condition like new
CR2	Condition as expected (no unusual degradation, functional as per design)
CR3	Signs of degradation
CR4	Poor condition

End of Life Criterion

An OCB with condition rating CR4 in a given maintenance category is assumed to be at the end of life (incipient failure) with respect to that maintenance category. A rating of CR3 means that remaining life is approximately 3 years. A rating of CR1 or CR2 is considered as the OCB in a good functional state as per design. The average SI maintenance interval is 7 years. Each task is assumed as independent degradation mechanisms; hence the estimation of lifetime of each degradation/task is essential for estimating the overall breaker lifetime. The results on lifetime analysis on each task are discussed in next section.

3.4.2.3 Statistical Lifetime Analysis

SI inspection data under each task is grouped to conduct lifetime analysis. Most of the breakers does not have record on the time of previous inspection and is thus assumed the average inspection interval of 7 years. Weibull distribution model is assumed to model the aging or deterioration effects in each task. The failure rate is assumed to linearly increase with time (Rayleigh Model) based on the preliminary analysis conducted on maintenance data. When the failure rate is assumed as constant (Exponential Model) the model underestimates the probability of failure, whereas when the failure rate is assumed highly nonlinear the model may overestimate the probability of failure.

The breakers were assumed to be in condition CR1 at the outset of the interval. The breaker with condition rating CR4 in a given maintenance category is considered as complete observation. The breaker with condition rating CR3 in a given maintenance category is considered as interval censored towards right of the observation since it is assumed that the remaining life is approximately 3 years. The breaker with condition CR1 and CR2 are considered as right censored observations. The estimation of lifetime distribution is conducted using maximum likelihood method discussed in Section 3.3.4. The mean lifetimes for different task categories is shown in the Table 3.9

Table 3.9: Mean lifetime of a breaker under different SI Inspection Tasks

Task	T2	T3	T4	T5	T6
Number of OCBs inspected	708	709	278	696	699
Mean Lifetime, Years (Rayleigh)	39	13	21	15	19
Mean Lifetime, Years (Exponential)	547	40	81	43	104

The mean life time is the lowest (13 years) with respect to the conditions of contacts and interrupters (T3). The mean lifetime is the highest (39 years) with respect to the insulation condition. The condition of tank (T6) reaches to CR4 on average in 19 years of service life. The mean lifetimes obtained from exponential distribution are much higher which underestimates the probability of failure.

The lifetime distributions are shown in Figure 3.17 and 3.18. The area under the distribution between 0 and 7 years shows the probability of a breaker reaching CR4. For example, the probability of reaching CR4 in the task T3 (contacts and interrupters) is approximately 20%, estimated from Figure 3.17.

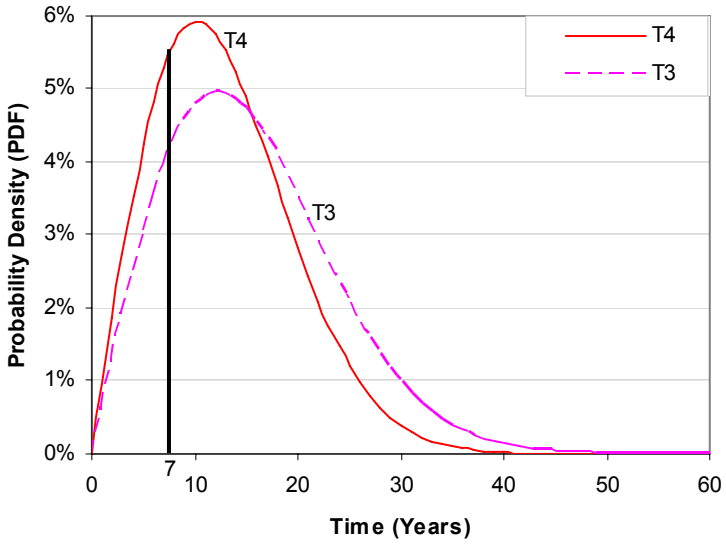

Figure 3.17: Lifetime distribution with respect to the tasks T3 and T4

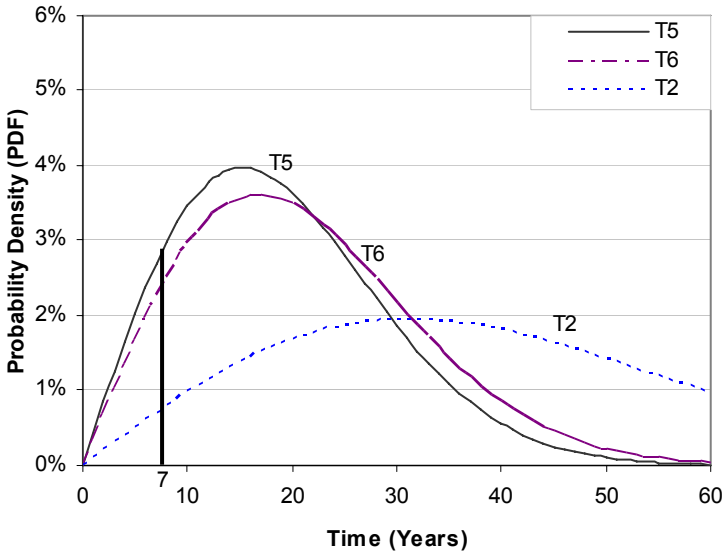

Figure 3.18: Lifetime distribution with respect to the tasks T2, T5 and T6

3.4.2.4 Maintenance Interval Optimization

The first step in optimizing a maintenance program is to increase the interval of SI maintenance from 7 years to say 8 or 10 years. An increase in SI interval will also increase the probability of the breaker reaching in CR4 condition. This will increase the probability of functional failure of a breaker. The contacts and the interrupters appear to be the most stressed parts of the breaker, since they have the lowest mean service life. If the SI interval is increased from 7 to 8 years, a maximum 5% increase in probability is estimated for the task T3 (contacts and interrupters). In other cases, the increase in probability is less than 5%.

The probability of a breaker reaching in CR4 condition for different inspection intervals is presented in the Table 3.10. The lifetime distributions given in Figure 3.17 and 3.15 were used to derive these probability estimates.

Table 3.10: Probability of an OCB reaching in CR4 condition under different SI task

Task	Mean Lifetime of Breaker (years)	Probability of Reaching in CR4 Condition		
		7 years (Current interval)	8 years	10 years
T2	39	2%	3%	5%
T3	13	20%	25%	37%
T4	21	8%	11%	16%
T5	15	15%	19%	28%
T6	19	10%	13%	19%

3.4.2.5 Remarks

The maintenance data collected on OCB gives very little information on component lifetimes. This creates difficulty in estimating the lifetime distribution of OCB. The time since previous inspection is taken as 7 years and the condition in each task define the lifetime of OCB. Weibull distribution with shape parameter 2 is assumed to model the lifetime in each task from aging effects. Lifetime distributions in each task are estimated from maximum likelihood method.

The probabilistic analysis of breaker inspection data enables the development of risk-based models to optimize the maintenance program and minimize the associated life-cycle costs. The service lifetime ends when a breaker enters in CR4 (poor condition), since it triggers a corrective maintenance of the breaker. It does not reflect the true probability of functional failure of the breaker. For the sake of a proper risk assessment, a correlation between the CR4 rating and breaker probability of failure must be investigated. The past records of breaker failure should be examined to establish this correlation. There is a potential to increase the inspection interval from 7 to 8 or 10 years for some of the SI tasks that can result in cost savings.

3.4.3 Estimation of Lifetime Distribution of Electric Insulators

3.4.3.1 Summary of Data

Electric insulators are an important component on power transmission lines for electric utilities. Insulators experience degradation with usage and eventually fail. Maintenance of such insulators is crucial in maintaining the network reliability of power infrastructure. The lifetime of the insulators is required for maintenance decisions. Probabilistic lifetime distribution for insulators can be estimated from field failure data. The insulators are designed with high lifetime and so the failures observed are very few.

A mockup inspection data on insulators obtained from the power utility for a specific population is shown in Table 3.11. The data shown in Table 3.11 is not considered in the analysis but reflects the actual data obtained from industry. The data obtained actually gives information on current status of insulators at the time of inspection. This is similar to the case of wood pole inspection but in this case there is insufficient data on aging population.

Table 3.11: Inspection data of insulators tested by power utility

Age (t_i)	**Number Defective (d_i)**	**Number Tested (n_i)**
21	0	25
24	0	100
25	2	500
26	5	1000
27	5	1000
28	30	6000
29	12	2000
30	10	1500
31	6	1000
32	7	500

The lifetime or failure of the insulator is defined as the time to enter defective state. The precise lifetime of the defective insulators is unknown, which happened sometime between installation and inspection time. The age of the insulators at

the time of inspection are derived from their installation dates. Such type of data is called left censored observations. This section discusses the problem of estimating the insulator lifetime distribution from current status data.

3.4.3.2 Statistical Data Analysis

The data from actual inspection of insulators similar to that shown in Table 3.11 is considered for the analysis. The non-parametric estimates are first calculated by Maximum Likelihood method as discussed in Section 3.3.3.4. The plot on the survival probability estimates along with 95% confidence limits is shown in Figure 3.19.

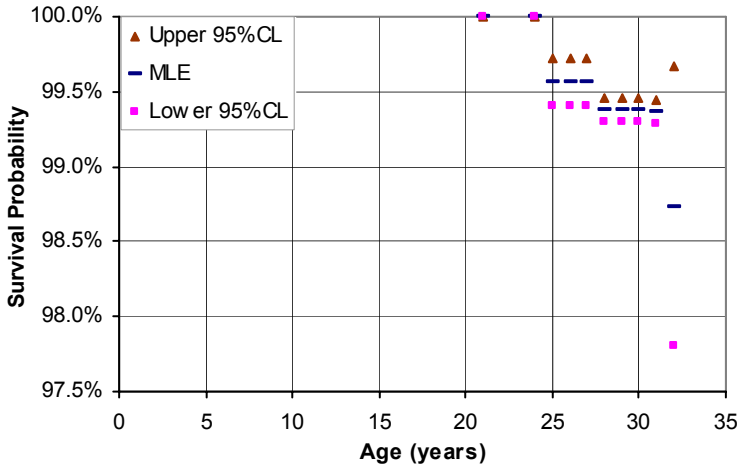

Figure 3.19: Non parametric MLE estimates of survival probabilities

The survival estimates of the insulators from Figure 3.19 are high indicating that the insulators have very high lifetime. The survival probability estimate for insulator age 32 years is 98.7% which is the oldest insulator in service. The parameters of Weibull distribution are estimated as discussed in Section 3.3.4.1. The maximum likelihood estimate in this case converged to a very high life expectancy of 521 years and C.O.V of 61%. Although there exists a local convergent solution with shape parameter as 5.27 and scale as 74.56 with life expectancy of 69 years and C.O.V of 22%. The reason for this discrepancy can be seen in Figure 3.20 where the MLE tries to fit observations collected in the early insulator lifetime.

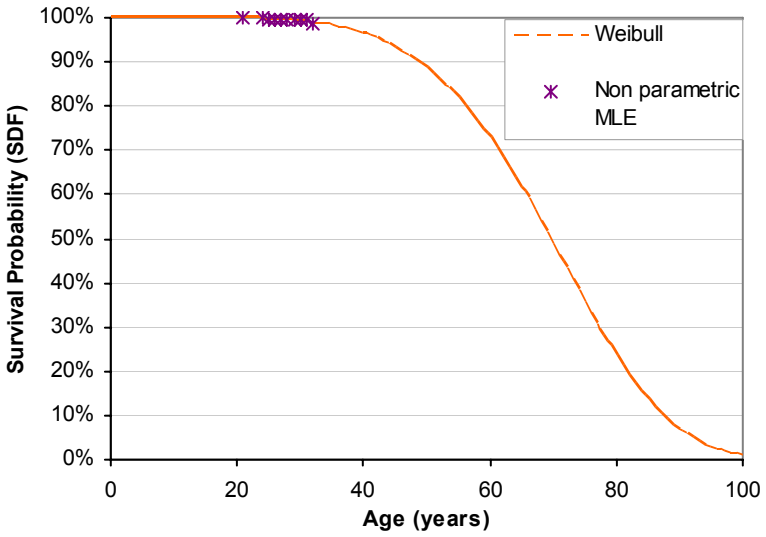

Figure 3.20: Weibull Survival Fit

It is therefore difficult to estimate a realistic parametric model with few observations in its initial lifetime. Parametric models are usually used to predict the remaining lifetime for maintenance decisions. In case of insulators as shown in Figure 3.20, many parametric models would be plausible and differ very much in the tail leading to different remaining life expectancy. Assuming Raleigh distribution resulted in a life expectancy of 320 years with C.O.V of 52.2% and parameters shape and scale are 2 and 365.23 respectively.

3.4.3.3 Remarks

The case of current status data obtained from field inspections from power utility is discussed in this section. Such data introduce a greater uncertainty in lifetimes of the components which can be estimated by maximum likelihood methods. The lifetime of the insulators are estimated to be very high from field inspection study. The few observations on insulator lifetimes create difficulty in estimating a reasonable parametric model and in predicting the remaining lifetime.

3.4.4 Analysis of Feeder Pipe Cracking

3.4.4.1 Summary of Data

The case study is from the inspection of 380 feeder pipes from a nuclear reactor. Feeder pipes are one of the critical components of primary heat transport system in nuclear reactor. The data consists of the time to crack detection of eight feeder pipes and time of last inspection for three of them. Out of the 8 feeder pipe cracks three are through wall cracks resulting in pipe leakage. Crack depth measurements on the 8 observations are used to estimate the growth rate (crack depth/detection time). Since the feeder pipes are not continuously monitored the growth of crack is assumed to follow linear growth model. The rest 372 pipes are still in service and have not shown any cracks.

Lifetime distribution model based on three leak observations and the rest 377 right censored observations is analyzed. Method of maximum likelihood assuming Weibull distribution resulted in life expectancy of 43 years and variance of lifetime as 95. The uncertainty in estimating the life expectancy is high due to sparse data on feeder lifetimes as shown in Table 3.12.

Table 3.12: Parameters of Weibull lifetime distribution

Model	Parameters	Estimate	Lower 95% CL	Upper 95% CL
Weibull	Shape (β)	5.06	1.65	15.54
	Scale (α)	47.06	15.82	139.98
	Mean Lifetime (μ_T)	43.24	15.58	120.04

This lifetime model ignores the fact that five feeder pipes having partial cracks. The problem can also be analyzed by modeling the crack growth rate. The problem is to estimate the lifetime distribution of pipe failure and annual probability of leak prediction in future time interval is discussed in the next section.

3.4.4.2 Statistical lifetime Model

One way to analyze the data is by estimating the uncertainty in crack growth rate by modelling the crack growth rate observations by Weibull distribution. The probability that a pipe with thickness h and with growth rate r fails at time t is given as $\Pr(t \times r \geq h)$, when growth rate follows a Weibull distribution with parameters (α, β)

$$\Pr\left(r \geq \frac{h}{t}\right) = \exp\left(-\left(\frac{h}{t} \times \frac{1}{\alpha}\right)^{\beta}\right) \tag{3.50}$$

$$F(t) = \exp\left(-\left(\frac{h}{t\alpha}\right)^{\beta}\right) \quad t > 0 \tag{3.51}$$

This shows that the derived distribution of t follows Inverse Weibull with parameters (h/α, β). The first moment or mean lifetime of the inverse Weibull is given as

$$\mu_t = \left(\frac{h}{\alpha}\right) \times \Gamma\left(1 - \frac{1}{\beta}\right) \tag{3.52}$$

The observations on growth rate are analysed by method of maximum likelihood to fit a Weibull distribution.

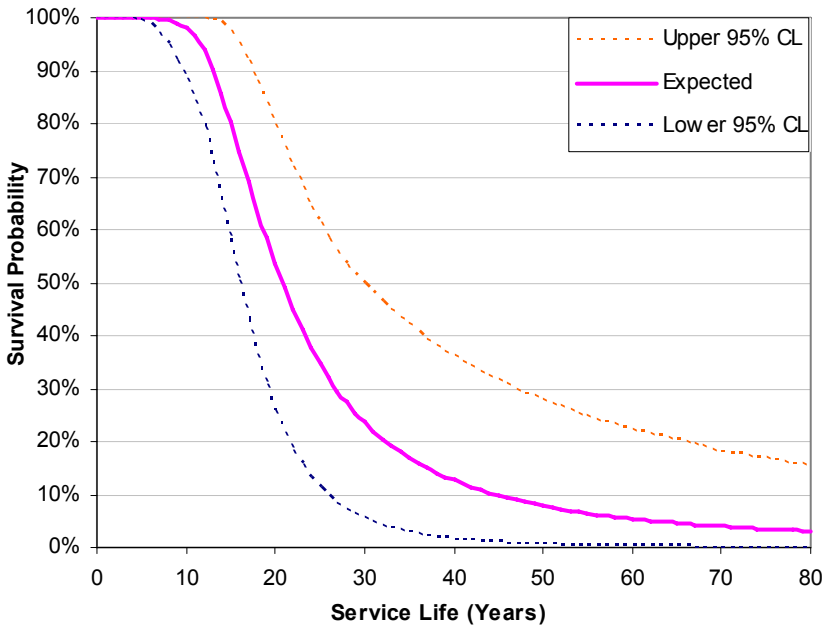

Figure 3.21: Survival Probability Curve of Feeder Lifetime

The parameters of the Weibull distribution for the growth rate model are calculated as (0.3844, 2.85). The probability of pipe failure follows inverse Weibull with parameters (18.21, 2.85) considering wall thickness of 7 mm. The survival probability plot along with 95% confidence limits is shown in Figure 3.21. The life expectancy of the feeder pipe is actually a function of wall thickness as shown in Eq.(3.52). With wall thickness of 7 mm, the life expectancy can be calculated from Eq.(3.52) as 25 years.

3.4.4.3 Probability of Failure Analysis

After estimating the lifetime distribution of the feeder pipes, the conditional probability of failure in future can be predicted. The probability that a feeder pipe following a lifetime distribution T fails in a particular year 't' given that it had survived until age x is given as

$$Ar(t) = \frac{S(t-1) - S(t)}{S(x)} \tag{3.53}$$

The above expression gives the annual probability of failure as a function of future year intervals. Considering lifetime of feeder pipe described by growth rate,

the annual probability of failure in future year intervals 21-40 years given that the population has survived at year 20 is calculated.

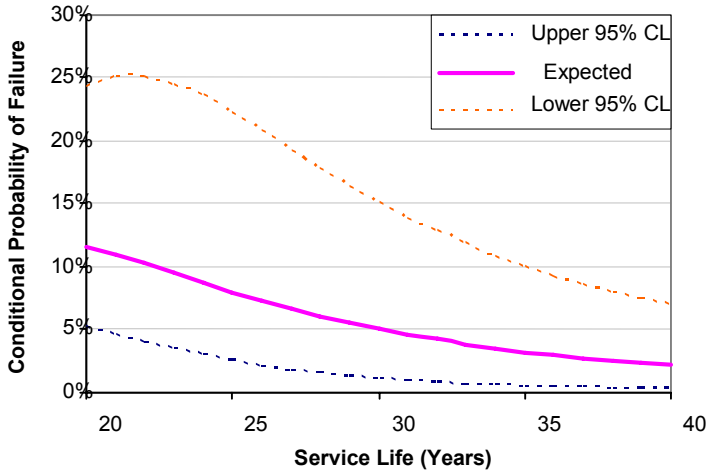

Figure 3.22 Probability of pipe failure in future operation

Figure 3.22 shows the annual probability of failure in future year intervals 21-40 along with 95% confidence bounds. The confidence limits show a higher uncertainty in estimating the annual risk due to very few observations. The annual probability of failure in future (conditioned on the information that the feeder pipe has survived at age 20 years) is relatively high (around 10%) in the initial period of operation but gradually decreases with time.

3.4.4.4 Remarks

The lifetime of feeder pipes is estimated from observed growth rates of feeder pipes. The distribution of pipe lifetime follows inverse Weibull assuming that the growth rate distribution follows Weibull. The uncertainty in rate of crack growth is assumed to follow a linear growth rate model. The annual probability of failure in the initial operation period is very high. It could be possible that the linear growth rate model estimates a higher feeder lifetime. The observations are also limited showing a greater uncertainty in estimating annual probability of failure.

3.5 Conclusions

It is not always possible to observe complete lifetimes through periodic inspections. In most cases, the observed lifetimes are either right-censored or interval-censored. The chapter presents statistical methods to analyze various types of incomplete data encountered from inspection of components in the energy industry. The effect of incomplete lifetime data in estimating the lifetime distributions is illustrated.

A comprehensive statistical analysis of realistic inspection data for estimating the lifetime distribution of wood pole distribution networks is discussed. The analysis concludes that the pole inspection data commonly collected by power utilities should be modeled as a combination of interval-censored and the right-censored sample of lifetimes. The analysis suggests that the pole survival curve is well approximated with the Weibull probability distribution, and from the data considered, the pole life expectancy is estimated at 69 years. The fitted distribution and life expectancy estimate are data dependent, although the methodology presented is general. A simplistic data analysis that ignores the censoring of lifetime can result in a severe underestimation of life expectancy.

In the case of oil circuit breakers, there is insufficient data to quantify the degradation. This is similar to the wood pole problem, in which the collecting of inspection data has lately started in the service of OCB and there is insufficient data to model the degradation by stochastic models. Lifetime models are therefore used in estimating the lifetime distribution, using condition data from selective intrusive inspections. The condition information on each task can be interpreted as censored and complete lifetimes. The lifetimes are assumed to follow Weibull distribution with linear failure rate (i.e shape parameter is fixed at 2) based on the preliminary assessment of maintenance data. The lifetime distribution in each task is estimated by the method of maximum likelihood. The estimated lifetime distributions suggest that there is a potential to increase the inspection interval from 7 years to 8 or 10 years, to achieve cost savings.

In case of electric insulators, the data obtained from power utilities is a snapshot of the state of insulators from a single inspection. The exact lifetimes of insulators are unknown, so the data type is therefore considered as current status. From the available data, the survival probability estimates of insulators are calculated to be very high. It is therefore difficult to estimate a realistic parametric model since the remaining lifetime of the current population is uncertain.

The feeder cracking problem is another case in which there are only three complete observations (leaks), and the rest as right censored. The life expectancy in such a case can be estimated as 43 years, but there is greater uncertainty in the estimate. The crack growth rate is of interest to engineers in feeder pipe life cycle management. The probability of failure due to through-wall leakage is of concern. The randomness in crack growth rate is used to derive the distribution of feeder lifetime. The lifetime distribution is derived as inverse Weibull, while the crack growth rate is assumed to follow Weibull distribution. The life expectancy is estimated to be 25 years, a value which keeps the current age of feeder pipe near life expectancy, leading to a higher annual probability of pipe failure after another five years.

The major contribution of the lifetime distribution chapter is to present the methodology for estimating realistic lifetime distribution from incomplete lifetime data usually obtained from field inspection studies in energy infrastructure. The chapter also discusses the difficulty in interpreting and estimating the lifetime distribution from highly censored observations.

CHAPTER 4
LCM MODEL USING LIFETIME DISTRIBUTIONS

4.1 Overview

This Chapter discusses the application of probabilistic models in equipment life cycle management. Firstly the age based replacement policy popular in energy industry is applied for wood pole management. The sequential inspection based component replacement models for a distributed population are illustrated. The effect of imperfect preventive maintenance on maintenance decisions is modeled using the concept of virtual age.

4.2 Age Based Replacement Policy

The age-based replacement policy is the conceptually simplest and an effective policy to implement in a system with large population of relatively inexpensive components (Barlow and Proschan, 1965). In this policy, a component is replaced at the age t_0 or at failure, whichever occurs first. The objective of the policy is to select the replacement age t_o that minimizes the life-cycle cost rate associated with the policy.

Consider the cost of preventive replacement as C_P, which includes the inspection, labour and equipment costs. An additional cost incurred due to failure is denoted as C_F, which includes additional costs due to power interruption and corrective repair to be done under an emergency.

According to the renewal theorem, the replacement age (t_o) should be selected to optimize the expected average cost rate, $Z(t_0)$, in a long run (Barlow and Proschan, 1965). The expected cost rate is defined as the ratio of the expected cycle cost to the expected cycle length:

$$Z(t_0) = \frac{E[C(t_o)]}{E[T_L)]} \tag{4.1}$$

where $C(t_o)$ is the life-cycle cost and T_L is the cycle length, defined as the time between replacements. It is a random variable that is related to the life time distribution and replacement age with cumulative distribution given as

$$F_{T_L}(x) = \begin{matrix} F_T(x) \\ 1 \end{matrix} \Bigg) \quad \begin{matrix} (x < t_o) \\ (x > t_o) \end{matrix} \tag{4.2}$$

The expected cycle length is obtained as

$$E[T_L] = \int_0^{\infty} (1 - F_{T_L}(x))dx = \int_0^{t_o} S_T(x)dx \tag{4.3}$$

The expected cost is derived as $\mathrm{E}[\mathrm{C}(t_o)] = C_P + C_F F_T(t_o)$. Finally, the expected cost rate is obtained as

$$Z(t_0) = \frac{C_P + C_F F(t_0)}{\int_0^{t_0} S_T(x)dx} \tag{4.4}$$

The optimum replacement time is determined by minimizing $Z(t_o)$ with respect to t_o as

$$\frac{dZ(t_0)}{dt_0} = 0 \tag{4.5}$$

which can be simplified to

$$S_T(t_0) + h(t_0)\int_0^{t_0} S_T(x)dx = 1 + \frac{C_P}{C_F} \tag{4.6}$$

where $h(t_o)$ is hazard rate at the replacement age. The optimum replacement age is the solution of Eq.(4.6) in terms of the cost ratio, C_P/C_F, and the survival function.

4.2.1 Wood Pole Replacement Problem

Figure 4.1 presents a generic plot of the optimal replacement age (t_{opt}) versus the cost ratio is obtained by numerically solving Eq.(4.6) and using the best-fit Weibull distribution derived for the three models discussed in Section 3.4.1.

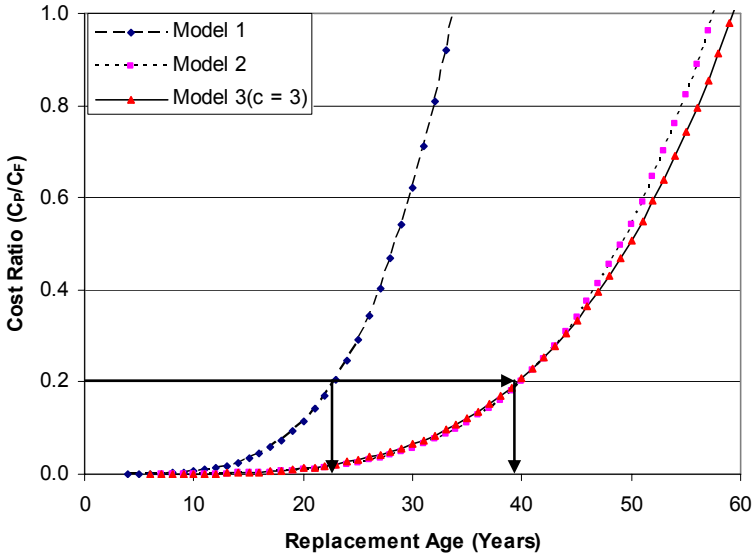

Figure 4.1: Optimal replacement age versus cost ratio

The use of this curve can be illustrated by an example. Typically, the preventive replacement cost of a wood pole is C_P = 1000 CAD$ and additional failure cost is C_F = 5000 CAD$. The optimal replacement age can be directly read from the plot for the cost ratio C_P/C_F = 0.2. The optimal replacement age obtained from Model 2 and 3 is 40 years, whereas Model 1 as expected provides a pessimistic estimate of 22 year. It is clear that an incorrect modeling of inspection data in Model 1 would lead excessively conservative replacement policy with very high refurbishment cost.

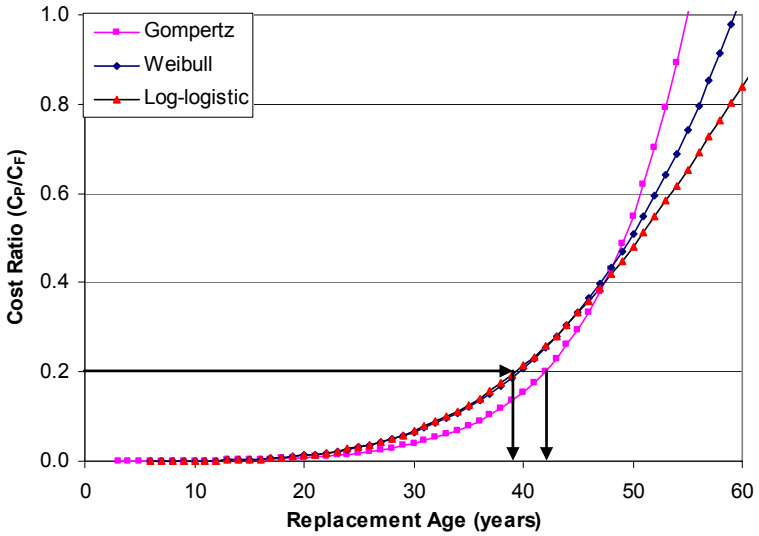

Figure 4.2: Optimal Age replacement policy for different distributions (Model 3, c=3)

The sensitivity of the replacement age to distribution type is illustrated in Figure 4.2 for Model 3. In the case of C_P/C_F = 0.2, the distribution type has a small influence on t_{opt}, which varies in a narrow range of 39 – 41 year. The reason for such observation is the survival curves of the distributions are not significantly different until age 50 years but differ significantly in the tail of survival curves. It is a remarkable that the optimization of replacement age (t_{opt}) is quite insensitive to the distribution over a practical and wide ranging values of the cost ratios, $0 < C_P/C_F < 0.6$. The distribution type matters more when the preventive cost is a large proportion of the failure cost ($C_P/C_F > 0.6$), though in such cases the age-based replacement policy may not be suitable.

4.2.1.1 Remarks

The analysis presents a generic method to optimize the age of pole replacement as a function of the life-cycle cost. For a cost ratio of C_P/C_F = 0.2, the optimal replacement age is estimated as 40 years. An interesting conclusion is that the type of lifetime distribution (Weibull, Gompertz or Log-logistic) has a limited sensitivity to the optimum replacement age and the expected life-cycle cost.

4.3 Sequential Inspection Based Replacement Model

4.3.1 Introduction

This section presents a risk based approach to manage components from a large distribution networks. Network components being large in number play a significant role in the overall Asset Management of the network system. Maintenance of such a large infrastructure is a major problem that the asset managers face in this competitive world. The population is so large that all components cannot be inspected in any one year due to a prohibitively high inspection cost and labour requirements. Therefore, there is need for the development of quantitative methods on decisions related to inspection and replacement strategies adopted by most network organizations.

The development of a probabilistic model for sequential inspection based maintenance program is addressed in this section. The impact of replacement strategies on life-cycle performance (i.e., risk and cost) is quantified. This analysis can then be used to optimize the maintenance interval and replacement rate in order to meet a performance target defined in terms the cost, risk or both cost and risk.

In summary, this section presents a complete probabilistic risk-based framework for life-cycle management of distribution networks. The approach has a significant potential in minimizing the maintenance cost and risk and improving asset management practices in general. The proposed model is generic, and is equally applicable to the asset management of large infrastructures.

4.3.2 Estimation of Substandard Component Population

A probabilistic method is presented to estimate the fraction of substandard components in the distribution network based on current component demographics and survival curve estimated from the inspection data.

The model predicts the component “failure rate”, which is the annual rate of components reaching the end of life in a specified year. The proportion of

substandard components in the distribution network is also estimated, which directly relates to risk of failure or vulnerability associated with the integrity of components in the network. The proportion of substandard components is essential to the assessment of life-cycle cost and reliability analysis. The proposed model will be applied to optimize component replacement strategies in the next section.

4.3.2.1 Model

The age-specific failure associated with a component of age X years in a future interval of t to $t+1$ year is estimated from the component survival curve, $S(t)$, as a conditional probability given as

$$\Pr(t \le T < t+1 \mid T \ge X) = M_X(t) = \left(\frac{S(X+t) - S(X+t+1)}{S(X)} \right) \tag{4.7}$$

An alternate expression for the conditional failure probability is given as

$$M_X(t) = \left(\frac{S(X+t)}{S(X)} \right) . (h(X+t)) \tag{4.8}$$

where the first term in the bracket is the probability of an age X component surviving up to age $X+t$, and the second term, $h(X+t)$, is the hazard rate at age $X+t$. The conditional failure probability in effect can be derived from the conditional life-time distribution given as

$$M_X(t) = \left(\frac{f_T(X+t)}{S(X)} \right) \tag{4.9}$$

where $f_T(x)$ denotes the component life-time density function.

A similar approach as shown in Eq. (4.7) is discussed by Li, et al., (2004) to predict the number of failures in a planning horizon. Since the population consists of components of different ages, as described by the age distribution, $f_A(x)$, the overall population failure rate in a future time interval t - t+1 year is obtained as

$$M_P(t) = \sum_{X=0}^{T} M_X(t) \times f_A(X) \tag{4.10}$$

The cumulative proportion of substandard components, referred to as vulnerability index (VI), in a time interval 0 (present) to *t* year is simply given by the summation of annual population failure rate over this interval

$$M_C(0,t) = \sum_{u=0}^{t} M_P(u) \tag{4.11}$$

4.3.2.2 Illustration of Conditional Failure Probability Estimation

The estimation of conditional failure probability of a 20-year component in future is considered. Since the component has survived up to age 20, the original life-time distribution (dotted curve) must be replaced with an updated conditional distribution as shown in Figure. 4.3 The bar at age 40-41 shows the conditional failure probability (4%) after 20 years, i.e., when the component age becomes 40 years. In simple terms, 4% of components at the current age 20 are expected to reach their end of life in a future interval in the 40th to 41st year.

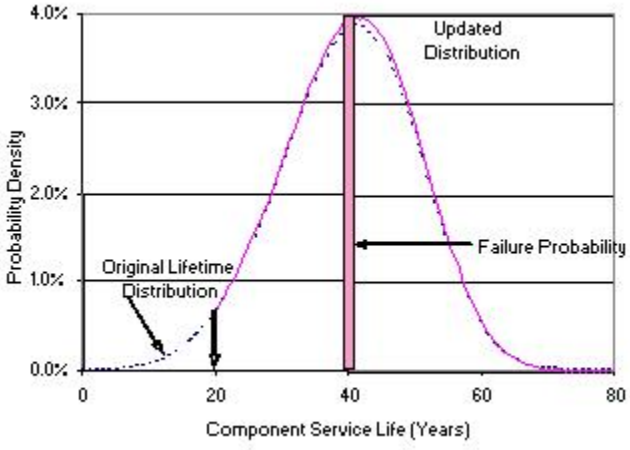

Figure. 4.3. Illustration of conditional failure probability estimation

4.3.2.3 Results

The estimates of cumulative number of substandard components as a percentage of the total component population are presented in Figure. 4.4 These results are obtained using the input data presented in Table 4.1

Table 4.1. Statistical input data for illustrative results

Item	Average (years)	Standard Deviation (years)	Distribution Type
Age Distribution	30	15	Weibull
Lifetime Distribution	40	10	Weibull

Figure. 4.4 show the substandard components in the population that are obtained from statistics from Table 4.1. The plot highlights the impact of component demographics on the number of substandard components in absence of an inspection and replacement program. For example, Figure. 4.4 show the total (cumulative) number of substandard components after 20 years is estimated as 70% on the basis of a component life expectancy of 40 years.

This analysis confirms the need for an effective inspection and replacement program to limit the number of substandard components to an acceptable level.

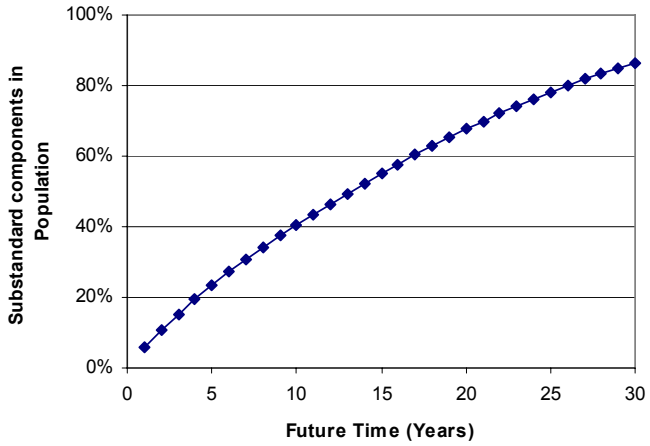

Figure. 4.4. Future projection of substandard components in the population

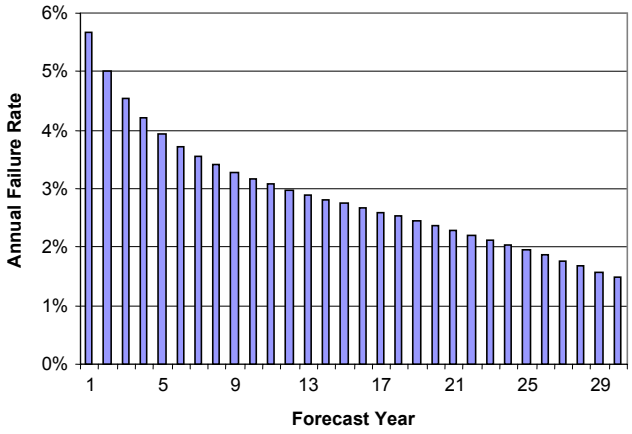

Figure. 4.5. Annual failure rate in component population

The analysis model can be used to provide further insight into component aging and failure rate. Considering the life expectancy as 40 years, the annual conditional failure rates are projected in Figure. 4.5 In early years, the conditional failure rate ranges from 3%-6%, but it declines rapidly after 20 years. The decline is due to the fact that most aged components have already vanished from the population leaving behind a much smaller cohort of relatively young components. In this analysis, component replacement is not considered. The analysis with component replacement is discussed in Section 4.4 using renewal theory.

4.3.2.4 Summary

A probabilistic model is presented for the estimation of the fraction of substandard components as well as the annual conditional failure rate.

From the point of view of the risk of line failure, the cumulative (total) number of substandard components is relevant. The conditional failure rate on the other hand plays a role in the estimation of replacement rate, as shown in the next section.

The number of substandard component is projected, which underscore the need for an effective component replacement program. Otherwise, the substandard component population would become so large that it would reduce

distribution network reliability and overwhelm maintenance activities in the future.

4.3.3 Probabilistic Asset Management Model

To maintain reliability of the distribution system network, an effective program for the replacement of substandard components is necessary. The replacement program has two main elements, namely the inspection interval and the component replacement rate.

The section presents a probabilistic model to quantify the impact of the inspection interval and the annual component replacement rate, and relates these to limiting the risk that the substandard components in the population may pose to the system. A sequential inspection based replacement strategy is discussed in this section. This analysis is essential to support the life-cycle cost estimation model presented in the next section.

4.3.3.1 Model for Sequential Inspection and Replacement Program

This section presents a conceptual model of the sequential inspection and replacement program. A sequential program means that only a part of the component population is inspected in a given year, such that it takes T years to complete the inspection of the entire population. It is in contrast with maintenance strategies used in other industries (e.g., aerospace and chemical), in which an entire component population is inspected in a given year of inspection.

To illustrate the concept of the sequential program, consider the case of a 5-year inspection cycle as shown in Figure 4.6. To begin with (year 0), the distribution component population is basically divided into 5 blocks, and one block will be sequentially inspected each year. Substandard components found during an inspection will be replaced by new components (age 0). It means that component replacement takes place in the population block under inspection only.

In year 1, block-1 is inspected and due to component replacement, the average component age is reduced and its age distribution is modified. Population blocks 2-5 are unattended.

In year 2, block-2 is subject to inspection and replacement, and blocks 1, 3-5 are unattended. The substandard components continue to accumulate in blocks 3-5.

In year 3, block-3 is subject to inspection and replacement work. Components in block 4-5 are not inspected so far. Furthermore, previously inspected blocks 1-2 experience progressive aging as well. However, the conditional failure rate in previously inspected blocks is expected to be smaller than that in non-inspected blocks. The difference between the two depends on the replacement rate during the inspection.

The process continues as shown in Figure 4.6, and all the blocks are inspected at the end of year 5. However, substandard components are not completely eliminated from the population due to progressive component aging in previously inspected blocks 1-4.

The inspection cycle continues to be repeated over the forecast period, typically 30 years.

Inspection Year	Category	Component Population Blocks
0	Non-Inspected Population Blocks	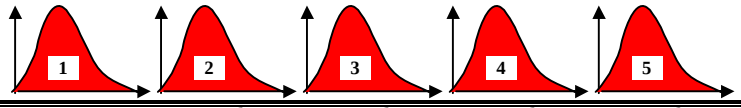
1	Non-Inspected Population Blocks	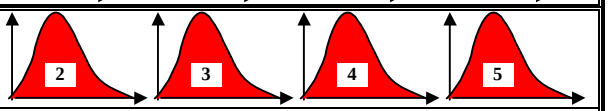
	Currently Inspected Block	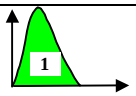
2	Non-Inspected Population Blocks	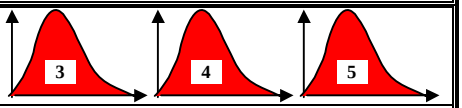
	Currently Inspected Block	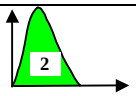
	Previously Inspected Blocks	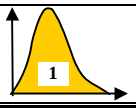
3	Non-Inspected Population Blocks	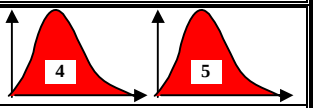
	Currently Inspected Block	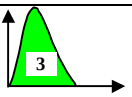
	Previously Inspected Blocks	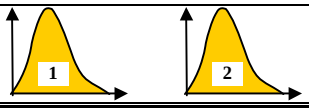
4	Non-Inspected Population Blocks	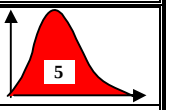
	Currently Inspected Block	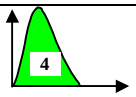
	Previously Inspected Blocks	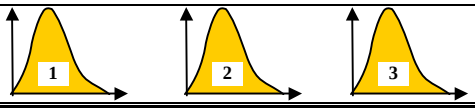
5	Non-Inspected Population Blocks	
	Currently Inspected Block	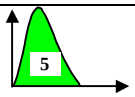
	Previously Inspected Blocks	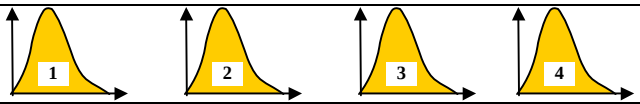

Figure 4.6: Illustration of component inspection and replacement strategy

4.3.3.2 Computation

In a distribution network, consider that the total number of components to be managed is *M*. It is planned to inspect these components over an *T* year inspection interval, so that the component population is divided into *T* blocks. The number of components in each block is $N = M/T$. The component sample size for annual inspection is $N_I = N$. The component replacement is carried out based on their condition. The blocks are inspected sequentially, and it takes *T* years to inspect the population completely. Considering a forecast period of T_F (= 30 years), the number of inspection cycles = T_F/T.

The probabilistic analysis model is developed to estimate:

(1) The number of remaining substandard components in the component population for a chosen inspection interval (*T* years). It is a proxy measure of residual risk or vulnerability to failure in the distribution network.

(2) The component replacement rate in any given year, which is needed to compute the cost of component replacement.

The proportion of components of age X_k in k^{th} block turning into substandard state in an interval $t_1 - t_2$ years is defined as

$$P_S(X_k, t_1, t_2) = \left(\frac{S(X_k + t_1) - S(X_k + t_2)}{S(X_k)} \right) \times f_A(X_k) \tag{4.12}$$

where $f_A(X_k)$ denotes the component age distribution at the time of reference *t* in a component block. Recall that *S(t)* is the survival probability.

The fraction (%) of substandard components in a k^{th} block is given as

$$D_S(k, t_1, t_2) = \sum_{X=1}^{100} P_S(X_k, t_1, t_2) \tag{4.13}$$

The total number of substandard components in the entire population is the sum of rates of substandard components over T blocks:

$$N_S(t_1, t_2) = N \sum_{k=1}^{T} D_S(k, t_1, t_2) \tag{4.14}$$

The fraction of substandard components in the entire distribution population is given as

$$Q_S(t) = \frac{N_S(T_{i-1}, t)}{M} \tag{4.15}$$

Note that $T_0 = 0$.

The number component replacement in a given year is an important input parameter for the cost analysis. If a population block were to be inspected in year $t_2 = t$, the replacement rate with reference to the time of the previous inspection, $t_1 = T_{i-1}$, is estimated as

$$D_R(k,t) = D_S(k, T_{i-1}, t) \tag{4.16}$$

The number of component replacements for the entire population is given as

$$N_R(t) = N\sum_{k=1}^{T} D_R(k,t) \tag{4.17}$$

The population wide replacement rate is estimated as

$$Q_R(t) = \frac{N_R(t)}{M} \tag{4.18}$$

Since substandard components are replaced with new components at the time of inspection T_i, the age distribution of the component block population must be updated. Firstly, the age distribution is corrected to reflect the removal of substandard components from different age groups:

$$f_A(X, T_i) = f_A(X, T_{i-1}) - P_S(X, 0, T_i) \tag{4.19}$$

Despite the conceptual simplicity of this model, the computer implementation is somewhat involved due to the following reasons. The progressive aging of multiple component block populations has to be tracked over the forecast period. Furthermore, each block population has to be updated at the time of inspection. Updating the population has to be repeated several times over the forecast period. Because of the time-dependent nature of the problem, the number of substandard components and replacements is variable over time and population block.

4.3.3.3 Replacement Strategy

In this strategy, only those components are replaced that are determined to be in substandard condition through inspection. This approach is economically beneficial because unnecessary component replacements are avoided. However, this approach has a drawback in case of a long inspection interval combined with an aged component population. The drawback is that it replaces substandard components that are present in the population only, but ignores components that have potential to reach end of life during the inspection interval. In summary, this strategy may not be effective when the inspection interval is long.

4.3.3.4 Results

4.3.3.4.1 General

The section illustrates the effect of the inspection interval (cycle length) affects on the remaining number of substandard components, an indicator of risk, and the replacement rate, a measure of cost of replacement program.

Table 4.2 describes three scenarios of the inspection program. The results are obtained corresponding to the component life expectancy of 40 years.

Table 4.2. Inspection interval date for component replacement program

No	Forecast Duration (T_F years)	Inspection Interval (T year)	Inspection Cycles (T_F/T)	Inspection Sample (%of population/year) (100/T%)
1	30	5	6	20%
2	30	15	2	6.67%
3	30	25	1	4%

4.3.3.4.2 Estimation of Remaining Substandard Poles

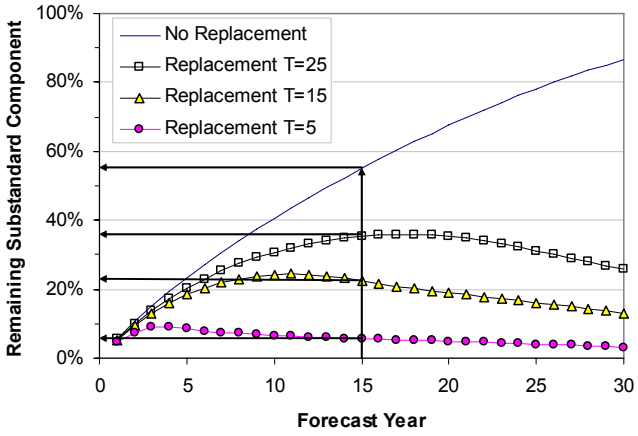

Figure. 4.7. Remaining substandard components

Figure. 4.7 show the effect of the inspection/replacement interval on the number of remaining substandard components as a percentage of the entire component population. It is obtained using the component life expectancy of 40 years. In absence of a replacement program, the number of substandard components would increase rapidly. In a 30 year period, almost 90% of population would turn into a substandard state. A 15-year program can eliminate almost 80% of substandard components in a 30-year period. Naturally, the number of substandard components decreases as the inspection/replacement interval decreases (i.e., more frequent inspections). It however has an implication on the maintenance cost, which is discussed in the next section.

4.3.3.4.3 Estimation of the Replacement Rate

An important parameter for life-cycle cost estimation is the number of component replacements that are expected under different inspection interval (T). The effect of the replacement rate with the inspection interval is shown in Figure. 4.8.

Initially the replacement rate in the 5-year program is the high due to frequent inspections and higher sample size. It however, declines after 10 years since population is substantially renewed in the first phase (t<10 years). The replacement rate picks up again after 25 years thereby reflecting the population aging effect.

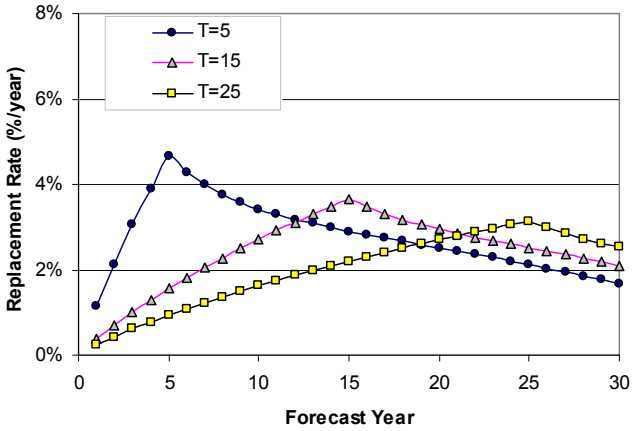

Figure. 4.8. Estimation of component replacement rate

In the 15 year program, the replacement rate continuously increases in the fist cycle (t ≤15 year) and reaches the peak value of 3.5%. In the second phase, however, the replacement rate levels off at about 2%/year value.

4.3.3.4.4 Summary

The section presents a probabilistic model for the sequential inspection based component replacement program. The model provides estimates of the remaining number of substandard components, an indicator of risk, and the replacement rate, a measure of the cost of the replacement program. The model illustrates the effect of inspection interval and component life expectancy on these two parameters. The model is the basis for life-cycle risk and cost analysis presented in the next section.

4.3.4 Life-Cycle Risk and Cost Estimation

The section presents a model for estimating the life-cycle risk and costs associated with the management of the distribution component asset. This model would allow the optimization of the replacement program for minimizing the cost and achieving a target reliability level.

4.3.4.1 Life-Cycle Risk

The substandard components are more vulnerable to failure under adverse weather conditions or an accidental overload. Therefore, as the number of substandard components increases in the distribution network, the risk of unexpected component failure also increases with it. In other words, the risk of component failure interrupting the electricity supply to customers is directly proportional to the number of substandard components in the population, which can be estimated from the model presented in this section.

The actual probability of failure of a substandard component is rather difficult to estimate. Nevertheless, an average probability of failure can be roughly estimated from the currently available component failure data.

Considering that approximately 250 component failures per year are currently attributed to substandard component, and that there are approximately 6% substandard components in 1.5 million distribution component population. The probability of failure is therefore estimated as $P_F = 250/(0.06 \times 1.5 \times 10^6) = 2.77\times10^{-3} \approx 3\times10^{-3}$ /substandard component/year. This estimate can be refined by a formal statistical analysis of historical component failure data and conducting a reliability analysis of component structure.

Conceptually, the annual rate of component failure in a forecast year t is estimated as

$$Q_F(t) = Q_S(t) \times P_F \tag{4.20}$$

where $Q_S(t)$ is the total fraction of substandard components in the distribution population as given by Eq.(4.15).

The economic cost of a component failure (C_F \$/component) includes the cost of emergency component replacement as well as the cost of supply interruption. The annual risk associated with an aging network is estimated as

$$R_F(t) = C_F Q_F(t) \tag{4.21}$$

4.3.4.2 Life-Cycle Cost

The life-cycle cost includes both maintenance cost and risk. The maintenance cost has two major components:

- Inspection Cost (C_I). It mainly involves the labour cost of inspecting a component visually.
- Preventive Replacement Cost (C_R). It is the cost of planned (preventive) replacement of a substandard component, which includes the cost of component and labour.

For a population of M components that is subject to an inspection and replacement cycle of T years, the annual maintenance cost (C_M) per component in a forecast year t can be estimated as:

$$C_M(t) = C_I Q_I + C_R Q_R(t) \tag{4.22}$$

where Q_I is the inspection sample expressed as a % of total population = $100/T$ %. The annual life-cycle cost (C_T \$ per component) in a forecast year t can be estimated as:

$$C_T(t) = C_M(t) + R_F(t) \tag{4.23}$$

Note that annual risk $R_F(t)$, is computed from Eq.(4.21).

The net present value of life cycle cost over a period of Y years is obtained as

$$C_{NP} = \sum_{t=1}^{Y} \frac{C_T(t)}{(1+r)^t} \tag{4.24}$$

where r is the annual interest rate.

4.3.4.3 Results

To illustrate the proposed model, life-cycle cost is estimated using the cost data shown in Table 4.3. All cost estimates are presented in a normalized form as \$ per component in a forecast year.

Table 4.3. Cost input data

Item	**Cost ($/component)**
Inspection Cost (C_I)	50
Preventive Replacement Cost (C_R)	1000
Failure Cost (Emergency Replacement Cost C_F)	6000
Failure Probability Estimate (P_F)	3×10^{-3}

The effect of replacement interval or inspection frequency on life cycle costs can be studied by applying the methodology described in Section 4.3.3 & 4.3.4. Firstly the annual maintenance cost over the forecast period calculated using Eq.(4.22) is shown below.

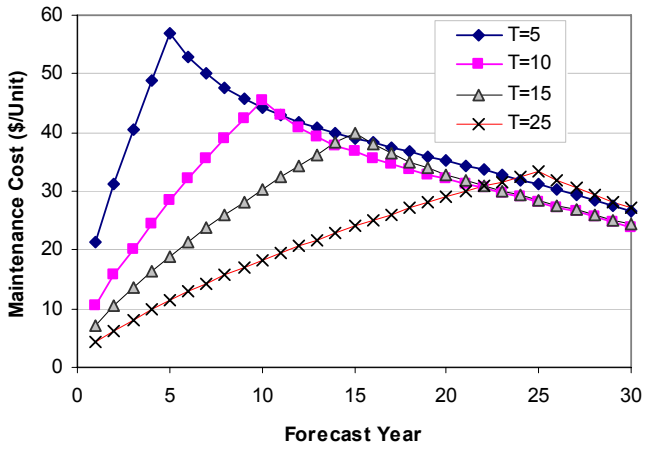

Figure. 4.9. Maintenance cost vs. inspection interval T

The maintenance cost decreases as the inspection interval (T) is increased from 5 to 25 years Figure. 4.9. The reason for such trend can be seen from Figure. 4.8, as the replacement rate decreases with increase in inspection interval.

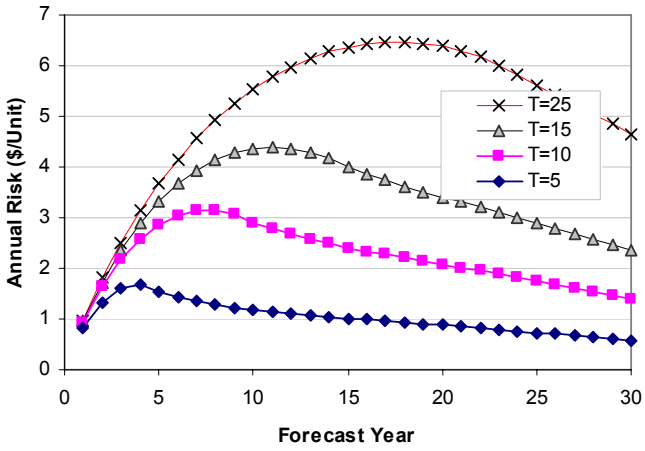

Figure. 4.10. Risk vs inspection interval T

The annual risk increases with increase in inspection interval as shown in Figure. 4.10. Because longer interval means a larger number of substandard components are vulnerable to failure. It must be stressed that the risk estimates are highly sensitive to the annual probability of failure of a substandard component, which is taken as 3×10^{-3} per year.

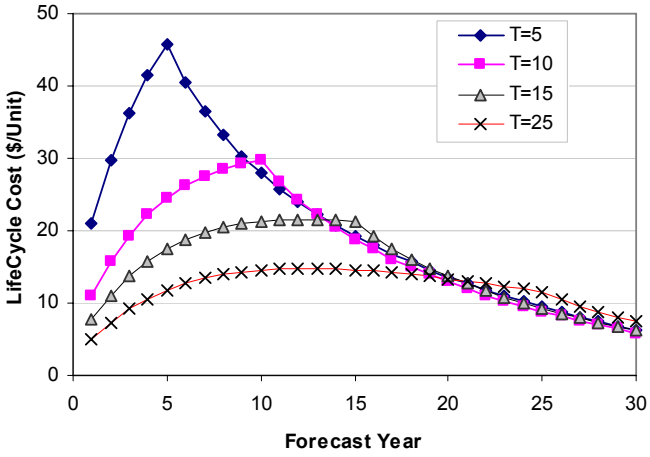

Figure. 4.11. Life cycle cost vs inspection interval T

The variation of life cycle cost, which is a sum of the maintenance cost and risk Eq.(4.23), and its net present value is shown in Figure. 4.11, which is qualitatively similar to the variation of maintenance cost shown in Figure. 4.9.

The reason is that the risk estimates typically ranging from \$2 - \$7 are much smaller in comparison to the maintenance cost, which is of the order of \$10 - \$60.

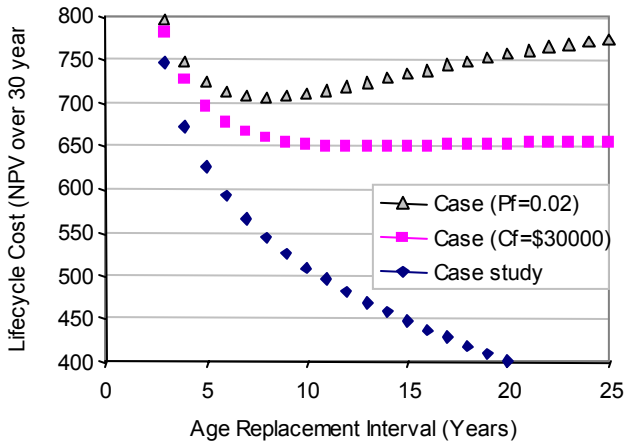

Figure. 4.12. Net present value (NPV) of life cycle costs for various cases

The net present value (NPV) of life cycle costs over a period of 30 years is illustrated here using Eq.(4.24). For the illustration purpose the annual interest rate is taken as 5%. For the case study considered as in Table 4.3 the net present value of the lifecycle costs over 30 year period is shown in Figure. 4.12. The NPV decreases with increase in replacement interval which suggests that higher replacement interval is more economical. Although these cost estimates are crucially dependent on input data, the risk (Figure. 4.10) appears to be smaller than the cost of maintenance (Figure. 4.9) program in this example. This observation underscores the need for a formal cost benefit analysis before implementing a particular maintenance strategy.

Considering another case by changing the cost ratios, in this case considering $C_F = 30000$ and conducting the lifecycle cost analysis as in Eq.(4.24). The net present worth over a period of 30 years with replacement interval is shown in Figure. 4.12. In this case the higher failure costs have an effect on lifecycle costs. Figure. 4.12 suggests that the lifecycle costs decreases with replacement interval and have a minimum and again increases. The observation for this example

suggests that there is an optimal replacement interval of 13 years based on minimum life cycle costs for maintenance.

It has been shown that the risk estimates are also sensitive to the annual probability of failure, another case is considered where the annual probability of failure of a substandard component as 2×10^{-2}. Similar calculations on lifecycle costs from Eq.(4.24) is done using the same input data from Table 4.3. The plot on lifecycle cost over a period of 30 year is shown in Figure. 4.12 with replacement interval on x-axis. The lifecycle costs here have a interesting profile and suggests an optimal replacement interval of 8 years. In this example for lower replacement interval the replacement costs dominate but in the later part when the replacement interval is high the failure costs dominate.

4.3.4.4 Summary

A probabilistic model is presented for the estimation of maintenance cost, risk and life-cycle cost associated with a maintenance program that involves sequential inspection based component replacement strategy.

As a general rule, increasing the inspection interval decreases the maintenance cost at the expense of increasing risk.

The time-dependent variation of life-cycle cost depends on the relative magnitude of risk and cost over time.

The ratio of component failure cost to replacement cost (C_F/C_R) is a critical parameter. The cost ratio should be sufficiently high, otherwise the benefit of the maintenance program would be less than the associated cost.

The risk and cost estimates presented here are considered illustrative, the input data pertaining to costs of inspection, replacement and failure of a distribution component can be arrived from field experts to get a more meaningful results. The estimation of probability of component failure must be refined through the statistical analysis of historical component failure data and/or structural reliability analysis of component structure.

4.4 Model Based on Renewal Theory

4.4.1 Introduction

A probabilistic method proposed by Van Noortwijk and Klatter, (2004) is presented to estimate the fraction of substandard component replacement in the distribution network based on current component demographics and lifetime distribution estimated from the inspection data. The results are then compared to the non-renewal case developed in Section 4.3.2.

The component replacement is assumed to follow discrete renewal process. The probabilistic method predicts the expected number of component replacements per unit time, which is the annual rate of components reaching substandard state in a specified year. The assumptions in renewal process for replacements are that the substandard components are detected and replaced in a short period.

A discrete renewal process $\{N(t), t=1,2,3,\ldots\}$ is a non-negative integer-valued stochastic process that registers the successive renewals in the time interval $(0, t]$. The renewal times T_1, T_2, $T_3,\ldots$, is assumed to be non-negative independent and identically distributed with discrete probability function given as

$$\Pr\{T_k = i\} = p_i = F(i \mid a,b,0) - F(i-1 \mid a,b,0) \tag{4.25}$$

$i = 1,2,...$, where p_i represents the probability of a renewal in unit time i. This probability function is a discrete Weibull distribution. The conditional probability that the life time X exceeds x given $X>y$ is given as

$$P\{X > x \mid X > y\} = 1 - F(x \mid a,b,y) = \exp\left\{-\left[\frac{x}{b}\right]^a + \left[\frac{y}{b}\right]^a\right\} \tag{4.26}$$

The probability of a renewal of an aged component in future time x with current age y can be calculated using Eq. (4.26). The expected number of renewals for a new component is given as a recursive equation according to Van Noortwijk (2003)

$$E[N(n)] = \sum_{i=1}^{n} p_i \left[1 + E[N(n-i)]\right] \tag{4.27}$$

for $n = 1,2,3,...$ and $N(0) \equiv 0$. This equation is based on the condition that the first renewal occurred at time T_i. The expected long term average number of renewals per unit time is given as

$$\lim_{n\to\infty} \frac{E[N(n)]}{n} = \frac{1}{\sum_{i=1}^{\infty} i p_i} = \frac{1}{\mu} \tag{4.28}$$

which is the reciprocal of mean lifetime μ. As $n \to \infty$, the expected long term average cost per unit time approaches c/μ, where c is the cost associated with each renewal and is assumed as constant with time. The developed methodology can also be extended for a component which has aged $y \geq 0$. The probability distribution of residual lifetime can be discrete as

$$\begin{aligned} P\{T = i \mid y\} &= q_i(y) \\ &= F(y+i \mid a,b,y) - F(y+i-1 \mid a,b,y) \end{aligned} \tag{4.29}$$

for $i = 1,2,3,....$ The expected number of renewals in the time interval (0, n] when the first component has age y is given as

$$E[\tilde{N}(n,y)] = \sum_{i=1}^{n} q_i(y)\left[1 + E[N(n-i)]\right] \tag{4.30}$$

where $E[N(n)]$ is given by Eq. (4.27). and $\tilde{N}(n,y)$ is called the delayed renewal process since the process starts at component age y. The expected cost of replacement from an aged population with current component ages $y_1,...,y_m$ can be obtained as

$$E[K(n)] = \sum_{j=1}^{m} c_j E[N(n,y_j)] \tag{4.31}$$

where c_j is the cost of replacing the j^{th} component. The expected cost of component replacement in unit time i can be obtained as

$$E[K(i)] - E[K(i-1)],\ i = 1,...,n \tag{4.32}$$

For a unit cost of component replacement, Eq. (4.32) gives the rate of component replacement per unit time.

4.4.2 Results

Considering the population demographics and the estimated lifetime distribution as presented in Table 4.4, the replacement cost of the population per unit time in future can be calculated.

Table 4.4. Statistical input data for illustrative example

Item	Average (years)	Standard Deviation (years)	Distribution Type
Age Distribution	30	15	Weibull
Lifetime Distribution	40	10	Weibull

The average age of the remaining population is 30 years and the average lifetime of the component is 40 years. Assuming that all age components are replaced with a new component with unit cost (c=1). The expected replacement cost per unit time or the expected number of renewals per unit time for the population can be calculated from Eq. (4.32) which is shown in Figure 4.13. The year zero is the current year and Figure 4.13 shows the predictions for a forecast period of 150 years. Figure 4.13 shows the expected cost of replacement per year for the population as a function of current component age.

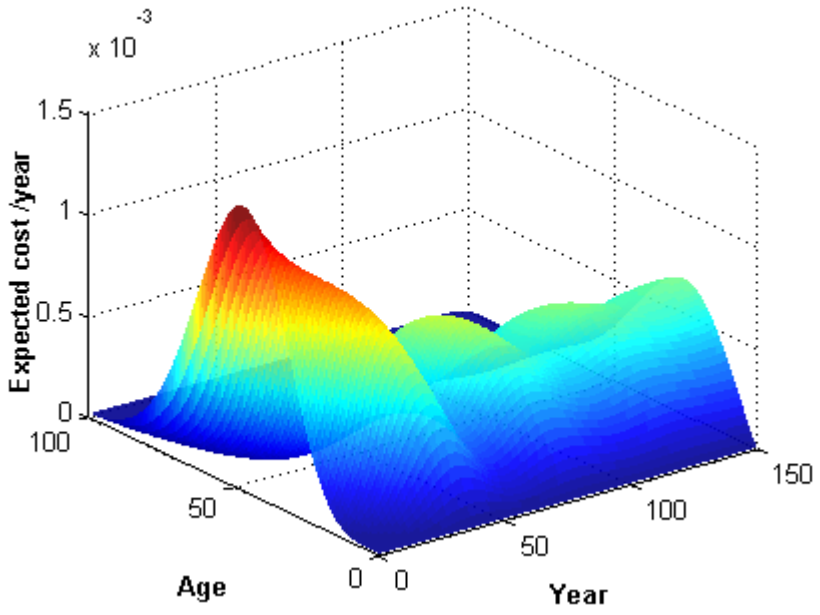

Figure 4.13: Expected cost of replacements per year as a function of age

The expected cost of replacements over all ages is shown in Figure 4.14. Figure 4.14 shows the expected cost of replacements per year over all ages of the population. The uncertainty in second replacement time is greater than the uncertainty in first replacement time. This kind of replacement is also termed as corrective replacement. The annual rate and hence the cost of corrective replacement policy can be shown by Figure 4.13 & Figure 4.14. It can be shown from Figure 4.14, that the expected number of replacements per year converges to 0.025 which is equal to the expected long term average number of replacements ($1/\mu=0.025$) as given in Eq. (4.28).

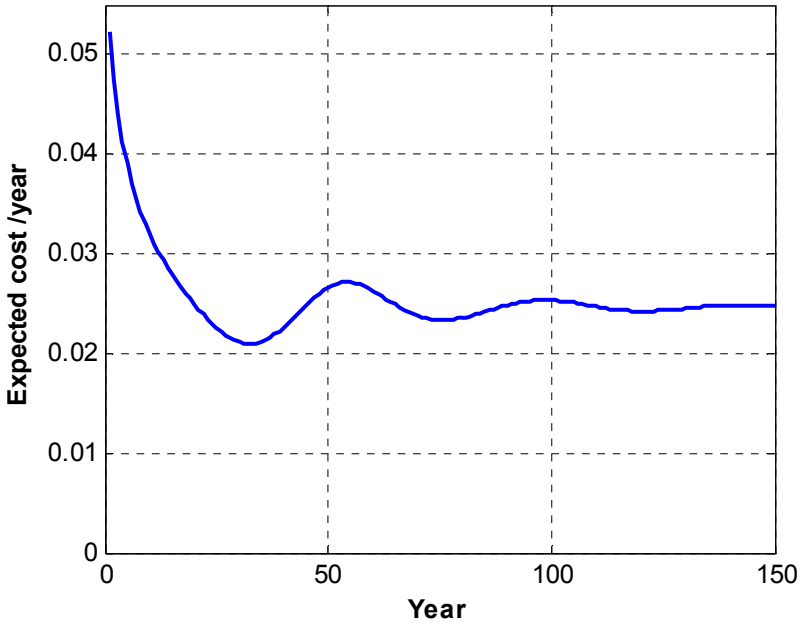

Figure 4.14: Expected cost of replacements per year among all ages

It is interesting to compare the result in Figure 4.14 to the non-renewal case shown in Figure. 4.5, since they predict the same replacement rate until around 20 years. The expected replacement rate decreases as the population ages but increases later with failure from first renewals and then converges to a constant replacement rate with subsequent renewals. Whereas in non-renewal case (Figure. 4.5) the expected replacement rate decreases as there are no renewals.

4.4.3 Summary

A probabilistic model is presented for the estimation of the annual replacement rate of the population and the expected replacement cost per unit time. The component replacements are modeled as a renewal process, where a substandard component is replaced by a new component. For the component maintenance management, the annual rate of replacement and hence the replacement costs per year are crucial in optimizing the maintenance actions by minimizing the life cycle costs.

4.5 Imperfect Preventive Maintenance

4.5.1 Background

Let a component with lifetime variable "*T*" be maintained to reduce the risk of failure. To minimize the risk of failure, preventive maintenance is performed at regular intervals. There are two kinds of preventive maintenance (PM), namely proactive and reactive. Proactive preventive maintenance (PPM) is done before the initiation of degradation such that the time of initiation is delayed. Reactive preventive maintenance (RPM) is done after the initiation of degradation such that the rate of degradation is reduced. In this section RPM is discussed in the case of component maintenance optimization. Essential maintenance or refurbishment is done after a component has failed. Generally, the cost of refurbishment is very high compared to the cost of PM. Therefore, PM actions are necessary to reduce the cost of refurbishment. If PM actions are more frequent maintenance costs increases, thereby reducing the refurbishment costs. Likewise, when PM actions are less frequent, maintenance costs are less but refurbishment costs increase. Therefore, there is a need for optimizing the number of PM actions over a component lifetime.

With preventive maintenance (RPM), a component is either as good as new (Perfect PM) or the rate of degradation is reduced (Imperfect PM). In case of perfect PM, the degradation of the component starts as if the component is new, this need not be true in reality. The effect of imperfect PM can be modeled as a virtual age model with a degree of imperfection (γ). Maintenance generally refers to as preventive maintenance in subsequent sections.

4.5.2 Virtual Age Model

A component with lifetime distribution $F_T(t)$ is considered by periodically maintaining at intervals t_p . After the first preventive maintenance, the degradation of the component is reduced by the introduction of a virtual age to the component. The concept of virtual age has been thoroughly discussed in the

literature and has its applications in a variety of probabilistic models (Pham and Wang, 1996). The virtual age after first maintenance action $v_1(t)$ is given as

$$v_1(t) = t - (1-\gamma)t_p \qquad t_p < t < 2t_p \tag{4.33}$$

where t_p is the time of first maintenance and γ is degree of maintenance imperfection ($0 \le \gamma \le 1$). In case of perfect maintenance (i.e γ=0), the virtual age $v_1(t) = t - t_p$ starts from zero age. In case of no maintenance (i.e γ=1), the virtual age $v_1(t) = t$ is the same as the component age *t*. The virtual age model can then be used to derive the component survival function as

$$\begin{aligned} S_{t_p}(t) &= \exp\left(-\int_0^{t_p} h(u)du - \int_{v_1(t_p)}^{v_1(t)} h(u)du \right) \\ &= \exp\left(-\int_0^{t_p} h(u)du \right) \times \exp\left(-\int_{\gamma t_p}^{v_1(t)} h(u)du \right) \qquad t_p < t < 2t_p \\ &= S_T(t_p) \times \frac{S_T(v_1(t))}{S_T(\gamma t_p)} \end{aligned} \tag{4.34}$$

where $S_T(t)$ is the component survival function without maintenance. When there is no maintenance done on the component (i.e γ=1), the survival function results in $S_{t_p}(t) = S_T(t)$, the original survival function. In the case of perfect maintenance (i.e γ=0), the survival function is given by

$$S_{t_p}(t) = S_T(t_p) \times S_T(t - t_p) \tag{4.35}$$

The methodology can be generalized for any number of preventive maintenance actions over the lifetime of the component. The virtual age of the component after *j* number of maintenance actions can be given as

$$v_j(t) = t - (1-\gamma) j t_p \qquad j t_p < t < (j+1)t_p \tag{4.36}$$

The component survival function after *j* number of preventive maintenance actions can be derived in the same way as done in Eq(4.34).

$$S_{t_p}(t) = \left\{ \prod_{i=1}^{j} \frac{S_T\left([1+(i-1)\gamma]t_p\right)}{S_T\left((i-1)\gamma t_p\right)} \right\} \times \frac{S_T(v_j(t))}{S_T(j\gamma t_p)} \qquad j t_p < t < (j+1)t_p \tag{4.37}$$

When there is no maintenance done on the component (i.e γ=1), the survival function results in $S_{t_p}(t) = S_T(t)$, the original survival function. In the case of perfect maintenance (i.e γ=0), the survival function after j^{th} PM is given by

$$S_{t_p}(t) = \left[S_T(t_p)\right]^j \times S_T(t - jt_p) \tag{4.38}$$

The survival probability as shown in Eq. (4.38) is greatly improved with frequent preventive maintenance when compared with no maintenance. Even with frequent preventive maintenance actions the survival probability decreases with time but rather slowly as compared to no maintenance.

The effect of imperfect preventive maintenance on survival probability is derived as in Eq. (4.37) and is very useful in maintenance optimizations decisions. The application of imperfect maintenance in maintenance optimization is illustrated by an example in the next section.

4.5.3 Illustrative Example

To illustrate the effect of imperfect preventive maintenance on component survival probability, a component with a mean lifetime of 36 years following Weibull distribution with shape parameter 3 and scale parameter 40 is considered. The component is maintained periodically at the interval (t_p) of 10 years. Three scenarios of imperfect maintenance are considered here. In the first case, the component is maintained perfectly (i.e γ=0), the second case when the component is maintained imperfectly with γ=0.2 and the third when no maintenance work is done (i.e γ=1). For all the three cases the survival probability function is plotted in Figure 4.15 over 100 years. Figure 4.15 clearly shows the improvement in survival probability in the case of perfect maintenance and the effect of imperfect maintenance on the component survival.

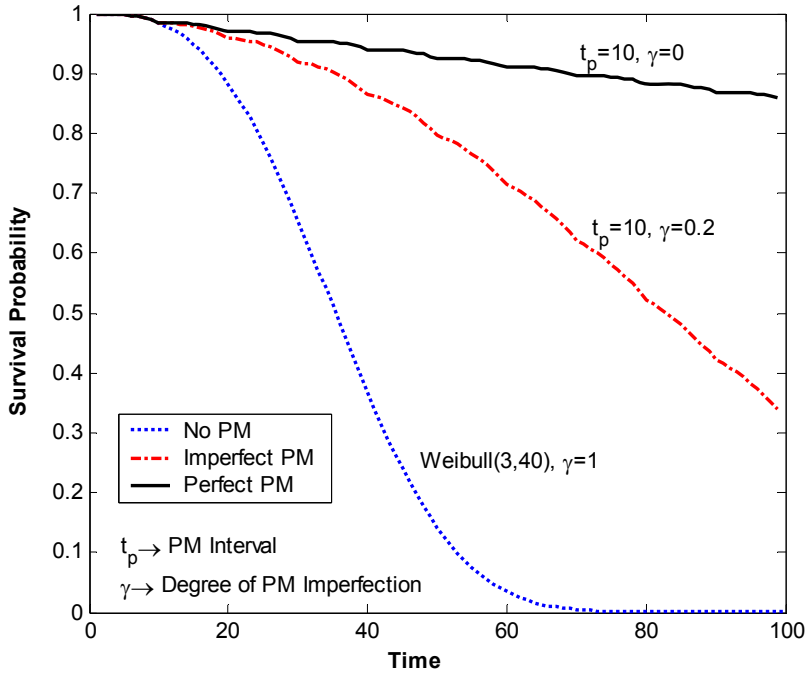

Figure 4.15: Survival probability curves in case of imperfect maintenance

The model can be used to quantify the effect of maintenance imperfection on component survival for life cycle management. The model can be used for each component in the system or the lifetime distribution of the whole system. The models flexibility can be exploited in various types of maintenance actions and to vary the effect of maintenance at each interval. Finally, the model can be helpful especially in component or system lifecycle management.

4.5.4 Cost Optimization

The effect of preventive maintenance of a system with lifetime of 100 years is studied by Yang et al. (2006). The survival function of the system is defined by a Weibull distribution with shape parameter 2.86 and scale parameter 94.34. The effect of preventive maintenance on the system is modeled according to Eq(4.37). Preventive maintenance actions are applied periodically at time intervals t_p of 2, 5, 10, 15, 20, 25, 30, 40, 50, 75 and 100 years. Yang et al. (2006) demonstrated the effect of perfect preventive maintenance to the problem described above. The

analysis conducted in this section extends this approach for the case of imperfect preventive maintenance actions.

The unit cost of failure is considered as 100 and the maintenance cost is varied to study for various cost ratios. The failure costs are calculated based on the probability of failure at the end of system lifetime of 100 years. The maintenance costs are calculated based on the number of maintenance actions at the end of system lifetime. Hence, the total cost at the end of system lifetime of 100 years is taken as the sum of failure cost and maintenance cost. The optimal maintenance interval is found to be the maintenance interval that leads to lowest total cost among all maintenance intervals considered.

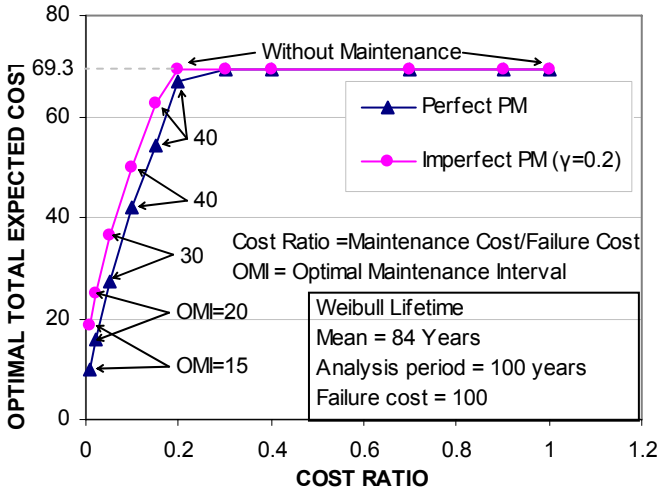

Figure 4.16: Optimal preventive maintenance

The optimal maintenance policy of the system for the various cost ratios considered is shown in Figure 4.16. The plot shows the effect of imperfect maintenance for two scenarios. The results from Figure 4.16 suggest that there is less effect on the optimal maintenance intervals but there is a significant difference in the optimal cost. Figure 4.16 illustrates the concept of an imperfect preventive maintenance model in maintenance optimization of systems.

4.6 Conclusions

The effect of maintenance actions can be quantified using probabilistic models for life cycle costs and equipment performance. This chapter discusses such application of maintenance models through the probabilistic approach, using component lifetime distributions.

Age-based replacement policy is simple and effective to implement in a system with a large population of relatively inexpensive components. An optimal age-based refurbishment policy for wood pole management is presented. For a cost ratio of $C_P/C_F = 0.2$, the optimal replacement age is estimated at 40 years. An interesting conclusion is that the type of lifetime distribution (Weibull, Gompertz or Log-logistic) has a limited sensitivity to the optimum replacement age and the expected life-cycle cost.

A sequential inspection-based replacement model is proposed to manage components from a large distribution network. The model is demonstrated to show the effect of an inspection interval in estimating the maintenance cost, risk, and life cycle costs. This approach is applicable to distributed populations in which inspections are scheduled as blocks of the populations. This approach is computationally complex and needs realistic cost input data to support decision making. As a general rule, increasing the inspection interval decreases the maintenance cost at the expense of increasing risk. The time-dependent variation of life-cycle cost depends on the relative magnitude of risk and cost over time.

A rather simplistic approach, in which components are replaced as they are detected to be in substandard state (Corrective Replacement), is demonstrated using renewal theory. The component replacement policy from renewal theory framework is presented in estimating the future expected replacement costs.

A probabilistic lifetime model is proposed to consider the effect of imperfect preventive maintenance on systems and components. The model has the flexibility to incorporate the imperfections of maintenance actions using the concept of virtual age. The model can consider the effect of maintenance imperfections at various maintenance intervals. The effect of imperfect preventive

maintenance in maintenance optimization is illustrated. The results show that imperfect preventive maintenance increases optimal total costs and the frequency of optimal maintenance intervals.

CHAPTER 5
STOCHASTIC MODEL FOR PITTING CORROSION IN STEAM GENERATORS

5.1 Background

The Steam generators (SG) are the most critical component of nuclear power reactor next to reactor core as shown in Figure 5.1. They are large heat exchangers that use the heat from primary coolant to produce steam in secondary side that is sent to steam turbines to produce electricity. A nuclear power plant may have multiple steam generators that are of shell-and-tube type heat exchangers each consisting of several thousand tubes. The steam generator tubes function as part of the nuclear reactor primary heat transport system pressure boundary. These tubes are generally thin walled for efficient heat transfer from primary side to the secondary side. In order to act as an effective barrier these tubes should be free of cracks, perforations and general degradation.

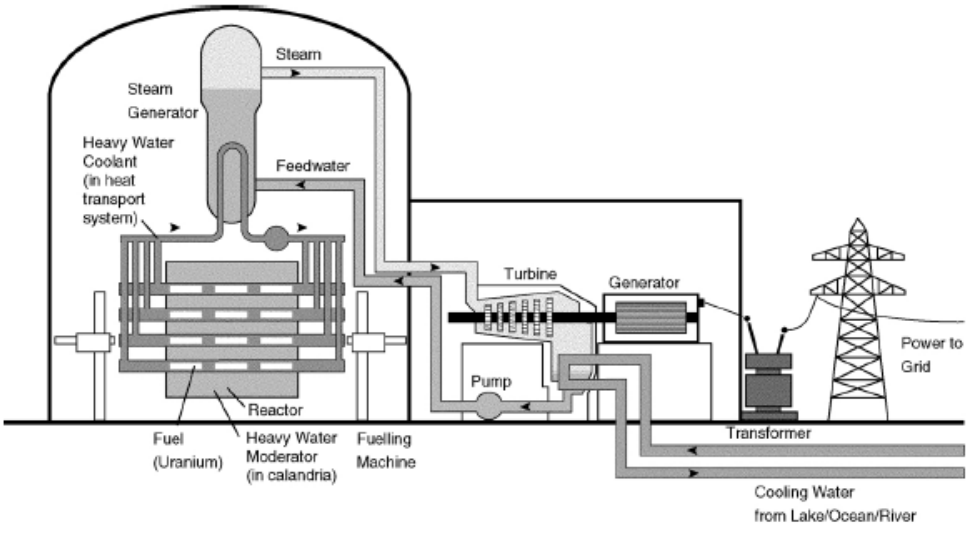

Figure 5.1: CANDU nuclear power plant (from http://canteach.candu.org/)

However in the past the steam generator tubes have experienced widespread degradation as observed at nuclear power plants [IAEA, 1997]. The degradation

mechanisms occur due to various factors such as: the material characteristics, operating and maintenance environment, water chemistry to name a few. Various degradation mechanisms affecting steam generator tubing are stress corrosion cracking, fretting, pitting, denting, erosion-corrosion, and fatigue as shown in Figure 5.2. Steam generators being critical components of nuclear power plant and the tubes being part of the primary pressure boundary can contribute significantly to plant outages due to tube leaks or rupture. Thus the risk of tube leak or rupture results in overall plant risk leading to plant shutdown. However, the utilities adopt various remedial and maintenance actions to reduce the risk of tube leak in order to ensure safe and reliable operation over its intended designed life.

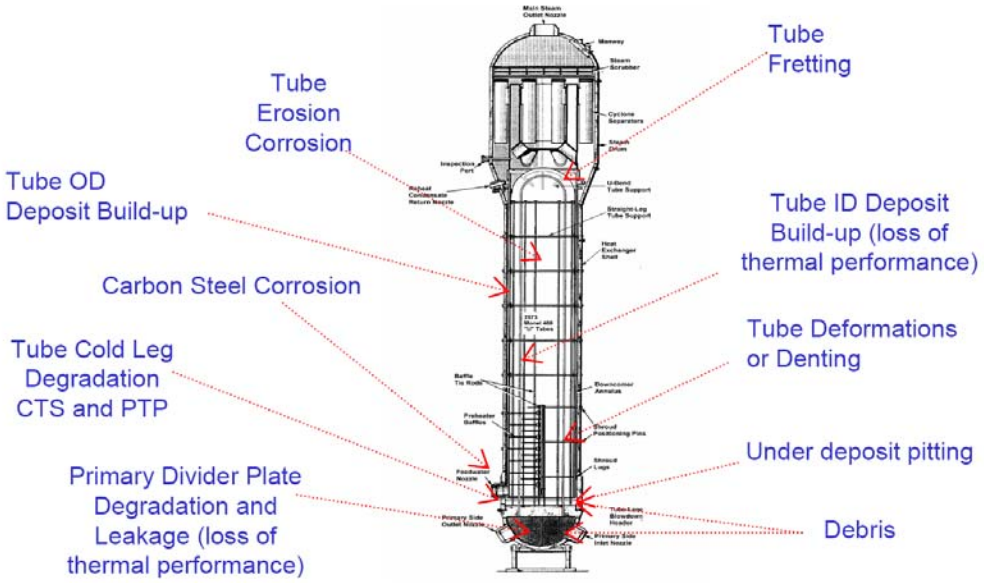

Figure 5.2: Steam generator degradation mechanisms (Maruska, 2002)

The degradation of steam generators has led to forced outages of nuclear power plants resulting in loss of revenue, and increase in the maintenance costs. Hence utilities resort to strategic life management process to efficiently run steam generators over its expected lifetime. Thus the major goals of the life management

strategies are to avoid surprises, learn from experience and manage the investment in steam generators (Tapping et al., 2000) in the most optimal way.

The methodology in implementing life management strategies is to first characterize the possible degradation mechanisms effecting the steam generator life and reliability. In order to achieve this, a sound fitness-for-service (FFS) plan, and good inspection capability is important. The possible remedial and maintenance actions are then assessed based on their merits in extending the service life of steam generator. The maintenance actions are then ranked based on risk reduction and cost effectiveness. However, even with best efforts on effective maintenance strategies uncertainties still lie with the aging of steam generators. The uncertainties also associated with how the flaws are characterized, detected, and mitigated. The success of life management strategies depend on minimizing these uncertainties. A risk based approach is therefore critical to life management strategies for its success. Such approach accounts for various uncertainties and quantifies them through probabilistic models for better decision making.

Pitting corrosion is a predominant form of degradation on the outside diameter (OD) of steam generator tubing of some nuclear power plants. This Chapter discusses the application of stochastic models for pitting corrosion degradation towards steam generator life cycle management.

5.1.1 Pitting Corrosion

During the course of normal operation of a nuclear power plant the impurities from make up water, the condenser leaks and the corrosion product oxides leached from feed train structural materials are carried along the feed water and get deposited over the steam generator surfaces. These deposits lead to problems such as under deposit pitting, tube failures and loss of production. The regions near the sludge pile at tube sheet and support plate experience crevice like conditions which favour pitting corrosion.

The pits are characterised as wide mouthed, dish shaped with low aspect ratio which could be described as localised wastage. Pitting corrosion typically occurs

at locally weak spots on tube where the passive layer breaks creating a local corrosion cell which is promoted by the presence of chloride and sulphate ions. The impurities such as sulphates and chlorides are produced from condenser leaks and chemicals used in chemical cleaning which result in local acidic conditions favourable to pitting process. The pitting process is accelerated in the presence of oxidizing conditions and copper deposits (IAEA, 1997). The accumulations of sludge act as barrier to diffusion accelerating the pitting process by enhancing chemical concentration.

The redox potential of the solution should exceed a critical value for the pits to initiate. This potential can be achieved by the presence of dissolved oxygen, oxidizing metal cations like $FeCl_3$ or $CuCl_3$ of higher redox potential than critical potential are more conducive to rapid pitting than dissolved oxygen. Any movement in the solution can remove the local concentration of Cl^- and H^+ ions that is required to continuous propagation thereby stopping pitting (Burstein et al., 1994). Laboratory studies and field observations have shown that the pitting rate could be very high resulting in through wall failure in a matter of days (Angell, 2002).

Severe pitting has been experienced in SG tubes in some nuclear reactors. Pitting observed in CANDU unit is described as under deposit pitting corrosion which is contributed due to presence of porous adherent deposits. The utility adopt aggressive water lancing and chemical cleaning to remove most of the deposits thereby mitigating pitting. Lancing uses high pressure jets to mechanically remove sludge from tube surfaces. By periodic lancing the depth of sludge is kept at reasonable levels. More advanced lancing equipment is used with multidirectional pressurized water jets which could remove tenacious sludge deposits (IAEA, 1997). Chemical cleaning is always preceded by water lancing such that they allow cleaning chemicals to access the crevices.

5.1.1.1 Chemical Cleaning

The sludge and deposits consist of feedtrain corrosion products (e.g., Fe_3O_4, Fe_2O_3, Cu, Cu_2O, CuO), impurities from condenser cooling water (e.g., SiO_2), and

water treatment chemicals (e.g., sodium phosphate). The chemical cleaning process commonly used is based on EPRI-SGOG (Electric Power Research Institute – Steam Generator Owners' Group) which is generally applied during plant outage (Semmler et al., 1998). If Cu is present an oxidizing step is applied whereas a reducing step dissolves Fe oxides. Of the various chemical cleaning formulations, the EDTA (Ethylene Diamine Tetra Acetic Acid) formulations are more popular in chemical cleaning of steam generators (Padma et al., 2001). The composition of chemical cleaning formulation consists of additives added to EDTA such as pH additive, reducing agent, oxidizing agent, and corrosion inhibitors. The compositions and conditions of chemical cleaning process are usually specific for a particular SG depending on the materials used and operating environment. Such chemical cleaning process has successfully been implemented by power utilities in extending the life of steam generators (Evans et al., 2002, Maruska, 2002).

5.1.1.2 Eddy Current Inspection

The most common tool for in-service inspection of SG tubing are eddy current probes which consists of small electrical coil enclosed in the probe head connected to an electric circuit. Eddy current probes are electro-magnetically coupled to the test specimen and generate eddy currents flowing in a direction parallel to the coil windings. An eddy current signal results from the disturbance in the magnetic field caused by the defect interfering with the eddy currents generated by the probe as it scans the defect. The amplitude and phase of the signal reflect the amplitude and phase of the affected part of the three dimensional eddy current field. The signal has a characteristic pattern that is used in identifying the type of defect.

The two basic types of eddy current probes used in SG inspection are "impedance" and "transmit-receive". The eddy current signals measured from the primary coil electric impedance induced by the eddy current magnetic field are of the impedance probes. In a transmit-receive (T/R) probe, the transit coil generates magnetic field and the eddy current signals are measured as the change in voltage

induced in the receive coil. The transmit-receive probe has proved to have a greater scope in eddy current testing and is currently used in most modern probes (Obrutsky, L., 2002).

Eddy current signal parameters are affected mainly by

- Tube thickness
- Defect type, size and orientation
- Test frequency of coil
- Magnetic properties of the material

The eddy current amplitude decays exponentially with depth from the surface of the probe and phase lag increases linearly with depth. The frequency of the test coil is selected based on the thickness of the tube, resistivity and permeability of tube material. It is quite common to use multiple frequencies on the same coil to test the probe characteristics (probe calibration) and also in characterizing various types of defects. Eddy current signals from a single coil are actually absolute measurements and are so called absolute probes. The differential probe consists of two coils side by side that measure the differential signal which is much sensitive to defects and insensitive to slowly varying properties like gradual dimensional or temperature variations and probe wobble. It's also common to have both absolute and differential setup in the same probe taking advantage of each. The three common types of probes used at CANDU steam generator tube inspection discussed in this Chapter are Carter-1, Carter 2 - Cecco 4, and X - Probe. There are a number of eddy current probes developed for specific applications and defect characteristics.

5.1.1.2.1 Carter-1 Bobbin Probe

The CTR-1-350, or Carter 1 probe uses absolute and differential bobbin coils that are coaxial with the inspected tube. The induced eddy current flows circumferentially in the steam generator tube, parallel to the coil windings. Hence these probes are not sensitive to circumferentially oriented defects. Bobbin probes are very good at volumetric defects. The volumetric material loss at a given

location is estimated by comparing the probe signal to amplitude calibration curves. The signal amplitude is sensitive to the morphology and circumferential extent of the flaw which could lead to potential sizing error. The main advantage of the bobbin probe is its speed which allows inspection in a short period of time thereby reducing unavailability and outage times.

5.1.1.2.2 Carter 2 - Cecco 4 Transmit-Receive Probe

The CTR2-C4, or Carter 2 – Cecco 4 probe is a multi-coil (array) transmit/receive eddy current probe, consisting of small coils aligned in the axial direction along the probe. Similar to the CTR-1 probe, the CTR2-C4 probe is generally not sensitive to degradation modes such as circumferential cracking, however it can detect multiple volumetric flaws such as corrosion pits at the same axial location around the circumference of the tube. Because of the multi-coil design, the CTR2-C4 probe has been shown to detect corrosion pits with higher accuracy, with negligible change in operational speed.

5.1.1.2.3 Transmit-Receive type X-Probe

The X-probe is a fast single-pass transmit/receive eddy current probe that combines the circumferential and axial modes in a single probe head. X-probe has a number of transmit/receive coils varying from 8 to 18 depending on probe diameter. The probe has a scanning speed comparable to the standard bobbin probes that is able to discriminate between axial, circumferential, and volumetric flaws in a single scan. X-probe is used in field recently and is only used at specific sections which need attention. X-probe is believed to characterize defects better than other probes available as it has greater resolution and stores lots of information on tube characteristics since it has more number of coils.

5.1.2 LCM Strategies

The goal of the steam generator life cycle management is to maximize value while ensuring safe and reliable operation until the expected end of life. The purpose of life cycle management plan is to provide both near term and short term strategies for inspection, cleaning, and modifications necessary for safe and

reliable operation. The objectives and scope of LCM plans is discussed in Chapter Chapter 2. In this section LCM strategies currently implemented in steam generator corrosion management is discussed.

5.1.2.1 Current LCM Strategies

The current steam generator remedial actions include extensive cleaning campaigns with the use of specialized water lancing equipment at low and high temperature chemical cleaning. Enhanced inspection is essential for an effective maintenance strategy. Advanced inspection technique such as X-probe is used for more rapid and accurate inspections. Degraded tubes are removed for metallographic assessments and fitness for service evaluations. Particular attention is given to chemistry control with improved water treatment plants and condenser. The copper components from the feedtrain and condenser are replaced. Much emphasis is given in maintaining chemistry specifications in secondary side chemistry within guidelines while maintaining high hydrazine chemistry regime. Currently work is undergoing on the development of tube sleeving in repairing the plugged tubes.

5.1.2.2 Fitness for Service Assessment

A sound fitness for service program is essential in characterizing degradation mechanisms. Fitness for service guidelines are therefore developed for each plant since the degradation mechanisms vary for each plant. Fitness for service assessment along with structural integrity and operational assessment is conducted at each inspection campaign to demonstrate the ability of steam generator to function safely until next inspection outage. The utility considers the primary objective of fitness for service is same as life cycle management; to assure the integrity of steam generators as a primary pressure and containment boundary, the difference being the time span of application.

5.1.2.3 LCM Issues

The utilities were successful in mitigating pitting degradation with aggressive cleaning campaigns and efficient chemistry control. Despite the remedial actions

new pits initiate and continue to grow rapidly. This presents a major challenge for steam generator LCM in predicting future equipment performance, estimating the remaining life, and the adverse economic consequences. The ageing of steam generator under pitting corrosion is not fully understood. Uncertainties also exist on how the flaws are characterized, detected and mitigated. A risk based approach is therefore essential for efficient life cycle management program which accounts for various uncertainties and to quantify them. A probabilistic based framework for pitting corrosion degradation is discussed in next section based on eddy current inspection data.

5.2 Stochastic Modelling of Pitting Corrosion

5.2.1 Introduction

The risks associated with steam generator tube pitting corrosion can be quantified through stochastic modelling. Estimating the expected number of tubes that require plugging and the probability of tube leakage in the future operating period are important input to risk based life-cycle management of steam generators (Harris, et al., 1997). When the extent of pitting is unacceptable, then the need for maintenance activities such as water lancing or chemical cleaning should be assessed in a risk-based framework. The model should be able to assess the impact of maintenance interval on the risk associated with the event of tube leakage and be able to carry out the cost benefit analysis. In technical terms, answering these questions requires distributions pit size, and rate of new pit generation. The objective of this study is to discuss various uncertainties with inspection data and develop probabilistic models to estimate probability distributions from existing inspection data and apply them to life cycle management.

5.2.1.1 Pit Generation Models

Localized pitting corrosion process is considered to have stochastic character in nature. Existing models are developed in idealized setting which utilizes laboratory data obtained from continuous monitoring of pit initiation and

propagation using potentiometers. As passivation breaks down, the potential difference increases sharply. This potential (pitting potential) depends on the nature and composition of the solution. Likewise the time interval needed to observe the drastic increase in potential is taken as the induction time. Stochastic models based on the statistical distribution of pitting potential and induction times for pit formation are proposed from such experimental observations (Shibata, 1996; Mola et al., 1990; Wu et al., 1997). The process of pit generation is modelled as a pure birth stochastic model. Opposite to pit formation, passive layer healing operates as a pit death process. These models are useful in investigating the experimental procedures in electrochemical systems. Such models may not be applicable in field applications because it's not practical to monitor the pitting potential in steam generator tubes.

Markov process model for the growth of maximum pit depth was discussed by Provan and Rodriguez, (1989) applied to oil and gas pipelines where corrosion is a very slow process. Hong, (1999) proposes the use of combined model by representing the pit generation process with Poisson model and the pit depth growth process by Markov process. The combined model is reported to give better estimate for the problems discussed by Provan and Rodriguez, (1989). These models are not directly applicable in analyzing pitting problems in steam generator for the reasons discussed in Section 5.1.1.

Pit generation and growth is fairly rapid in some CANDU reactors. It is believed oxygen intake during shut down and start-up cycles promotes the pitting, which is a kind of inter-granular attack. The time of rapid growth is random and then growth stops. There is evidence to suggest that most pits don't grow after this initial period of generation and growth. Thus pit size also becomes a random variable. Such a process is also referred to as marked point process as shown in Figure 5.3.

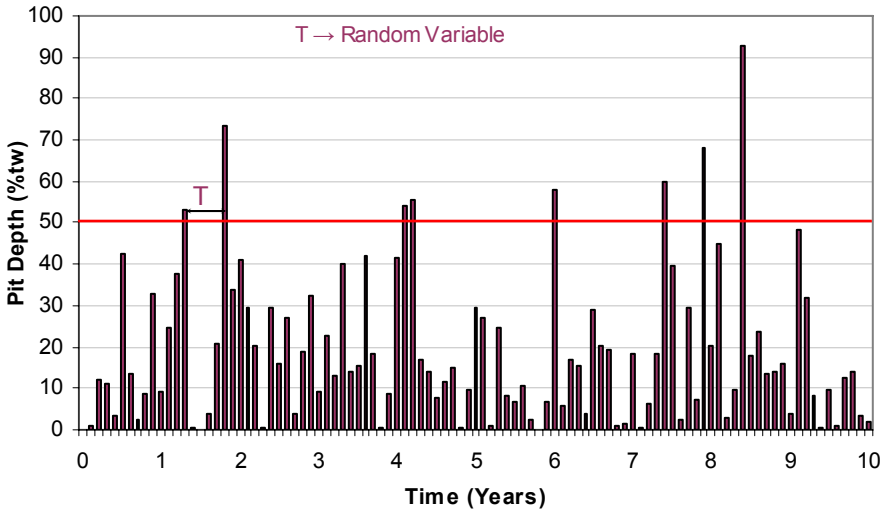

Figure 5.3: Plot to illustrate marked point process for pits > 50%tw

Model pit initiation is random in time and pit assumes a random size from a distribution. Small size pits can not be reliably detected or measured. The focus of attention is on relatively large pits of size (≥ 50% tw). The idea is that pits exceeding a relatively high threshold (50%) follow the Poisson process as shown in extreme value theory (Smith, 2004). The pit generation is assumed to follow Poisson process which falls under stochastic birth process. The pit generation model following NHPP is discussed in next section along with parameter estimation from observed inspection data.

5.2.2 Stochastic Pit Generation

Let the number of pits *N(t)* in the interval [0-*t*] follow a Non-Homogenous Poisson Process (NHPP) with intensity function $\lambda(t)$. The mean value function $\Lambda(t)$ or the expected number of pits $E[N(t)]$ per SG following Weibull Power law is given as (Ross, 2000)

$$E[N(t)] = \Lambda(t) = \int_0^t \lambda(s)ds = \frac{\alpha}{\beta} t^{\beta} \qquad (5.1)$$

The parameters α, is a scale parameter and β is the shape parameter. When shape parameter β=1, the intensity function is constant and the process is defined as a Homogeneous Poisson process (HPP).

5.2.3 Inspection Process

In practice it is quite difficult and uneconomical to inspect the equipment continuously with time. Inspection of equipment is usually conducted at periodic or non periodic inspection time intervals. Consider an inspection process of a single SG from the start of its operation as shown in Figure 5.4, where non-destructive inspections are conducted at times t_1, t_2, t_3 and t_4.

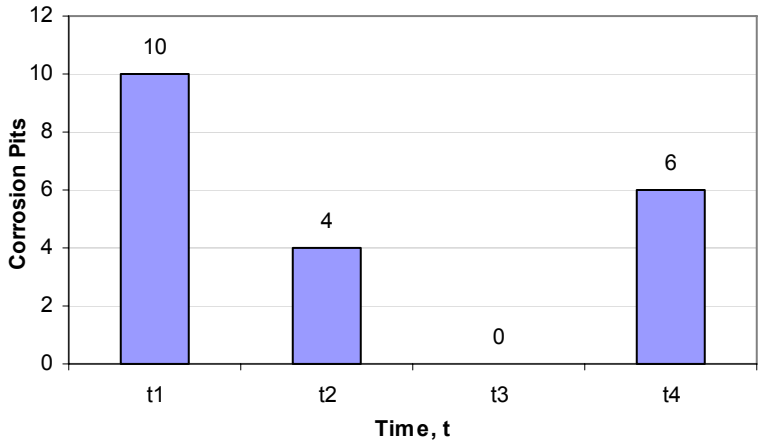

Figure 5.4: SG pitting corrosion inspection data

The number of pits observed at time t_2 is the number of new pits generated during the interval [t_1-t_2]. The number of pits generated during inspection interval [t_1-t_2] follows a Poisson distribution which is given as

$$P\{N(t_2) - N(t_1) = n\} = e^{-[\Lambda(t_2)-\Lambda(t_1)]} \frac{[\Lambda(t_2) - \Lambda(t_1)]^n}{n!} \quad n \geq 0, t_2 > t_1 \tag{5.2}$$

If at the time of inspection t_3 there are no observed new pits, such kind of data are called censored data. The censored data gives us the information that there are no new pits observed in the interval [t_2-t_3] with probability given as

$$P\{N(t_3) - N(t_2) = 0\} = e^{-[\Lambda(t_3)-\Lambda(t_2)]} \quad t_3 > t_2 \tag{5.3}$$

By assuming a probability model for pit generation rate, the probability of observing these pits in an inspection process as shown in Figure 5.4 is calculated by a likelihood method. The parameters of the model are then estimated by maximizing this likelihood function. The theory and methodology of likelihood

method is explained further in subsequent sections. The advantage of likelihood method is that it can handle censored data.

5.3 Estimation of Pit Generation Rate

From inspection data, the number of pits generated in different intervals can be obtained as shown in Figure 5.4 throughout the service life of the system.

Suppose in a k^{th} interval $[t_{k1}\text{-}t_{k2}]$, n_k pits are generated and that there are in total M intervals for which data are available. The maximum likelihood function for this sample can be set up as (Lawless, 2003):

$$L(\alpha,\beta)=\prod_{k=1}^{M}\frac{[\Lambda(t_{k2})-\Lambda(t_{k1})]^{n_k}}{n_k!}\exp\{-[\Lambda(t_{k2})-\Lambda(t_{k1})]\} \tag{5.4}$$

By substituting the mean rate function, the log-likelihood is derived as

$$l(\alpha,\beta)\propto\sum_{k=1}^{M}\left[n_k\log\left(\frac{\alpha}{\beta}\left\{t_{k2}^{\beta}-t_{k1}^{\beta}\right\}\right)-\frac{\alpha}{\beta}\left\{t_{k2}^{\beta}-t_{k1}^{\beta}\right\}\right] \tag{5.5}$$

The unknown parameters are estimated from the conditions of maximization as

$$\begin{aligned}\frac{\partial l(\alpha,\beta)}{\partial\alpha}&=\sum_{i=1}^{M}\left[\frac{n_k}{\alpha}-\frac{1}{\beta}\left\{t_{k2}^{\beta}-t_{k1}^{\beta}\right\}\right]=0\\ \frac{\partial l(\alpha,\beta)}{\partial\beta}&=\sum_{k=1}^{M}n_k\left[\frac{\left\{t_{k2}^{\beta}\log t_{k2}-t_{k1}^{\beta}\log t_{k1}\right\}}{t_{k2}^{\beta}-t_{k1}^{\beta}}-\frac{1}{\beta}\right]-\frac{\alpha}{\beta^2}\left[\beta\left\{t_{k2}^{\beta}\log t_{k2}-t_{k1}^{\beta}\log t_{k1}\right\}-\left\{t_{k2}^{\beta}-t_{k1}^{\beta}\right\}\right]=0\end{aligned} \tag{5.6}$$

The parameters $\hat{\alpha},\hat{\beta}$ can be estimated by trial and error from Eq. (5.6). Standard maximization codes can also be applied to Eq. (5.5) to estimate the parameters. The Fisher information matrix is derived as the negative of the second derivative of the log likelihood function with respect to the parameters. The asymptotic covariance matrix of the maximum likelihood estimators is an inverse of the Fisher information matrix. Using the estimates of asymptotic variance, the approximate confidence limits for the distribution parameters can be obtained under the assumption of normality.

5.3.1 Test for Homogenous Poisson process

In case of the HPP model (β=1), the pit generation rate is constant with time. A statistical test, such as the likelihood ratio test, can be applied to test the null hypothesis that β=1. The likelihood ratio statistic (LRS) is given as

$$LRS = -2\{l_1(\beta \neq 1, \alpha_1) - l_0(\beta = 1, \alpha_0)\} \tag{5.7}$$

where $l_0(\beta = 1, \alpha_0)$ and $l_1(\beta \neq 1, \alpha_1)$ are the log likelihood functions for the homogeneous and non-homogeneous Poisson process models, respectively. The LRS follows the Chi-square distribution with one degree of freedom. The null hypothesis is rejected at the 5 % level of significance when p-value is less than 5%, and it can be concluded that the pit generation rate is not constant or otherwise.

5.4 Extreme Pit Depth Model

5.4.1 Pit Depth Distribution

The pit depths are measured using NDE techniques which are used to evaluate flaw distribution in tubes. The measured pit depths pose challenge in modeling probability distribution as they are associated with detection uncertainty and measurement error. Measured pit depths of size less than 30% through wall depth (TWD) is based on expert judgment due to relatively small size of pits for a tube of wall thickness in range of 1-2 mm. All new pits greater than 50% TWD is considered for the analysis as the measurement error effects are minimal to larger pits. Pit depths exceeding a threshold of 50% TWD can be treated as extreme (or peaks) of the pit generation process. The distribution of these peaks over the threshold can be modeled using the generalized Pareto distribution (GPD), commonly used in the extreme value theory (Smith, 2004). The generalized Pareto distribution (GPD) for peaks over thresholds ($x > u$) is given by

$$F_X(x) = 1 - \left(1 - \xi \frac{x-u}{\sigma}\right)^{1/\xi} \tag{5.8}$$

where σ is the scale parameter and ξ is the shape parameter. When $\xi \le 0$, the GPD has a long and unbounded tail. When $\xi > 0$, the distribution is right bounded at σ / ξ. In the limiting case when $\xi \to 0$ the distribution takes exponential with mean equal to σ. When $\xi = 1$, GPD model becomes the uniform distribution. The GPD model is commonly used in extreme value analysis of engineering and environmental systems (Smith, 2004).

The distribution parameters can be estimated by method of moments using the sample mean (m) and standard deviation (s) computed from the pit depth data based on the following relations (Hosking and Wallis, 1987)

$$\xi = \frac{1}{2}\left[\left(\frac{m-u}{s}\right)^2 - 1\right] \tag{5.9}$$

$$\sigma = (m-u)(1+\xi) \tag{5.10}$$

5.4.2 Extreme Pit Depth Distribution

In order to estimate probability of the tube leakage in a steam generator, the distribution of the largest (extreme) pit size is required. Since the pit occurrence is described by a non-homogeneous Poisson (Weibull) process, the rate of occurrence of pits exceeding a size z at time t is given as

$$\lambda_z(t) = \lambda(t)[1 - F_X(z)] \tag{5.11}$$

The expected number of pits exceeding depth >z % TWD in the interval [0-t] per SG, i.e, the mean rate function, is given as

$$E[N_z(t)] = \Lambda_z(t) = \Lambda(t)\left[1 - F_X(z)\right] \tag{5.12}$$

The distribution of the number of these large pits is given by the Poisson distribution as

$$P_N(n) = \frac{[\Lambda_z(t)]^n}{n!}\exp\{-\Lambda_z(t)\} \tag{5.13}$$

From the principles of extreme value theory, the distribution of the largest pit among all generated n pits in [0-t] can be expressed as

$$F_Y(z) = \sum_{n=0}^{\infty} [F_X(z)]^n \frac{[\Lambda(t)]^n e^{-\Lambda(t)}}{n!} = \exp\{-\Lambda(t)[1-F_X(z)]\} = \exp\{-\Lambda_z(t)\} \quad (5.14)$$

The distribution $F_Y(z)$ is also referred to as the Generalized Extreme Value (GEV) distribution, which encompasses all three limiting forms of the extreme value distributions, namely, the Gumbel, Frechet and Weibull distributions (Smith, 2004). It can be used to estimate the probability of tube leakage per operating year.

If the reactor unit has *n* number of SGs, each with leak probabilities p_{L_i} acting as a series system independent of each other, then the probability of having a leak in the unit p_L^U can be calculated as

$$p_L^U = 1 - \prod_{i=1}^{n} (1 - p_{L_i}) \quad (5.15)$$

The number of extreme pits for the Unit is actually a sum of independent Poisson processes from all SGs. The expected number of extreme pits with depth *z %* TWD in the interval [0-*t*] per unit can be calculated as

$$E[N_z(t)] = E[N_{z_1}(t)] + E[N_{z_2}(t)] + ... + E[N_{z_n}(t)] \quad (5.16)$$

The expected number of extreme pits per unit can be used in developing unit life-cycle management plans.

5.5 Gamma Frailty Poisson Model

The Poisson models discussed earlier in the preceding sections are proposed in the context of pitting corrosion process. The pitting observed from a single SG is usually in negligible amount considering large pits. Pitting processes from all the SGs in a reactor unit are assumed as realizations from a random pitting process model of a single SG. It is quite reasonable to pool the data from all the SGs of a reactor unit to model the random pitting process of a single SG. However the unobserved randomness among the different SGs can be accounted for using frailty model. Such frailty Poisson models are used in demographic studies such as in panel count data (Lawless, 1987, Zhang and Jamshidian, 2003). The frailty model on Poisson process is defined as

$$\Lambda(t \mid \gamma) = E(N(t) \mid \gamma) = \gamma \Lambda_0(t) \tag{5.17}$$

where the frailty random variable γ follows Gamma $(\delta, 1/\delta)$ distribution with mean as one and variance δ. The unconditional mean function is thus $E(N(t)) = \Lambda_0(t)$ which can be considered to follow power law model given in Eq. 5.17. The unconditional probability of observing *n* pits in time [0, *t*] can be derived as

$$\Pr\big(N(t) = n\big) = \frac{\Gamma(n + \delta^{-1})}{n!\Gamma(\delta^{-1})\delta^{\delta^{-1}}} \frac{\left[\Lambda_0(t)\right]^n}{\left[\Lambda_0(t) + \delta^{-1}\right]^{n+\delta^{-1}}} \tag{5.18}$$

The probability of observing number of pits in an interval shown in Eq. 5.18 is actually follows a negative binomial distribution. The frailty random variable usually introduces greater dispersion in observing the number of pits in an interval. Such high variance is observed from data obtained by industry and is usually modeled as negative binomial distribution (Camacho and Pagan, 2006). Hence frailty model seems to be appropriate in case of relatively insufficient observations of pitting corrosion from steam generators. Such frailty models can be directly applied in modeling pitting corrosion and the parameters are estimated by Maximum Likelihood method as described in Section 5.3.

5.6 Some Results Applicable to Life Cycle Management

5.6.1 Time to First Leak

The probabilistic pitting corrosion model developed in Section 5.2.2 can be further applied in estimating the time to first failure distribution. The definition of failure is taken in general, which can be considered as the leak criterion or the plugging criterion. Let T_1 denote the time from $t = 0$ until the first failure. The survival function of T_1 is given as

$$P(T_1 > t) = P(N_z(t) = 0) = e^{-\Lambda_z(t)} \tag{5.19}$$

Where $N_z(t)$ is the number of failures at time *t,* and $\Lambda_z(t)$ is the mean value function of extreme pits. The expected time to failure can now be calculated by integrating the survival function in Eq. (5.19).

$$E[T_1] = \int_0^\infty e^{-\Lambda_z(t)} dt \tag{5.20}$$

If the mean value function follows Weibull power law as shown in Eq**.** (5.1), the expected time to first leak and its variance formula can be derived as shown below.

$$E[T_1] = \left(\frac{\beta}{\alpha}\right)^{1/\beta} \Gamma\left(1 + \frac{1}{\beta}\right) \tag{5.21}$$

$$Var[T_1] = \left(\frac{\beta}{\alpha}\right)^{2/\beta} \left[\Gamma\left(1 + \frac{2}{\beta}\right) - \Gamma^2\left(1 + \frac{1}{\beta}\right)\right] \tag{5.22}$$

Considering the generalized Pareto distribution for the pit depth as discussed in Section 5.4.1 and NHPP model for pit generation discussed in Section 5.2.2, the time to first leak distribution can be estimated as

$$P(T_1 > t) = e^{-\frac{\alpha}{\beta} t^\beta \left(1 - \xi \frac{z-u}{\sigma}\right)^{1/\xi}} \tag{5.23}$$

5.6.2 Time to nth Failure/Leak

The probabilistic corrosion pitting model can be used in estimating the time to n^{th} failure distributions. Let S_n denote the time until failure n for $n = 1,2,...$, where $S_0 = 0$. The distribution of S_n is given by

$$P(S_n > t) = P(N_z(t) \le n-1) = \sum_{\nu=0}^{n-1} \frac{\Lambda_z(t)^\nu}{\nu!} e^{-\Lambda(t)} \tag{5.24}$$

The expected time to n^{th} failure can be calculated by integrating the survival function Eq. (5.22) which is given as

$$E[S_n] = \int_0^\infty \sum_{\nu=0}^{n-1} \frac{\Lambda_z(t)^\nu}{\nu!} e^{-\Lambda_z(t)} dt \tag{5.25}$$

Considering the generalized Pareto distribution for the pit depth discussed in Section 5.4.1 and NHPP model for pit generation discussed in Section 5.2.2, the time to n^{th} failure distribution can be estimated as

$$P(S_n > t) = \sum_{\nu=0}^{n-1} \frac{\left[\frac{\alpha}{\beta} t^{\beta}\left(1-\xi\frac{z-u}{\sigma}\right)^{1/\xi}\right]^{\nu}}{\nu!} e^{-\frac{\alpha}{\beta}t^{\beta}\left(1-\xi\frac{z-u}{\sigma}\right)^{1/\xi}} \tag{5.26}$$

5.7 Uncertainties Associated with Pit Depth Model

Eddy current (ET) inspection process is aimed to produce reliable information for engineers to ensure structural integrity of SG. However there are various uncertainties involved in each stage of inspection process that hinders the overall reliability of ET inspection process. The major reliability issues of eddy current inspection relevant for engineers are the detectability and accuracy issues. It is required that defects greater than critical size should be detected by ET inspection. The detectability issue is addressed using Probability of Detection (POD) curves for the technique as well as for analysis/analyst. The major factors that affect POD are

- Probe sensitivity to defect orientation
- Human factors
- Poor signal to noise ratio
- Material characteristics
- Probe wear
- Internal and external deposits
- Scan rate

Most of the factors discussed above are minimized by selecting an appropriate probe and better inspection procedures. Even with the best efforts in minimizing the uncertainties there still lies a residual uncertainty that constitute toward inspection reliability. It is therefore necessary to demonstrate the POD curves for the inspection process along with the inspection results.

Sizing accuracy reveal how close the technique defect size match to that of true defect size. The sizing accuracy is addressed by means of root mean squared error (RMSE) by comparing eddy current measurements to that of the actual depths from a pulled tube. The major factors affecting the accuracy of eddy current technique are

- Defects on Calibrated tube may not depict actual defects on field
- Probe wear
- Signal to noise ratio
- Human factors

Most of the factors can be minimized by selecting an appropriate probe and by customizing calibration standards. As discussed above for detection uncertainty, it is difficult eliminate uncertainties completely. It is therefore necessary to demonstrate the sizing accuracy of the inspection process along with the eddy current inspection results.

The effects of sizing accuracy and detectability are minimized when considering relatively larger pit depths. The effect of sizing accuracy on pit depth distribution is illustrated in Section 5.8. The pit depths with size ≥50%tw are considered for modelling the depth distribution. Generalized Pareto distribution is considered for modelling pit depths exceeding a threshold of 50%tw as discussed in Section 5.4.1.

5.7.1 Measurement Error Analysis from Field Inspections

The probabilistic model for pit depth should take into account the measurement error in Non-destructive test (NDT) tool. Statistical methods have been used for evaluation of measurement error from such NDT tools by laboratory studies. The statistical methods applicable in Non-destructive evaluation (NDE) are reviewed by Olin&Meeker (1996) and Sweeting (1995). They show the application of regression models on the measured flaws and the true flaws in characterizing the measurement errors of NDT tools. Inspection data on flaws using multiple NDT tools can also be used in characterizing the measurement error of each tool. In this

section such application in nuclear steam generator tubes non-destructive inspection are discussed.

Non-destructive inspection of steam generator tubes has played a major part in its safe and successful operation. Periodic inspection database on SG tubes reveal corrosion pit depth measurements from various eddy current probes. In some cases corrosion pits are measured using multiple probes to gain more insight, especially on larger pit depths which could potentially leak. The corrosion pit depth data measured from multiple eddy current probes can be used to quantify the measurement error for each measuring probe. The EPRI guidelines for inspection of SG only refer to root mean squared error/differential (RMSE/D) in accessing the quality of an inspection instrument. The methodology discussed here follows the paper from Morrison, et al. (2002) where he discusses the application of Grubbs Method from multiple inspection data.

5.7.1.1 Estimation of Measurement Errors from Inspection Data for Each of Two Probes

The root mean squared error/differential (RMSE/D) calculates the total scatter from the two tools being compared. If the measured values from Probe 1 and Probe 2 are x_i and y_i, the RMSE/D is calculated as

$$RMSE / D = \sqrt{\frac{1}{n}\sum_{i=1}^{n}(x_i - y_i)^2} \tag{5.27}$$

From RMSE/D it is not possible to decompose the total scatter and assign it to each tool. This approach is helpful only if one of the measuring probe is assumed to be perfect. In most of the cases this approach penalizes bad probe unnecessarily by assigning the total scatter to bad probe.

5.7.1.2 Grubbs Method

Grubbs (1948) suggested the use of sample variance and covariance to estimate measurement errors for individual probes. The measured pit depths (x_i, y_i) from each probe is assumed to follow the model given as

$$x_i = \mu_i + \alpha_1 + e_{i1}, \qquad \text{and} \qquad y_i = \mu_i + \alpha_2 + e_{i2} \tag{5.28}$$

where μ_i is the true value for the i^{th} pit depth, α_1 and α_2 are the constant biases and e_{i1} and e_{i2} are the measurement error (ME) in observing μ_i. It is assumed that the ME of a probe is independent of the true value of the pit depth and is also independent of the ME for the other probe. The randomness in ME is assumed to follow normal distribution with mean zero and standard deviation σ. The variance of measured pit depths ($\sigma_x^2 = \sigma_\mu^2 + \sigma_1^2; \sigma_y^2 = \sigma_\mu^2 + \sigma_2^2$) consists of the variance of the true value of pit depth and the variance of measurement error of its measuring probe. The covariance between the observed measurements ($C[x, y] = \sigma_\mu^2$) from each probe gives an estimate on the variance of true value of pit depth. The measurement error for each probe can be estimated by subtracting the variance of true value from the variance of measured values from that particular probe.

Grubbs estimates the variance of measurement error of each measuring probe and variance of true values of pit depths by the method of moments on the model described in Eq. (5.28). The variance of true value of pit depth is estimated as the unbiased sample covariance ($\sigma_\mu^2 = s_{12}$) and the variance of measurement error for each measuring probe is estimated as

$$\sigma_1^2 = s_1^2 - s_{12}, \text{ and } \sigma_2^2 = s_2^2 - s_{12} \tag{5.29}$$

where s_1, s_2 are the unbiased sample variance of each measuring probe pit depths and s_{12} is the unbiased sample covariance which are calculated as

$$s_1^2 = \frac{1}{n-1}\left[\sum_{i=1}^{n} x_i^2 - \frac{1}{n}\left(\sum_{i=1}^{n} x_i\right)^2\right],$$

$$s_2^2 = \frac{1}{n-1}\left[\sum_{i=1}^{n} y_i^2 - \frac{1}{n}\left(\sum_{i=1}^{n} y_i\right)^2\right], \text{ and} \tag{5.30}$$

$$s_{12} = \frac{1}{n-1}\left[\sum_{i=1}^{n} x_i\, y_i - \frac{1}{n}\left(\sum_{i=1}^{n} x_i\right)\left(\sum_{i=1}^{n} y_i\right)\right]$$

The measurement errors estimated in Eq. (5.29) are obtained from one inspection sample which could differ from another inspection sample. The variability in estimating the measurement error $\hat{\sigma}_j^2$ of the *j*-th probe (*j* = 1, 2) can be estimated as

$$V(\hat{\sigma}_j^2) = \frac{2\sigma_j^4}{n-1} + \frac{\sigma_\mu^2\sigma_1^2 + \sigma_\mu^2\sigma_2^2 + \sigma_1^2\sigma_2^2}{n-1} \tag{5.31}$$

The variance parameters in the above equation are taken as the respective sample estimates. The bias parameters in Eq. (5.28) cannot be estimated unless the true value μ_i is known. However, the difference or the relative bias of Probe 1 with respect to Probe 2 can be given as

$$\alpha_1 - \alpha_2 = \bar{x} - \bar{y} \tag{5.32}$$

where $\bar{x}$ and $\bar{y}$ are the average of the measurements of Probe 1 and Probe 2. The total scatter between two probes can be decomposed into three separate components, the relative bias component and measurement error estimate for each probe. The three components are related to the RMSD by

$$RMSD = \sqrt{(\text{Bias})^2 + \sigma_1^2 + \sigma_2^2} \tag{5.33}$$

where σ_1^2 and σ_2^2 are the variances of the measurement errors of Probe 1 and Probe 2 respectively.

5.7.1.3 Constrained Expected Likelihood Method

Grubbs method can only work if the variance of the error estimates are positive, in case of $s_1^2 < s_{12}$ or $s_2^2 < s_{12}$ the standard deviation of ME from Eq. (5.27) cannot be obtained from Grubbs Method. In such situations the constrained expected likelihood method proposed by Jaech (1985) is used. Positive estimates on measurement error can be derived by finding the expected likelihood estimates of σ_1^2 and σ_2^2, where the expectation is restricted to the space of nonnegative values for both the parameters. Jaech (1985) provides a maximum likelihood approach to Grubbs Estimates and uses the results in deriving the constrained

expected likelihood estimates for measurement error. The MLE of $\left(\sigma_1^2 + \sigma_2^2\right)$ is S which is the total scatter given by

$$S = \frac{(n-1)(s_1^2 + s_2^2 - 2s_{12})}{n} \tag{5.34}$$

The CEL estimators are considered such that they lie in the first quadrant on the line $\left(\sigma_1^2 + \sigma_2^2\right) = S$ in a proportion v such that

$$\begin{aligned} &\sigma_{1v}^2 = vS; \qquad 0 \le v \le 1 \\ &\sigma_{2v}^2 = (1-v)S \end{aligned} \tag{5.35}$$

The CEL estimate of measurement error is then derived as the weighted average with respect to likelihood in the transformed space as defined in Eq. (5.35). The expressions for the CEL estimate of measurement error as given by Jaech (1985) are

$$\hat{\sigma}_1^2 = \frac{SI_0}{I_1}; \qquad \hat{\sigma}_2^2 = S - \hat{\sigma}_1^2 \tag{5.36}$$

where

$$\begin{aligned} I_0 &= \int_0^1 vf(v)dv \\ I_1 &= \int_0^1 f(v)dv \\ f(v) &= \left[s_1^2(1-v)^2 + v^2 s_2^2 + 2v(1-v)s_{12}\right]^{-n/2} \end{aligned} \tag{5.37}$$

Morrision (2002) suggests that the CEL estimates have to be checked to see if they are reasonable and they also suggest that when the covariance between the Probes is negative the CEL estimate does not seem appropriate.

5.8 Effect of Measurement Error and POD on Pit Depth Distribution

The main objective of this section is to illustrate the effect of uncertainty in detectability and measurability of pit depths or flaw depths in general. The source of such uncertainties in eddy current inspection process is already discussed in

Section 5.7. This section covers the technical details in accounting for measurement error and probability of detection.

The pit depths observed from eddy current inspection are associated with uncertainties with inspection process and tools. In addition to measurement error and probability of detection the pit depths are also associated with censoring. Due to the inherent noise from the eddy current probe, pit depths with sizes <30% TWD cannot be measured and hence designated as censored observations. Such uncertainties on pit depth greatly effect the predictions on the leak probability estimates. Simulation study is conducted to quantify the effect of uncertainties in pit depth measurements.

5.8.1 Simulation Analysis

Considering that the true pit depths follows exponential distribution with mean 15% TWD. The probability density function of the true pit depth is shown in Figure 5.5.

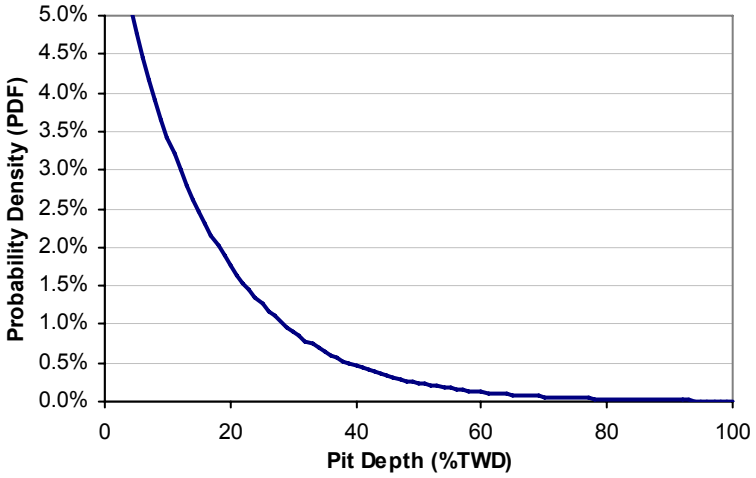

Figure 5.5: Probability density plot for true pit depth

The event of interest to most utilities is the probability of tube leak and the number of tubes plugged in a given outage. The tube leak probability is associated with the probability of pit depth exceeding 95% TWD. The number of tubes plugged is associated with the probability of pit depth exceeding 51% TWD. The

probability of exceedence can be calculated from Figure 5.5 by integrating the PDF exceeding 51% or 95% TWD. The probability of pit depth exceeding 95% TWD is calculated to be 0.18%, and the probability of pit depth exceeding 51% TWD is calculated to be 3.34%. The effect of measurement error and detection uncertainty is quantified in estimating the probabilities calculated above.

5.8.1.1 Effect of Detection Uncertainty

The uncertainty in pit detection comes from the eddy current probe resolution on pit sizes and also from eddy current data acquisition as described in Section 5.7. The uncertainty in pit detection is characterized by probability of detection (POD) function on pit depths. In general, pits with larger sizes can be detected with great certainty. The POD model quantifies the uncertainty in pit depth detection from eddy current inspection. The POD function considered here is the exponential model which is given as

$$POD(x) = 1 - \exp(-\lambda x) \tag{5.38}$$

where λ is the parameter of the exponential POD model. The POD for pit depth 60% TWD is considered as 95% with parameter $\lambda = 0.05$ as shown in Figure 5.6 to reflect actual industrial practice.

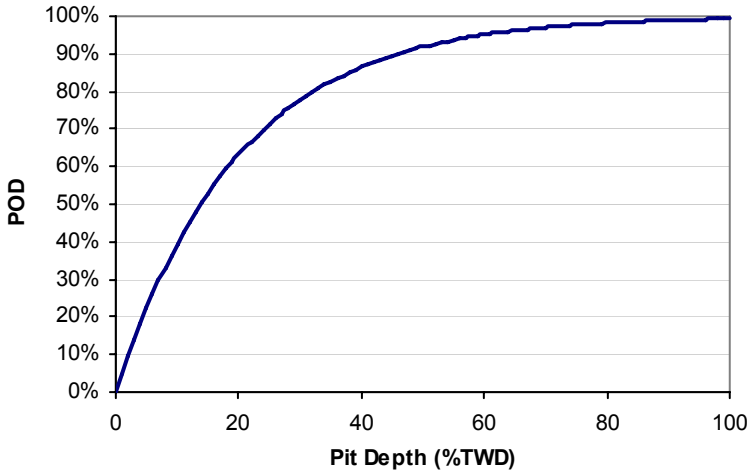

Figure 5.6: Probability of Detection Plot

The detection probability is lower for shallow pit depths and increases with higher pit depths. Detection uncertainty is introduced into the true depth distribution to obtain detected population of pit depths. Simulation analysis is conducted to introduce detection uncertainty to true pit depth measurements which follows the probability model

$$\begin{aligned} f_d(x) &\propto POD(x) f_T(x) \\ f_{ud}(x) &\propto \big(1 - POD(x)\big) f_T(x) \end{aligned} \tag{5.39}$$

where $f_d(x)$ is the probability density of detected pits, $f_{ud}(x)$ is the probability density of undetected pits, and $f_T(x)$ is the probability density of true pit depth distribution.

True pit depth is simulated from an exponential distribution as shown in Figure 5.5. A Binomial random number is used to generate a detected pit depth, the parameter of the Binomial distribution is taken from Eq. (5.38). A large population of true pit depths (10 million) is simulated to obtain a sample of detected pit depths. The probability is obtained empirically as the fraction of detected sample exceeding 95% TWD to the number of detected pit depths. The probability of pit depth exceeding 95% TWD is calculated to be 0.4% which is higher than 0.18% obtained from true depth distribution. Similarly the probability of pit depth exceeding 51% TWD is calculated to be 7.43%. The simulation study indicated that the detection uncertainty on pit depths over estimates the probability of tube leak when compared to the true estimate of leak probability. The probability of pit depth exceeding 95% TWD from the undetected sample is conducted in the same way from a large sample (10 million) of true pit depths which is calculated to be very low (0.0021%).

Since the detection uncertainty affects the leak probability estimates it is therefore needed to account for detection uncertainty in probability modeling. The detection uncertainty can be accounted for in estimating the true depth distribution from the detected depth distribution. The true depth distribution of corrosion pits can be derived by

$$f_T(x) \propto \frac{f_d(x)}{POD(x)}$$
$$f_T(x) = \frac{1}{k}\frac{f_d(x)}{POD(x)}; \quad k = \int_0^\infty \frac{f_d(x)}{POD(x)}dx \tag{5.40}$$

where $f_d(x)$ is the probability density of detected pits and $f_T(x)$ is the probability density of true pit depth distribution and k is a normalizing constant. The mean and variance of the true pit depth distribution can be calculated as

$$\mu_T = \int_0^\infty x f_T(x)dx = \int_0^\infty x\frac{1}{k}\frac{f_d(x)}{POD(x)}dx$$
$$\sigma_T^2 = \int_0^\infty (x-\mu_T)^2 f_T(x)dx \tag{5.41}$$

Similarly, the distribution of the undetected pit depths can be derived using the probability of detection concept which is given as

$$f_{ud}(x) \propto \big(1 - POD(x)\big)f_T(x)$$
$$f_{ud}(x) = \frac{1}{k_u}\big(1 - POD(x)\big)f_T(x); \qquad k_u = \int_0^\infty \big(1 - POD(x)\big)f_T(x)dx \tag{5.42}$$

where $f_{ud}(x)$ is the probability density of undetected pits and $f_T(x)$ is the probability density of true pit depth distribution and k_u is a normalizing constant. The mean and variance of the undetected pit depth distribution can be calculated as

$$\mu_{ud} = \int_0^\infty x f_{ud}(x)dx = \int_0^\infty x\frac{1}{k_u}\big(1 - POD(x)\big)f_T(x)dx$$
$$\sigma_{ud}^2 = \int_0^\infty (x-\mu_{ud})^2 f_{ud}(x)dx \tag{5.43}$$

Considering the detected pit depth distribution and probability of detection (POD) function from Eq. (5.38), the probability density function for true pit depth and undetected pit depths can be estimated.

5.8.1.2 Effect of Measurement Error

The measured pit depths from eddy current probes are associated with measurement error due to uncertainties from various sources as discussed in Section 5.7. A simplistic model to account for measurement error (ME) is a linear effect model as given by

$$Y = X + \mathrm{E} \tag{5.44}$$

where Y is the random variable for measured pit depth, X is the random variable for actual pit depth, and E the measurement error variable. It is assumed that the measurement error is independent of actual pit depth. The measurement error is generally assumed to be normally distributed with mean zero and a specified standard deviation. The measurement error of eddy current inspection probe is usually quantified by calibrating the measurements from sample observation of pulled tubes. The measurement error of inspection probes can also be quantified from repeat inspection data as demonstrated in Section 5.7.1. For the case of illustration the measurement error is assumed to follow normal distribution $\mathrm{N}(0,\sigma)$ with mean zero and standard deviation σ of 10% TWD.

A random number for true pit depth is simulated from the exponential distribution as shown in Figure 5.5. The measured pit depth is then indicated by assigning a random number from normal distribution to the true pit depth. A large population of true pit depths (10 million) is simulated to obtain a sample of measured pit depths. The probability of pit depth exceeding 95% TWD is obtained as the fraction of measured sample exceeding 95% TWD to the sample size. The probability of pit depth exceeding 95% TWD is calculated to be 0.22% which is slightly higher than 0.18% obtained from true depth distribution. Similarly the probability of pit depth exceeding 51% TWD is calculated to be 4.16%. The simulation study indicated that the effect of measurement error over estimates the probability of exceedences when compared to the true estimates.

Since the measurement error effects the estimation of tube leak probability it therefore accounted in probability modeling. The distribution for measured pit depth can be derived as using the measurement error model given in Eq.(5.44).

The conditional distribution on measured pit depth given the distribution of actual pit depth can be obtained as

$$F_{Y|X}(y) = \Pr(\mathrm{E} < y - x \mid X = x) \tag{5.45}$$

The marginal distribution of observed pit depth can then be obtained as

$$F_Y(y) = \int_0^\infty \Phi\left(\frac{y-x}{\sigma}\right) f_X(x)dx \tag{5.46}$$

Similarly the probability density function for observed pit depth can be obtained as

$$f_Y(y) = \int_0^\infty \frac{1}{\sqrt{2\pi}\sigma} \exp\left(-\frac{(y-x)^2}{2\sigma^2}\right) f_X(x)dx \tag{5.47}$$

The probability of observing *n* number of pit depths from eddy current inspection is given by the likelihood function given as

$$L(\Theta, \sigma) = \prod_{i=1}^{n} \left\{ \int_0^\infty \frac{1}{\sqrt{2\pi}\sigma} \exp\left(-\frac{(y_i - x)^2}{2\sigma^2}\right) f_X(x;\Theta)dx \right\} \tag{5.48}$$

The parameters of the likelihood function can then be estimated by maximizing the logarithm of likelihood function using standard maximization routines. The distribution of actual detected pit depth distribution can be estimated by likelihood method as described in this section.

5.8.1.3 Combined Effect of Detection and Measurement Error Uncertainty

In actual field measurement the pit depths are usually associated with detection uncertainty and measurement error of the eddy current inspection process. In this simulation study the true pit depth distribution considered in Figure 5.5 is introduced with probability of detection (POD) and measurement error as discussed in previous sections. Detection uncertainty is introduced first as the POD in Eq. (5.36) is defined on the true pit depth to obtain detected pit depths which is then introduced with measurement error. A large sample (10 million) of true pit depths is simulated by introducing detection uncertainty and measurement error to obtain a realistic sample of detected pit depths. The probability of pit

depth exceeding 95% TWD is obtained empirically as the fraction of detected sample exceeding 95% TWD to the number of detected pit depths. The probability of pit depth exceeding 95% TWD is calculated to be 0.51% which is higher than 0.18% obtained from true depth distribution. Similarly the probability of pit depth exceeding 51% TWD is calculated to be 9.02%.

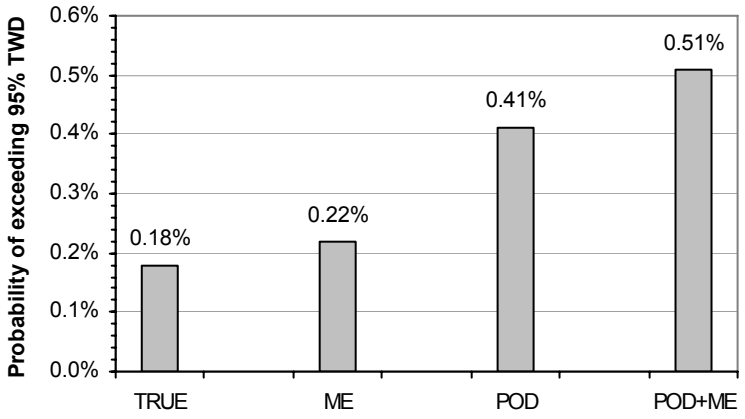

Figure 5.7: Effect of pit depth uncertainties on probability of pit depth exceeding 95% TWD

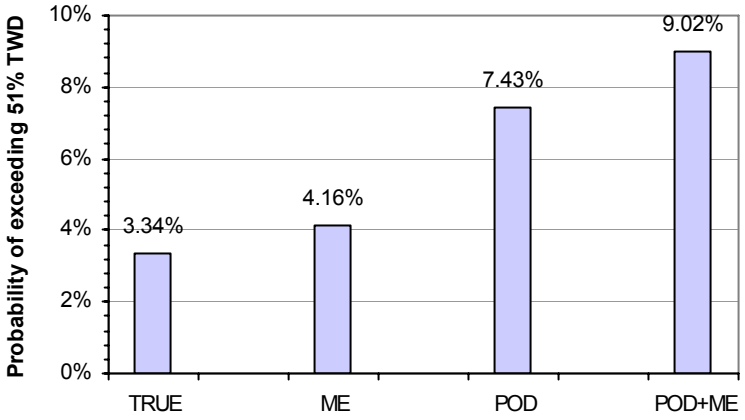

Figure 5.8: Effect of pit depth uncertainties on probability of pit depth exceeding 51% TWD

The effect of pit depth uncertainties on estimating the probability of exceeding 95 % TWD is shown in Figure 5.7. The results indicate that the

uncertainty in detection (POD) and measurement error (ME) over estimates the true estimate of the probability of exceedences. It is therefore required to account for measurement error and probability of detection on pit depths in probability modeling.

5.8.2 Remarks

The event of interest in the context of life cycle management is the probability of tube leak which results in forced outage and the number of tubes plugging. In order to estimate the tube leak probability from eddy current inspection data it is required to account for uncertainties in pit depth measurements. In this section a simulation study is conducted to estimate the effect of uncertainties in pit depths towards estimation of probability of pit depth exceeding 95% or 51% TWD. The results indicate that the measurement error and detection uncertainties over estimate the exceedence probabilities when compared to the estimate from true pit depth distribution. The uncertainties in pit depth measurements are therefore needed to account for in probability modeling. The section also discusses the probability models in accounting for such uncertainties in estimating the true pit depth distribution.

5.9 Inspection Uncertainty in Modeling Pitting Corrosion of Steam Generators

Due to costs involved in eddy current inspection of SG tubes it is not economical to conduct frequent inspections. Usually the SG tubes are either partially inspected every 2-4 years or more frequently depending on the extent of aging SG tubes. Such situations limit the amount of data required to model the random pitting process of a particular SG. The detected pit depths from eddy current inspections are also associated with probability of detection, measurement error and censoring of pit depths. Corrosion pits with depth $\leq$ 30% TWD cannot be measured accurately due to inherent noise in eddy current probes and therefore indicated as censored pit depths. Such uncertainties in inspection process hinder the estimation of realistic tube leak probability.

5.9.1 Simulation Analysis

The standard practice in industry is to plan a scheduled outage every two years. For a reactor unit the number of SGs inspected usually depends on the extent of degradation in SGs. For the simulation study conducted in this section the reactor unit is considered to have 12 SGs each experiencing similar pitting corrosion degradation process. Hence the data from the SGs inspected are grouped to model the uncertainty in corrosion pitting process for a single SG. The objective of this study is to quantify the uncertainty in estimating the tube leak probability and number of tubes plugged per SG under different inspection plans. The inspection plans considered are the number of SGs (3, 6, 9, and 12) inspected every two years.

The analysis considers a known pit generation process for a particular SG in estimating the probability of tube leak in the next outage from the pit depth data obtained from simulation. The pit occurrence follows a Poisson distribution with mean rate following Weibull power law rate as discussed in Section 5.2.2. The parameters for the SG pit generation model per SG are taken as 1.382 as scale (α) and 2.5 as scale parameter (β) to reflect the actual observation from industry. Assuming the process starts at year 0, the mean rate of pitting in an interval [0 t] in a single SG for a period of 16 years is shown in Figure 5.9.

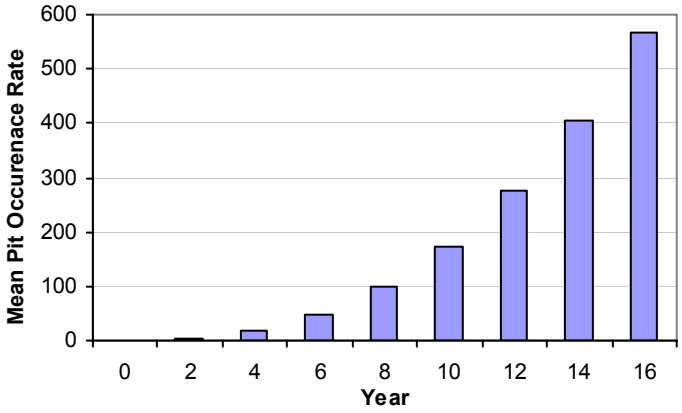

Figure 5.9: Mean pit occurrence rate plot

Using the Pit occurrence rate from Figure 5.9 and considering the true pit depth distribution from Section 5.8 the extreme pit depth model from Section 5.4 is applied to estimate the mean occurrence rate of extreme pits (Eq. 5.12) and the expected annual leak probability (Eq. 5.14) as described in Section 5.4. The tube leak probability in next outage is calculated by considering the leak criterion (z) as 95% TWD.

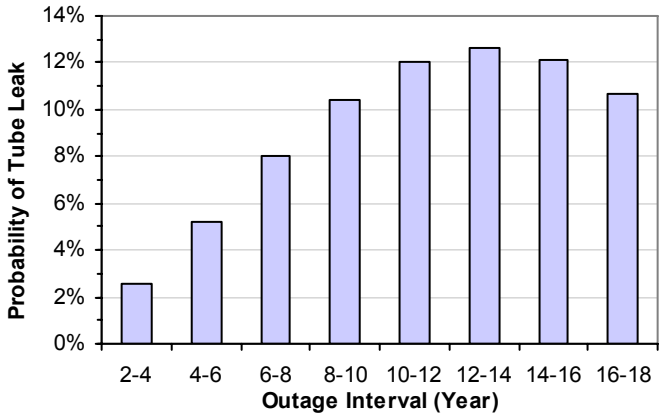

Figure 5.10: Probability of tube leak in next outage

The probability of tube leak predicted in next outage is shown in Figure 5.10 at each inspection outage for a period of 16 years using true pit depth distribution. The probability of tube leak prediction in outage years 2-4 is calculated as 2.5% at outage year 2 as shown in Figure 5.10. Simulation study is conducted by introducing the detection uncertainty and measurement error on pit depths. The results from the analysis are then compared to the probability of tube leak in next outage calculated from true pit depth (Figure 5.10).

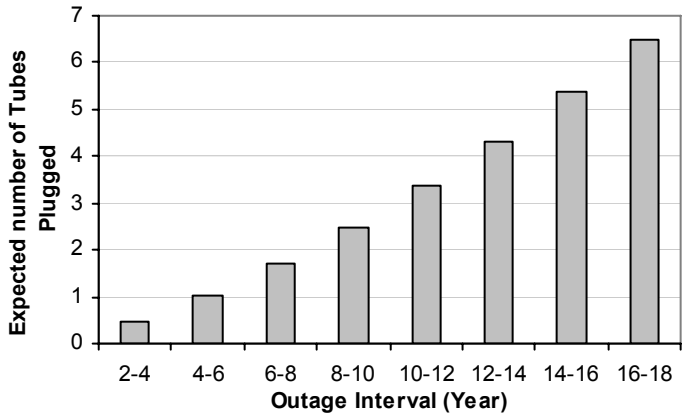

Figure 5.11: Expected number of tubes plugged in next outage

Similarly the expected number of tubes plugged predicted in next outage is shown in Figure 5.11 at each inspection outage for a period of 16 years. The results from the simulation analysis are then compared to the expected number of tubes plugged in next outage calculated from true pit depth distribution as shown in Figure 5.11.

5.9.1.1 Procedure

The inspection plans are designated as plans 1-4 for inspecting 3, 6, 9, and 12 SGs at each inspection outage. Under an inspection plan the pit generation is simulated using the model shown in Figure 5.9 for a period of 16 years. Since pit depth is a random variable, the pit depths are simulated from a true pit depth distribution as shown in Figure 5.5. Probability of detection and measurement error uncertainty is then introduced as discussed in Section 5.8.1 to obtain a realistic detected sample in each outage. The detected pit depth sample is then grouped from all SGs from all previous inspection outages to estimate the pit depth distribution and pit generation rate. The pit depth distribution is assumed to follow exponential where the distribution parameter is estimated from maximum likelihood method to account for censored sample with pit depth $\leq$ 30% TWD. A flow chart of the simulation analysis procedure is shown in Figure 5.12. The probability of tube leak and the number of tubes plugged for the next outage per SG are estimated at each inspection outage.

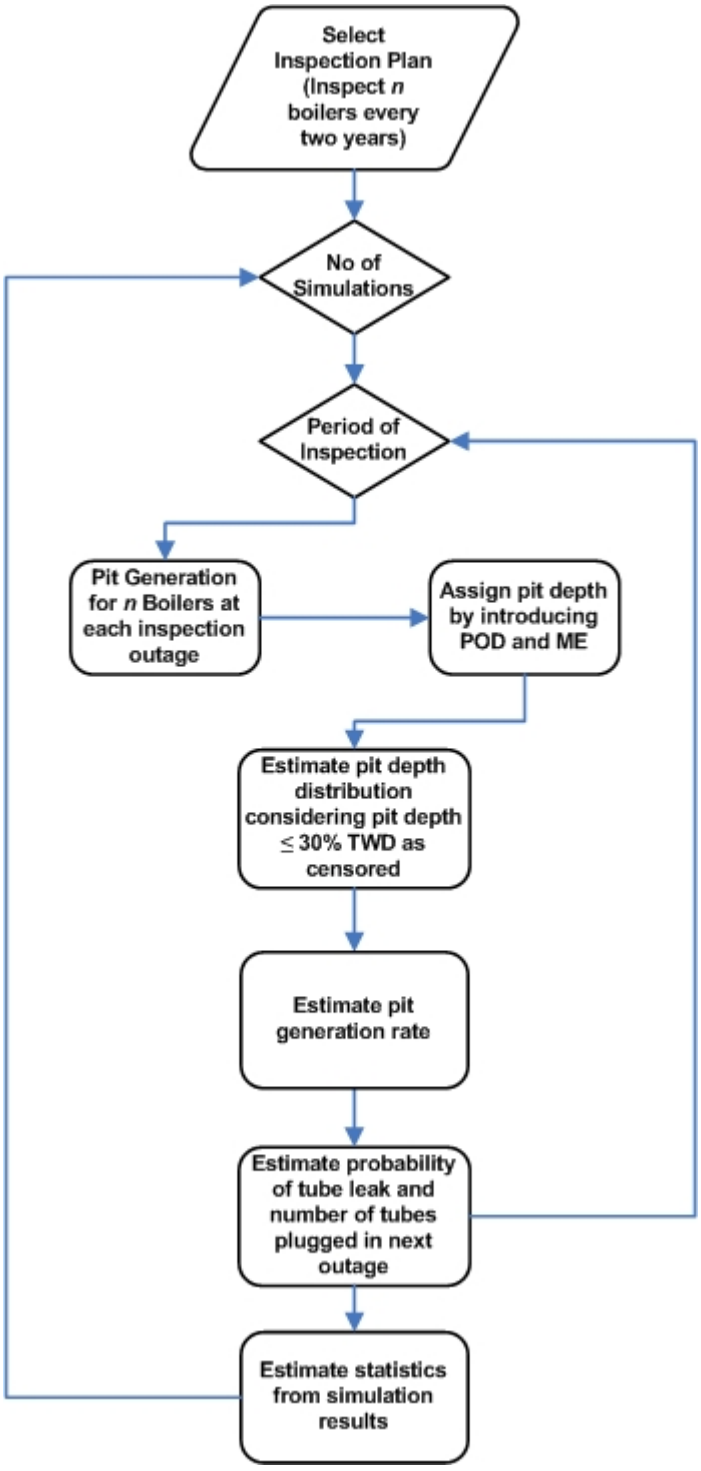

Figure 5.12: Flow chart on simulation analysis procedure

Under each inspection plan 10000 simulations are conducted to obtain the statistics on the estimate of tube leak probability and number of tubes plugged at

next outage. The results on probability of tube leak prediction from simulation analysis are shown in Figures 5.13-5.16.

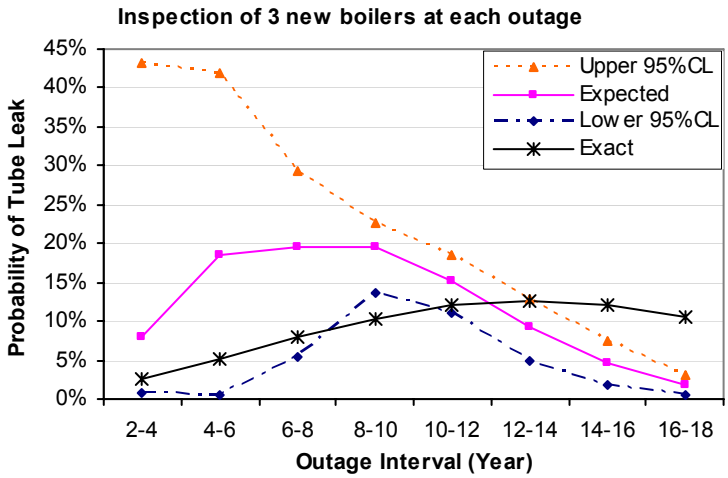

Figure 5.13: Probability of tube leak prediction in next outage under inspection plan 1

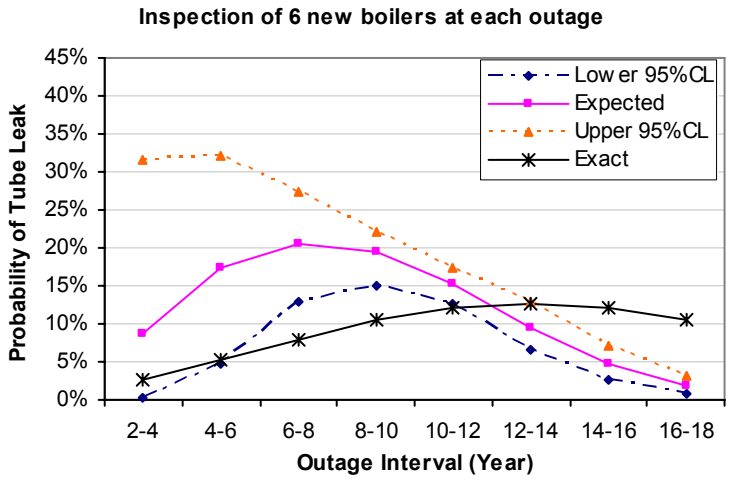

Figure 5.14: Probability of tube leak prediction in next outage under inspection plan 2

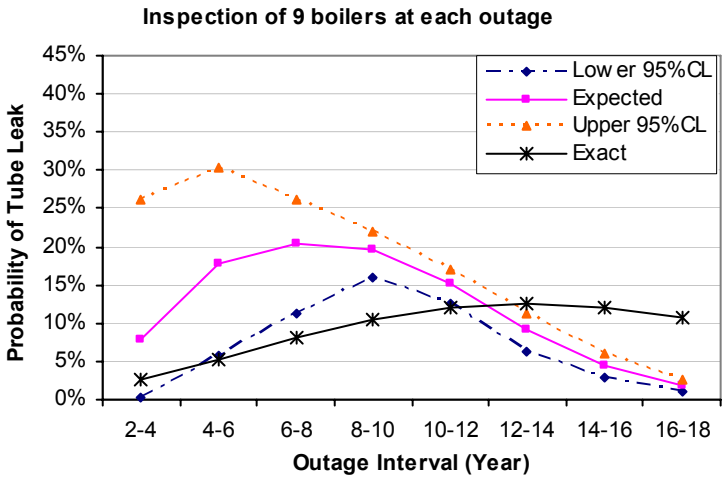

Figure 5.15: Probability of tube leak prediction in next outage under inspection plan 3

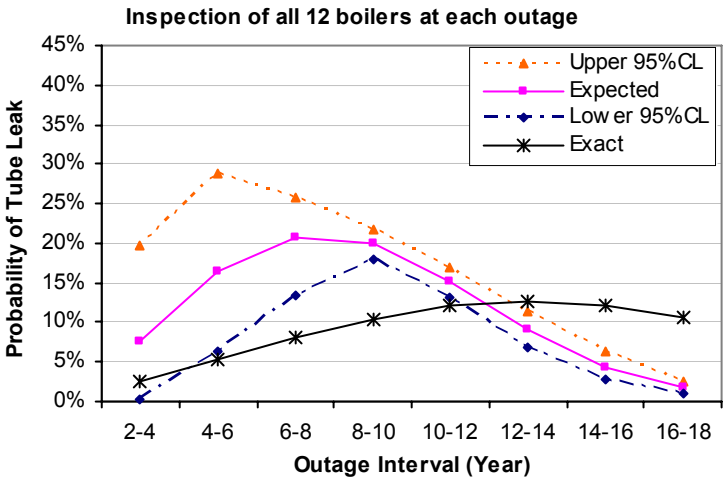

Figure 5.16: Probability of tube leak prediction in next outage under inspection plan 4

The obvious result from Figures 5.13-5.16 is that, the more the number of SGs inspected the lesser is the sampling uncertainty in estimating the leak probability estimate. The results indicate that inspecting more than 6 SGs at each outage provide reasonable estimates on probability of tube leak predictions. Since the uncertainty in estimating the leak probability is mostly from the number of pit depth measurements recorded. The results from simulation analysis in Figures

5.13-5.16 indicate that the uncertainty in eddy current inspection of pit depths greatly bias the estimate on leak probability. The results indicate that the uncertainty in pit depth measurements result in over estimating the leak probability estimate until around year 10 and under estimating the true leak probability estimate in the later years.

The results on predicting the number of tubes plugged from simulation analysis are shown in Figures 5.17-5.20.

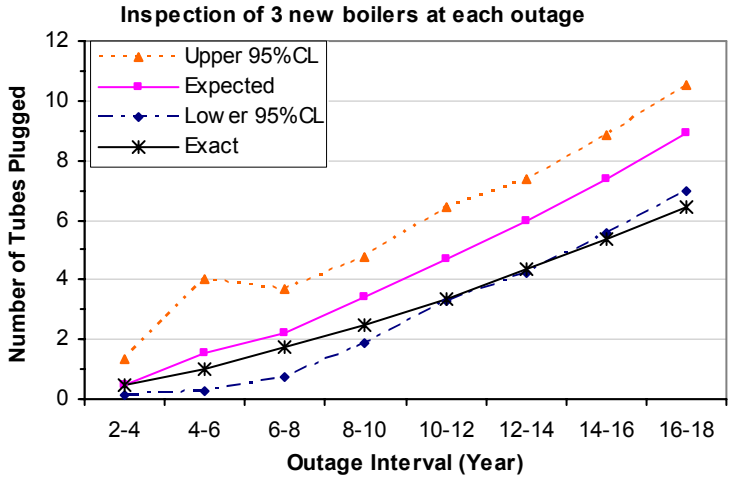

Figure 5.17: Number of tubes plugged predicted in next outage under inspection plan 1

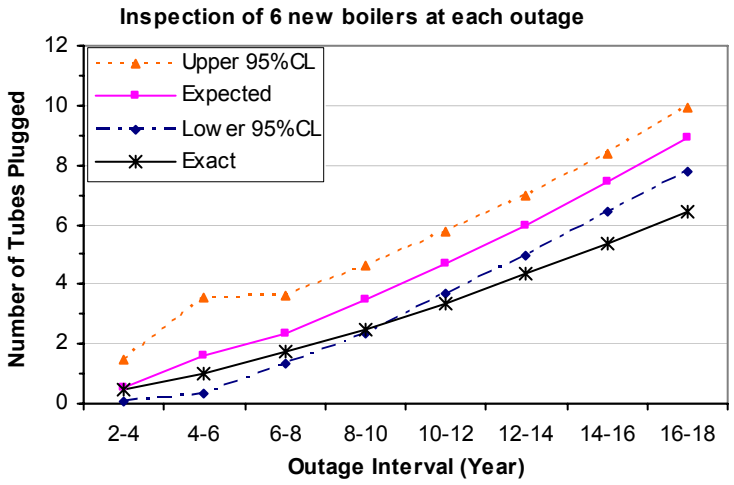

Figure 5.18: Number of tubes plugged predicted in next outage under inspection plan 2

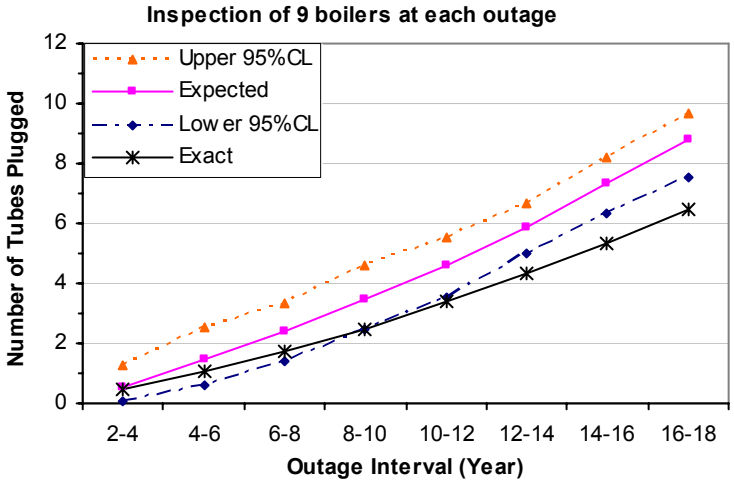

Figure 5.19: Number of tubes plugged predicted in next outage under inspection plan 3

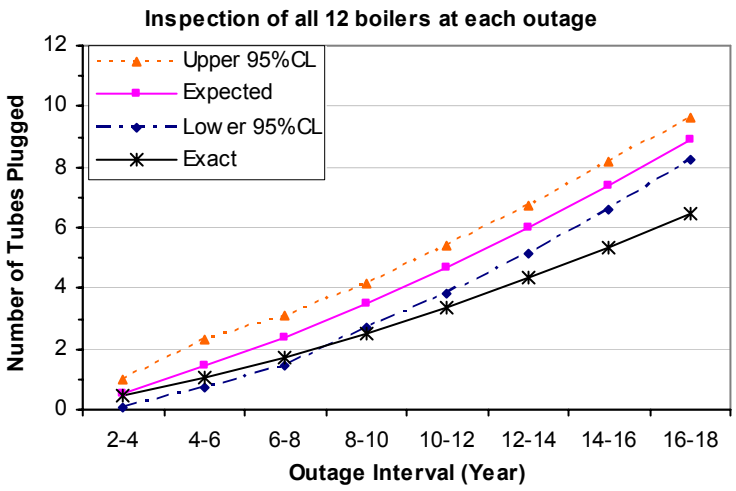

Figure 5.20: Number of tubes plugged predicted in next outage under inspection plan 4

The sampling uncertainty in predicting the number of tubes plugged in the next outages decreases with the number of SGs inspected as shown Figures 5.17-5.20. But the sampling uncertainty in predicting the number of tubes plugged is not significant when compared to the results from leak probability predictions. The uncertainties in pit depth measurements over estimate the prediction of number of tubes plugged in next outage when compared to exact predictions from true pit depth distribution.

5.9.2 Remarks

The prediction of probability of tube leak in next outage is greatly biased by uncertainties in eddy current inspection of pit depths as shown in Figure 5.21. This result is independent of inspection plans considered. The uncertainties in pit depth measurements over estimate the probability of tube leak prediction in next outage until around 10 years, and under estimate the leak probability prediction in the later years when compared to the leak probability estimate from true depth distribution. The effect of sampling uncertainty for different inspection plans towards probability of leak predictions is shown in Figure 5.22. The sampling uncertainty decreases as more data is collected in each outage. The increase in

COV in later years as shown in Figure 5.22 is due to the expected value of leak probability is lower in later outage interval..

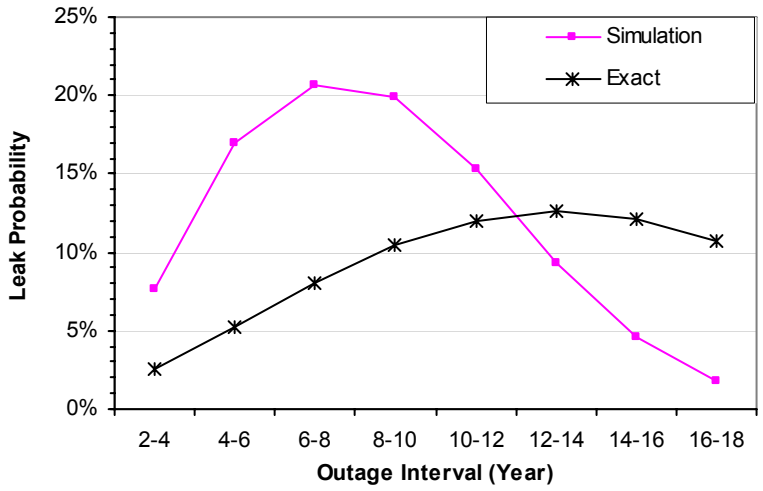

Figure 5.21: Comparison of the exact and simulation results for leak probability

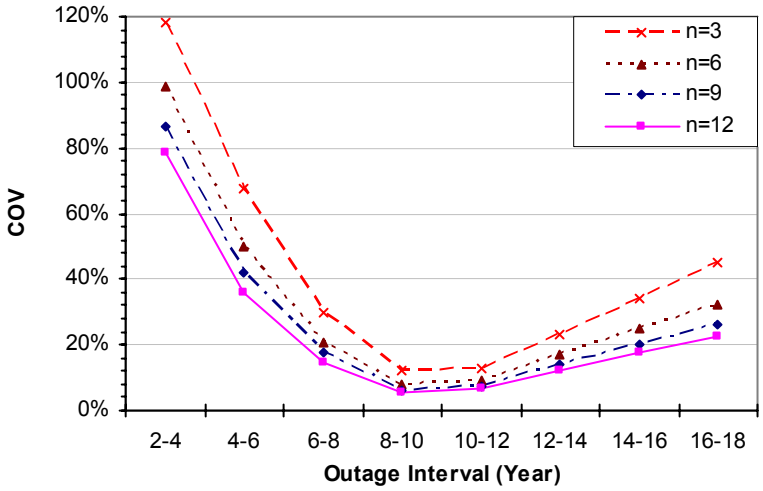

Figure 5.22: COV in leak probability prediction for different inspection plans

The prediction on number of tubes plugged in not greatly biased by uncertainties in eddy current inspection of pit depths as shown in Figure 5.23. The uncertainties in pit depths over estimate the prediction on number of tubes plugged in next outage at in later years of inspection. The sampling uncertainty in inspection plans is not very significant in prediction of number of plugged tubes as shown in Figure 5.24 at least in later outage intervals.

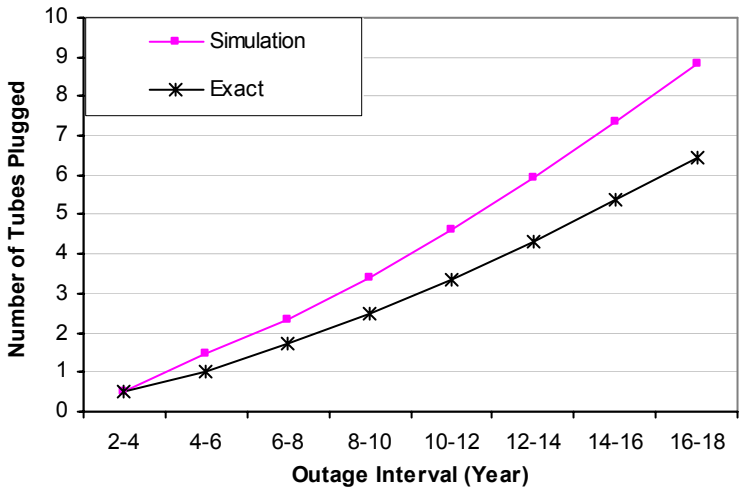

Figure 5.23: Comparison of the exact and simulation results for number of tubes plugged

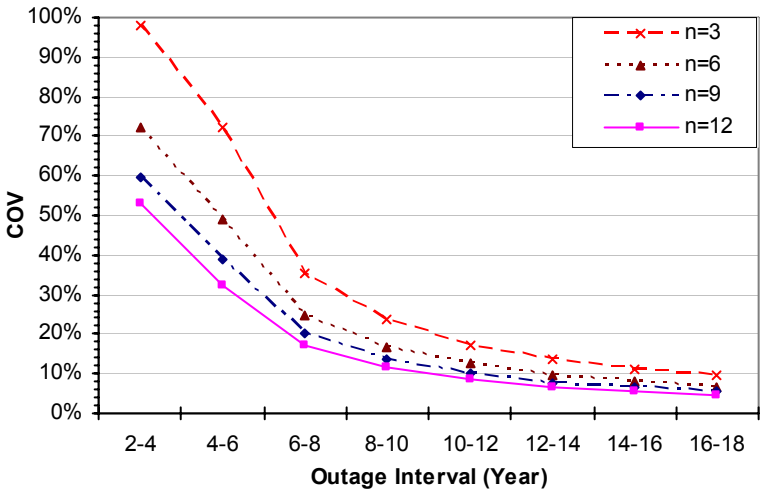

Figure 5.24: COV in number of tubes plugged under different inspection plans

5.10 Conclusions

An overview of life cycle management issues in steam generators of nuclear power plants is discussed. There is a need for efficient life cycle management decisions based on the current degradation of SGs. Probabilistic modelling of steam generator degradation mechanisms provides a great tool for quantifying the uncertainties in degradation and for modelling optimal maintenance decisions.

In the case of steam generator pitting corrosion, the rate of pit generation is modeled as a non-homogeneous Poisson process which falls into the class of stochastic birth process model. The pitting activity is observed during various outages of the plant's history by the use of eddy current inspection. The parameters of the pit generation process are estimated by taking into account both censored observations and non-censored observations. The pit depth distribution exceeding a threshold pit depth is modeled as the generalized Pareto distribution (GPD), which falls into the class of extreme value distribution. The generation of extreme pits also follows Poisson process, with pit depth distribution following GPD which can be characterized as a marked point process.

The results are presented from the stochastic model in estimating the expected number of extreme pits and the annual leak probability during future operation crucial for steam generator life management decision modelling. Some results on probability of first leak or n^{th} leak can be applicable to steam generator fitness for service assessments and life cycle management planning.

The effect of measurement error and detection uncertainty in eddy current inspections on measured defect depths is presented from simulation results. The results indicate that the measurement error and detection uncertainties overestimate the exceedence probabilities compared with the estimate from true pit depth distribution. The probability models provide a framework in quantifying the uncertainties and in estimating the true defect distribution models. The probability model on true defect distribution is needed for a realistic estimate of the uncertainty in pitting corrosion degradation of steam generators.

The effects of uncertainties in the eddy current inspection process for a reactor unit are demonstrated through a simulation study. Pitting corrosion degradation in each SG is simulated from a known stochastic model for a period of 16 years. The pit depth measurements are introduced with uncertainties from detection and measurement error. The censoring in pit depths is considered in estimating the pit depth distribution from simulated observations due to threshold limits on measuring pit depth from eddy current probes. The parameters of the

stochastic model are estimated by grouping the data from all SGs at an inspection outage to predict the probability of leak and the number of tubes plugged in next outage.

The prediction of the probability of tube leaks in next outage is greatly biased by uncertainties in eddy current inspection of pit depths. The uncertainties in pit depth measurements overestimate the probability of tube leak prediction in next outage until around 10 years, and underestimate the leak probability prediction for the later years compared with the leak probability estimate from true depth distribution. The prediction on number of tubes plugged in not greatly biased by uncertainties in eddy current inspection of pit depths. The uncertainties in pit depths overestimate the prediction on number of tubes plugged in next outage in later years of inspection. However, the sampling uncertainty in inspection plans is not very significant in predicting the number of plugged tubes.

CHAPTER 6
STEAM GENERATOR LCM APPLICATION

6.1 Introduction

Previous chapter discuss the pitting corrosion model and estimation methods applicable to steam generator life cycle management. This chapter deals with actual field inspection data obtained from industry. The application and benefits of the model are illustrated in the context of lifecycle management of a steam generator. Optimization on the chemical cleaning cycle of a SG is presented.

6.2 Data Analysis

The probabilistic modelling of pitting corrosion in this chapter is based on the reported results from eddy current inspection of several steam generators at a nuclear generating station. The SGs considered in this study have undergone two separate water lancing and chemical cleaning (WL/CC) campaigns in a period of approximately eight years. Therefore, only data between two WL/CC campaigns (i.e maintenance interval) will be used.

Only pits greater than or equal to 50% through-wall depth (TWD) observed during maintenance interval is considered for extreme pit generation model. There is less uncertainty in the detection of these deeper pits, and also higher confidence in the reported depths. Furthermore, deeper pits have higher significance in the context of steam generator LCM with regards to tube plugging and potential for through-wall penetration.

The database provided by industry consists of 122 pits $\geq$ 50% TWD, and their distribution is shown in Figure 6.1. Due to similar operating environment the results from all SGs are considered together as one sample.

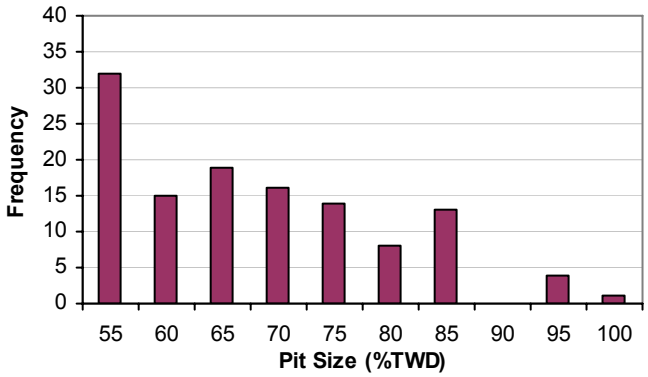

Figure 6.1: Distribution of pit sizes ≥ 50% TWD

The number of new pits generated gradually increases with the time of inspection, as shown in Figure 6.2. An increase over time is also related with the increase in sludge that provides favourable crevice conditions for pit generation.

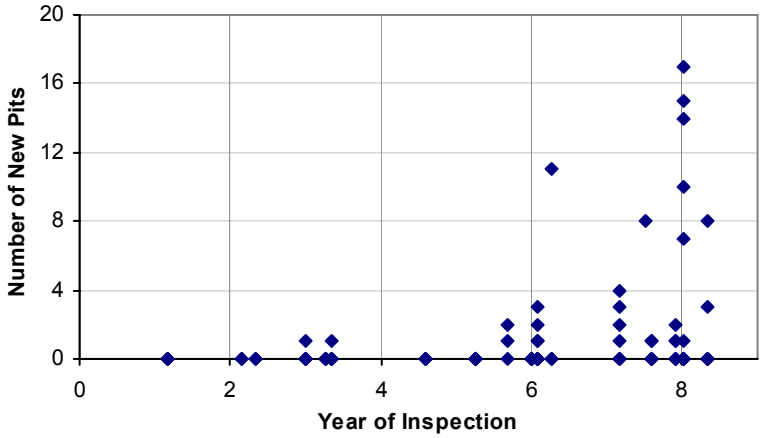

Figure 6.2: Generation of new pits during different inspection outages

6.2.1 Model Parameter Estimation

6.2.1.1 Estimation of the Pit Generation Rate

The pit generation rate is estimated from maximum likelihood method as described in Section 5.3 following Poisson process. The maximum likelihood estimates of the parameters of the Poisson models are presented in Table 6.1.

Table 6.1: Parameters of the pit generation process

Model	Parameters	Estimate	Standard Error
Homogeneous Poisson Process (HPP)	Mean Rate (λ)	0.373	0.034
Non-Homogeneous Poisson Process (NHPP)	Shape (β)	4.526	0.530
	Scale (α)	0.0014	0.0014

The sampling uncertainty in estimating the mean rate function of the NHPP model with confidence limits (CL) is shown in Figure 6.3.

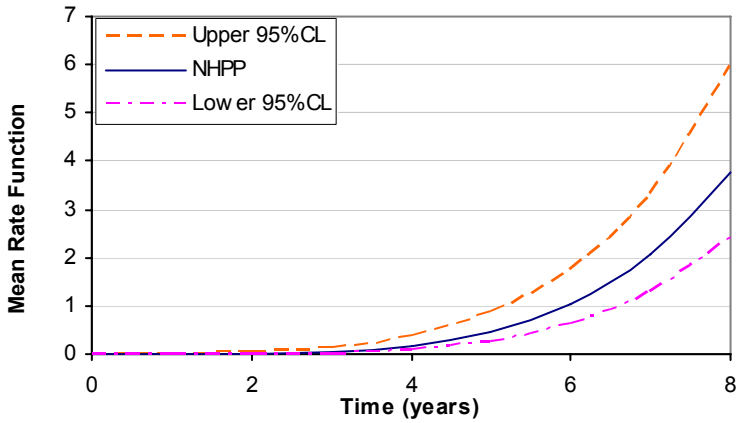

Figure 6.3: Mean rate function of NHPP process of pit generation in a SG

The likelihood ratio statistic (LRS) as described in Section 5.3.1 is conducted to the test for HPP. An $LRS = 119.6$ is obtained from the likelihood analysis for which the p-value is zero. Therefore, the null hypothesis is rejected at the 5 % level of significance, and it is concluded that the pit generation rate is not constant in time and does not follow the homogeneous Poisson Process (HPP).

6.2.1.2 Estimation of the Pit Depth Distribution

From the pit data (Figure 6.1) the parameters of the generalized Pareto model are estimated by using the method of moments. The estimated parameters are given in Table 6.2.

Table 6.2: Parameters of the pit depth distribution

Method	**Shape (ξ)**	**Scale (σ)** (% TWD)	**Threshold (*u*)** (% TWD)
Method of moments	0.509	25.51	49

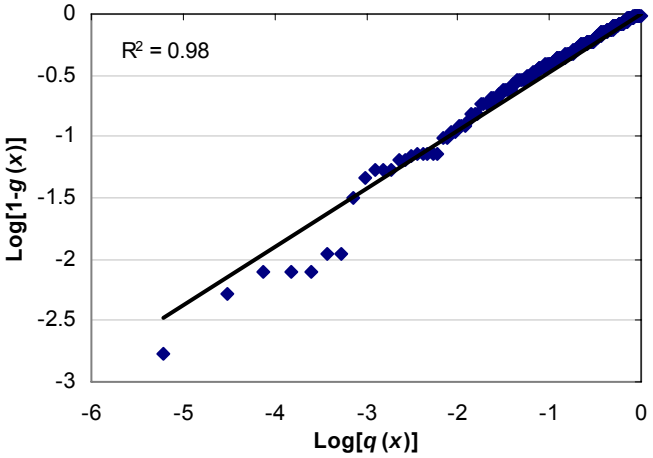

Figure 6.4: The GPD probability paper plot of the pit depth data

The goodness of fit of the GPD model is investigated using the probability paper plot. To derive axes of the probability plot, Eq. (5.8) is rewritten as

$$Log\left(1-\xi\frac{x-u}{\sigma}\right)=\xi Log(1-F_X(x)) \tag{6.1}$$

The X-axis of the plot is defined as Log(1- $F_X(x)$) = Log($q(x)$) and the Y-axis as Log(1- $g(x)$), where $g(x) = \xi(x - u)/\sigma$. The sample data are plotted along these axes, as shown in Figure 6.4. The R^2 value of 0.98 confirms that the GPD model provides a good fit to the data.

6.3 Model Application

Assessing the risk associated with tube leakage and the exceedance of the tube plugging margin in the next operating period are important considerations for steam generator life-cycle management. The proposed probabilistic model for pitting corrosion can be used to answer these questions.

6.3.1 Probability of Tube Leak

Operational experience and other evidence suggest that a corrosion pit may leak when its depth is of the order of 95 % TWD. Therefore, the probability of tube leakage per SG in a time interval (0 - t) can be computed from the extreme value distribution (Eq. 5.14) for z = 95%.

As shown by the results in Figure 6.5, the probability of tube leakage in the early years in a SG is negligible, but it increases rapidly in later years, exceeding 1 % in the 8th year.

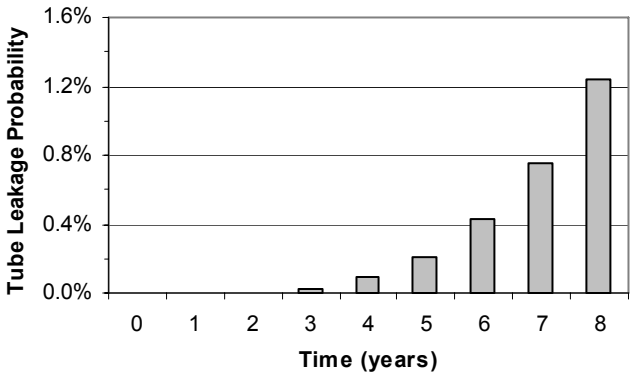

Figure 6.5: Annual probability of tube leakage in a SG

6.3.2 Tube Plugging

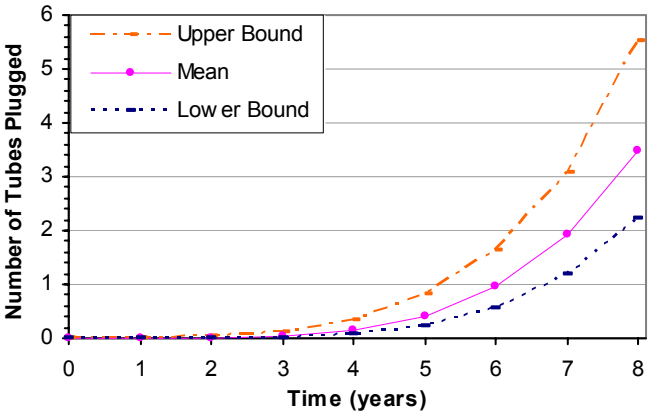

Figure 6.6: Expected number of plugged tubes

From the proposed model, the average number of tubes to be plugged in an 8-year interval is estimated as 3.5 tubes per SG using Eq. (5.12). Note that the plugging limit is assumed to be equal to 51 % TWD. The sampling uncertainty in estimating the expected number of tubes plugged is shown in Figure 6.6. In fact, the distribution of the number of tubes plugged in an 8 year interval follows the Poisson distribution as shown in Figure 6.7.

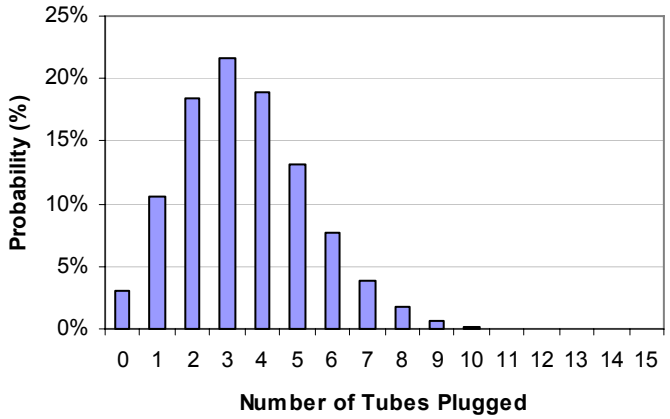

Figure 6.7: Distribution of the number of tubes plugged per SG

6.3.3 Time to Leak

Based on the results from pit generation rate and pit depth distribution, the time to leak as discussed in Section 5.6 can be estimated. Considering z = 95 %TWD as leak criterion, Eq. (5.23) gives the survival distribution for time to first leak.

$$P(T_1 > t) = \exp\left(-2.28 \times 10^{-06} \times t^{4.526}\right) \tag{6.2}$$

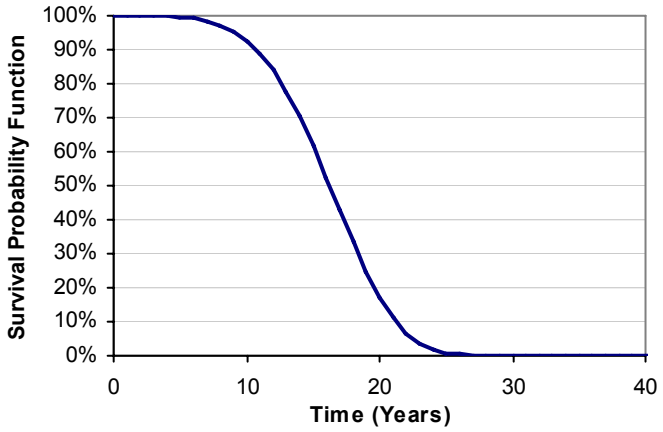

Figure 6.8: Survival probability function plot for time to first leak

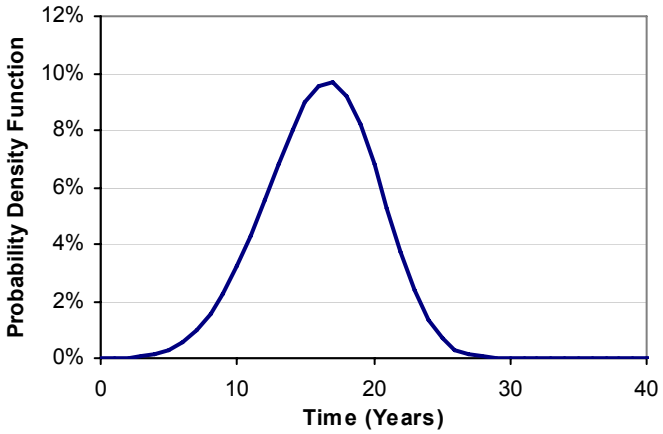

Figure 6.9: Probability density function plot for time to first leak

The survival probability plot is shown in Figure 6.8 along with probability density function plot as shown in Figure 6.9. The expected time to first leak is calculated from Eq. (5.21) as 16.1 years.

Similarly considering x = 51 %TWD as plugging criterion, Eq. (5.23) gives the probability distribution for the first time to meet plugging criterion. The expected time to first failure /SG can be calculated from Eq. (5.21), the results are shown in Table 6.3.

Table 6.3: Expected time to first failure per SG

Failure Event	Pit Depth (Criterion)	Expected time to first failure
Leak	95 % TWD	16.1 Years
Plugging	51 % TWD	5.5 Years

Considering z = 95 %TWD as leak criterion, Eq. (5.26) gives the probability distribution for time to n^{th} leak. Considering z = 51 %TWD as plugging criterion, Eq. (5.26) gives the probability distribution for the time to n tubes plugged. The expected time to n^{th} failure per SG is shown in Table 6.4.

Table 6.4: Expected time to n^{th} *failure per SG*

Event	n^{th} Failure	Pit Depth (Criterion)	Expected time to n^{th} failure
Leak	3^{rd} leak	95	22.3 Years
Plugging	20 tubes	51	12.2 Years
Plugging	40 tubes	51	14.2 Years

6.4 Measurement Error Analysis from Field Inspections

6.4.1 Data Summary

The corrosion pit data observed during inspection outages from a nuclear generating station of steam generator using probes C1, C2, and X. The measuring probes in order of increasing resolution are C1<C2<X, where the X-probe is the latest addition in SG tube inspection due to higher resolution and characterization of flaws as discussed in Section 5.1.1.2. The pit depths measured by at least two probes in an inspection outage are paired for the analysis discussed in Section 5.7.1.2. Most of the observations from C1 probe are censored and hence not considered in the analysis. The data from all the SGs of a nuclear generating station are grouped together for the analysis of probe measurement error as described in Section 5.7.1.

6.4.2 Statistical Analysis

6.4.2.1 C2 Probe and X Probe

X probe is recently introduced in SG tube inspection whereas C2 has been used for many years. The repeat observations from these two probes are 191 pit depths and are non-censored observations. The plot on all pit indications from C2 and X is shown in Figure 6.10 along with linear regression estimate.

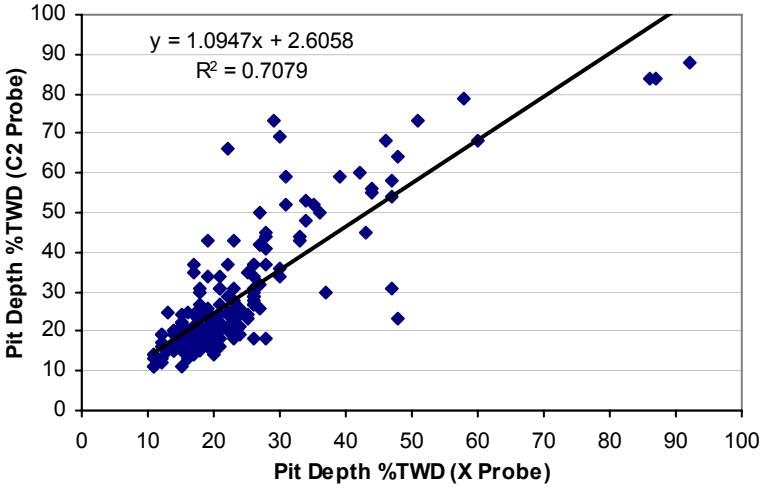

Figure 6.10: Repeat measurement on pit depth from C2 and X probe

Most of the data is populated around pit depths <30%tw, the plot also shows a good linear fit with R^2 of 0.7. The results from statistical analysis as described in Section 5.7.1 is summarised in Table below

Table 6.5: Summary on statistical results of repeat inspection data

Probes	Mean (%TWD)	Variance (%TWD)	COV	Relative Bias	RMSD	ME (%TWD)	SE (%TWD)
C2	27.9	254.9	164.8	4.8	9.9	8.5	11
X	23.1	150.6				1.7	8.2

In practice the RMSD of 9.9%tw between C2 and X probe is assigned to bad probe. Actually the RMSD is contributed from the uncertainties in both probes as

well as bias in measuring the actual pit depths. The constrained expected likelihood (CEL) method is used to quantify the measurement error in each probe. The measurement error is 8.5 %TWD on C2 and 1.7 %TWD on X probe respectively. The standard error in estimating the measurement error is large as shown in Table 6.5. The sampling uncertainty can be minimized with collection of more data.

6.5 Steam Generator LCM Model

6.5.1 Life Cycle Costing

All future costs of maintaining equipment are calculated in present value terms using the net present value (NPV) approach.

$$NPV = \sum_{i=0}^{T} C_i \left[\frac{1 + k/100}{1 + d/100} \right]^i \tag{6.3}$$

Where C_i is the cost incurred in year i, $k\%$ & $d\%$ are the inflation and discount rates. The net present value as given in Eq. (6.3) is the amount of money to be invested at the present time to pay the future costs incurred during a period of T years. The inflation rate is not considered in this section ($k = 0\%$).

This approach is generally accepted in power industries to compare various alternating course of actions over a range of future years. Life cycle costing usually involves optimizing maintenance decisions which is done by minimizing the expected value of NPV.

Attention should be paid in reviewing and planning maintenance models to ensure that costs associated with maintenance and those resulting from failures are properly reflected. The costs associated with maintenance are usually the planned preventive maintenance activities and the unplanned corrective maintenance actions resulting from unexpected failures. Unexpected failures also results in value of lost production and other consequential costs from failure. All such costs are important to include in the maintenance model to ensure that the

best policy is not just minimizing the maintenance cost but in maximizing the value of the asset.

6.5.2 SG LCM Costing

To extend the life of steam generators utilities adopt various life management strategies. To compare the merit of such life management strategies the net present value approach as discussed in the preceding section is applied. The current life management strategy in industry is to implement preventive maintenance action like water lancing for every 4 years and chemical cleaning for every 8 years to mitigate pitting corrosion degradation of steam generators.

The SG tube leakage due to tube pitting results in an unexpected plant outage and various consequential costs due to tube leak. Corrective maintenance cost due to tube leak is associated with the number of tube leaks (forced outages) in a given period. The expected NPV of corrective maintenance cost in the time period [0 t] (Hong, et al., 2006) for a cleaning cycle is given as

$$C_{CM}(t) = c_f \int_0^t \lambda_Z(u) \exp(-d \times u) du \tag{6.4}$$

where $\lambda_Z()$ is the intensity function of number of tube leaks assuming leak criterion $z = 95\%\text{TWD}$ and c_f is the cost of failure per outage due to tube leak. The failure costs include loss of revenue due to outage, tube plugging costs, additional inspection cost of SG tubes etc.

Preventive maintenance costs are fixed costs associated with the number of inspections and chemical cleaning campaigns on SGs. The periodic inspection on SG tubes doesn't affect the corrosion pitting process whereas the chemical cleaning actions mitigates corrosion pitting and the pitting process starts fresh (i.e the intensity function $\lambda_Z()$ starts from zero). The net present value of total cost of SG maintenance $C(t)$ in time period [0 t] is given as

$$C(t) = C_{PM}(t) + C_{CM}(t) \tag{6.5}$$

where $C_{PM}(t)$ & $C_{CM}(t)$ are the preventive maintenance and corrective maintenance costs in time period [0 t]. The NPV as calculated from Eq. (6.5) can be used in evaluating various preventive maintenance actions to be conducted on the steam generator life management program.

6.5.2.1 Illustrative Example

In this section the pitting corrosion problem as discussed in Section 6.2 is considered. The probabilistic pitting corrosion model developed in Section 6.2.1 is used in the cost model. The input data for the cost model is summarised in the Table 6.6.

Table 6.6: Input data for cost model per SG

Input Data	**Value**
Discount Rate (d)	5%
Inflation Rate (k)	0%
Inspection Cost	\$20K every 2 years
Chemical Cleaning (PM) Cost	\$100K every 8 years
Corrective Maintenance Cost (c_f)	\$1000K/outage
Forecast Period	24 Years

The maintenance costs considered as in Table 6.6 are assumed as fixed costs and are not time dependent. In this section implementing chemical cleaning action every 8 years for SG based on the Net Present Value approach is discussed. It is assumed that with each chemical cleaning action the pitting corrosion degradation is mitigated and the pitting process starts fresh again with SG usage.

The total expected maintenance cost in NPV as calculated from Eq. (6.3) is shown in Figure 6.11 & Figure 6.12 with and without chemical cleaning over a forecast period of 24 years. The plot shows a histogram of total costs showing both corrective and preventive maintenance costs. With chemical cleaning as shown in Figure 6.11, there is an abrupt increase in cost due to chemical cleaning

at 8th year and 16th year of operation. The chemical cleaning actions although resulting in high maintenance costs in that particular year of action reduces significantly the expected corrective maintenance costs in subsequent years. For the case without chemical cleaning as shown in Figure 6.12 the expected corrective maintenance costs increases greatly over the forecast period.

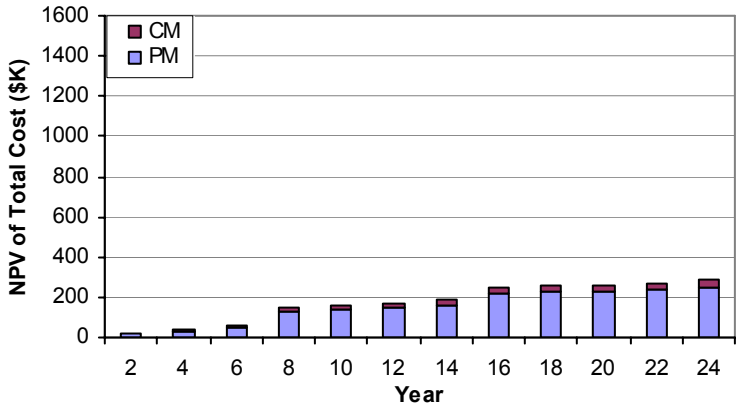

Figure 6.11: Expected total costs in NPV with Chemical Cleaning

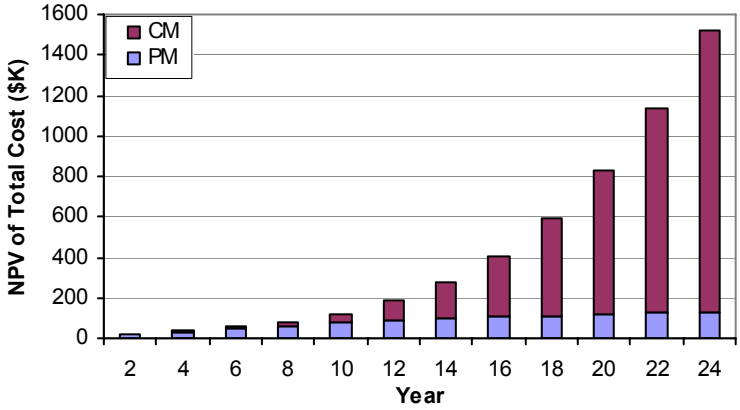

Figure 6.12: Expected total costs in NPV without Chemical Cleaning

The cumulative cost of maintenance at the end of forecast period of 24 years in NPV is summarised in the Table 6.7.

Table 6.7: Expected total Maintenance Cost in NPV over a forecast period of 24 years

Decision	NPV
Chemical Cleaning every 8 years	$283 K
Without Chemical Cleaning	$1521 K

The results in Table 6.7, show that the SG maintenance with chemical cleaning actions conducted every 8 years results in much lower total expected costs based on NPV over a forecast period of 24 years.

6.5.3 Maintenance Optimization

The NPV approach as discussed in preceding section is used to optimize the frequency of chemical cleaning. Frequent chemical cleaning actions may reduce the risk of tube leakage greatly due to pitting corrosion but the maintenance costs will be much higher. On the other hand deferring the chemical cleaning actions may reduce the high maintenance costs but results in high risk of tube leakage which could result in high corrective maintenance costs. Considering the effect of chemical cleaning on reducing the tube leak probabilities, it is shown that chemical cleaning actions every 8 years lead to less maintenance cost in NPV over a forecast period of 24 years. Similar calculations as done in Section 6.5.2.1 are conducted by changing the frequency of chemical cleaning actions. The effect of chemical cleaning cycle on the overall NPV of maintenance over a forecast period of 24 years is shown in Figure 6.13.

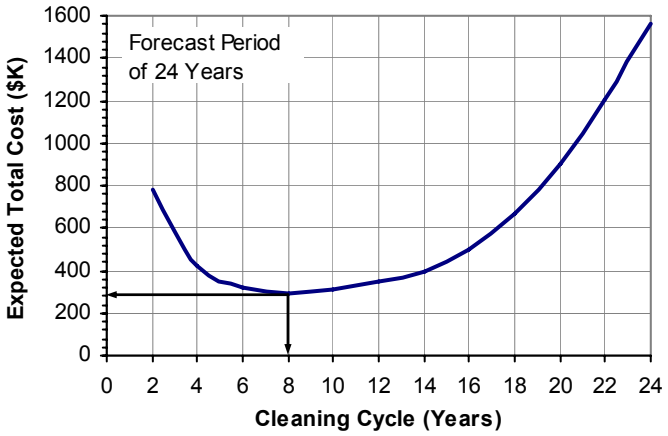

Figure 6.13: NPV of Maintenance cost Vs Chemical Cleaning Cycles

Interestingly, the optimal cleaning cycle shown in Figure 6.13 is 8 years which results in least expected total cost. The optimum chemical cleaning cycle of 8 years is sensitive to the input cost data considered which could vary on the choice of maintenance actions and cost estimates. The discount rate has no effect on optimum cleaning cycle of 8 years.

6.6 Conclusions

The application of the pitting corrosion model to actual field inspection data obtained from industry is presented. The data from industry is associated with uncertainties in the inspection process and in measuring and detecting pit depths. This fact makes it difficult to develop realistic probability models. Pit depths exceeding 50% TWD is considered for the analysis so that the uncertainties with detection and measurement are minimized. Pitting corrosion process within the maintenance interval of 8 years between cleaning campaigns is considered for the analysis. The data from all units of the nuclear generating station are pooled as one sample to model the stochastic pit generation of a SG.

The application of the proposed probabilistic model for pitting corrosion degradation in SG LCM is presented. The model can be used to predict the probability of tube leak and expected number of tubes plugged during the next operating period. The model can also be applied to predict the probability

distribution of time to first leak. The expected time to the n^{th} leak or n^{th} plugging can also be estimated from the model.

The measurement error of eddy current probes from field inspection is presented. The traditional approach in industry is to use RMSD to quantify measurement error, which assigns measurement error to the bad probe. Actually, the RMSD embodies uncertainties in both probes as well as bias in measuring the actual pit depths. The Grubbs method and CEL methods are used to quantify the measurement error in each probe. Measurement error analysis is conducted on the repeat inspection data from a nuclear generating station of pit depth measurements from C2 and X probe. The CEL method is used to quantify the measurement error in each probe. The measurement error is calculated as 8.5% TWD on C2 probe and 1.7% TWD on X probe respectively.

The steam generator LCM model for pitting corrosion degradation is presented. The effect of chemical cleaning interval on expected total costs over a forecast period is illustrated using the NPV approach. Maintenance optimization on a chemical cleaning cycle for SG pitting corrosion degradation is demonstrated. The pitting corrosion model for a SG estimated from actual plant data is considered for maintenance optimization. The optimum cleaning cycle is calculated to be 8 years for the cost data considered. The discount rate has no effect on an optimum cleaning cycle of 8 years.

The main contribution of the thesis is the application of stochastic pitting corrosion model for steam generator LCM.

CHAPTER 7
CONCLUSIONS AND RECOMMENDATIONS

7.1 Conclusions

The thesis presents application of probabilistic models to support risk-based life cycle management of energy infrastructure systems. Statistical techniques to analyze incomplete, censored and truncated data collected from inspection of components in the energy industry are addressed. The thesis presents detailed practical applications of LCM models to energy systems and discusses the practical difficulties associated with remaining lifetime prediction.

Probabilistic models for asset management of infrastructure components in estimating the life cycle costs associated with component replacement are investigated. Age-based replacement policy is simple and effective to implement in a system with a large population of relatively inexpensive components. A sequential inspection-based replacement model is proposed to manage components from a large distribution network. The proposed model has a significant potential in minimizing the maintenance cost, risk, and improving the asset management of distribution network components.

A probabilistic lifetime model is proposed to consider the effect of imperfect preventive maintenance on systems and components. The model has the flexibility to incorporate the imperfections of maintenance actions using the concept of virtual age. The results show that imperfect preventive maintenance increases optimal total costs and the frequency of optimal maintenance intervals.

The limitation of the work presented in the thesis is that the optimal maintenance actions are based on life cycle cost estimates only. Although the parameters of the model can be updated with availability of more data, Bayesian updating is not considered in the thesis.

A stochastic model for the pitting corrosion process in a SG is proposed. The occurrence of large pits is modeled as a non-homogeneous Poisson process. The pit depth distribution exceeding a threshold pit depth is modeled as the generalized Pareto distribution (GPD), which falls into the class of extreme value distribution. The model can be applied in estimating the expected number of extreme pits and the annual leak probability during future operation crucial for steam generator life management decision modelling.

The effect of measurement error and detection uncertainty in eddy current inspections on measured defect depths is investigated from simulation results. The results indicate that the measurement error and detection uncertainties overestimate the exceedence probabilities compared with the estimate from true pit depth distribution. The probability models developed provide a framework in quantifying the uncertainties in estimating the true defect distribution models.

The effect of uncertainties in the eddy current inspection process in predicting tube leak probability and number of tubes plugged in next outage is investigated through a simulation study under different inspection plans. The prediction of the probability of tube leaks in next outage is greatly biased by uncertainties in pit depths.

The uncertainties in pit depth measurements overestimate the probability of tube leak prediction in next outage during initial period of operation, and underestimate the leak probability prediction for the later years when compared to the leak probability estimate from true depth distribution. The uncertainties in pit depths also overestimate the prediction on number of tubes plugged in next outage at later years of inspection. The sampling uncertainty under different inspection plans is significant for tube leak predictions but is not that significant in prediction of number of tubes plugged.

The thesis presents the practical application of stochastic model for pitting corrosion degradation in steam generator tubing. The application and benefits of the model are illustrated in the context of a steam generator life cycle

management. The model presents a significant potential in optimizing the chemical cleaning cycle for a steam generator life cycle management.

Although the methodology presented in the thesis is based on illustrative case studies, they are generic, and therefore applicable to other component LCM in energy infrastructure. The probabilistic models developed in this thesis help engineers in the energy industry to quantify uncertainties in inspection data and provide a framework for practical application of probabilistic models towards life cycle management decisions.

7.2 Recommendations for Future Research

The thesis work is a part of broad research that focuses on developing a risk based approach to life cycle management of energy infrastructure systems. Various research issues related to development of probabilistic models in the context of inspection of equipment, data acquisition, degradation modelling, maintenance alternatives, and cost models are relevant.

Although the thesis addresses issues in estimating the lifetime distribution models from incomplete observations it does not deal with covariate data. The variables affecting the equipment lifetimes (covariates) are important and there is a need for advanced statistical techniques to account for covariates in estimating equipment lifetime.

Maintenance models discussed in this thesis is based on a single component in a distribution network. Maintenance model for systems with different component lifetimes is another research area which has a great potential in energy infrastructure systems. The cost data for maintenance models in the thesis are considered as constants. It is difficult to get actual costs from industry, therefore there is a need for better cost models which takes into account the uncertainties in cost estimates.

The Gamma frailty Poisson model (Negative Binomial Process) as discussed in chapter 5 takes into account large variability in pitting process among SGs which is not investigated in this thesis. Further research work is needed to

investigate if it is a better model for pitting corrosion degradation and its practical implementation in SG LCM.

The practical application of the proposed stochastic modelling for pitting corrosion to other degradation mechanisms in other nuclear components could be future scope of this thesis.

References

Akaike, H. (1985). Prediction and Entropy. Pages 1-24 in A. C. Atkinson, and S. E. Fienberg, (eds.) A Celebration of Statistics. Springer-Verlag, New York Inc.

Anders, G. J. and Leite da Silva, A. M. (2000). "Cost related reliability measures for power system equipment." *IEEE Trans. Power Systems*, Vol. 15, No. 2, pp. 654-660.

Anders, G.J., Endrenyi, J. and Yung, C. (2001). "Risk-based planner for asset management." *Computer Applications in Power*, IEEE, Vol. 14, Issue 4, Oct. 2001 pp.20-26.

Angell, P. (2002). "Development of pitting models to aid steam generator life management." *4th CNS international steam generator conference*, Toronto, Ontario, Canada. May 2002.

Awad, A.M. (1996). "Properties of the Akaike information criterion." *Microelectronics Reliability*, 36(4), pp.457-464.

Baker, R. (1990). "Probability estimation and information principles." *Structural Safety*, No. 9, pp.97-116.

Barata, J., Soares, C. G., Marseguerra, M. and Zio, E. (2002). "Simulation modeling of repairable multi-component deteriorating systems for 'on condition' maintenance optimization." *Reliability Engineering and System Safety*, Vol. 76, pp.255-264.

Barlow, R. E. and Proschan, F. (1965). "Mathematical Theory of Reliability." *SIAM Publication*, Philadelphia, PA.

Barlow, R. E. and Proschan, F. (1975). "Statistical theory of reliability and life testing." *Rinehart and Winston, Inc. Holt*, New York.

Bertling, L., Allan, R. N. and Eriksson, R., (2005). "A reliability centered asset maintenance method for assessing the impact of maintenance in power distribution systems." *IEEE Trans. Power Systems*, Vol. 20, No. 1, pp. 75-82.

Bhuyan, G. S. (1998). "Condition based serviceability and reliability assessment of wood pole structures." *Proceedings of IEEE 8th International Conference Transmission and Distribution Construction, Operation of Live-Line Maintenance*, ESMO-98, 26-30 April 1998, pp. 333-339.

Brown, R.E. and Spare, J.H. (2004). "Asset management, risk, and distribution system planning." *Power Systems Conference and Exposition*, IEEE PES, 10-13 October 2004, pp.130 – 135.

Burstein, G. T., Shrier, L. L. and Jarman, R. A. (1994). "Corrosion Volume 1-Metal/Environmental Reactions." *Butterworth-Heinemann*, Oxford.

Butera, R. (2000). "Asset management for the distribution pole plant-closing the performance gap between traditional maintenance and asset management." *Power Engineering Society Summer Meeting*, IEEE, Volume 1, July 2000. pp.561-565.

Camacho, F. and Pagan, S. (2006). "Statistical methods for darlington steam generator tube fitness-for-service assessments." *5th CNS International Steam Generator Conference*, November 2006, Toronto, Ontario, Canada.

Cavanaugh, J.E. (1997). "Unifying the derivations for the Akaike and corrected Akaike information criterion." *Statistics and Probability Letters*, No.33, pp.201-208.

Chan, M.L, (2004), "Transmission and distribution system asset management." *Power Systems Conference and Exposition*, IEEE PES, October 2004, pp.983-984.

Cox, D. R. and Oakes, D. (1984). "Analysis of Survival Data." *Chapman and Hall*.

Cox, D. R. and Isham, V. (1980). "Point Processes." *Chapman and Hall*, New York.

Datla, S. V. and Pandey, M. D. (2006). "Estimation of life expectancy of wood poles in electrical distribution networks." *Structural Safety*, Vol.28, pp.304-319, 2006.

Dekker, R. (1996). "Applications of maintenance optimization models: a review and analysis." *Reliability engineering and system safety*, Vol.51, pp.229-240.

Elandt-Johnson, R.C. and Johnson, N.L. (1999). "Survival Models and Data Analysis." *John Wiley & Sons*, New York, NY.

Electric Power Research Institute. (1998). "Nuclear plant life cycle management implementation guide." *EPRI Report TR-106109*. EPRI, Palo Alto, CA.

Electric Power Research Institute. (2001). "Demonstration of life cycle management planning for systems, structures, and components." *EPRI Report 1000806*, EPRI, Palo Alto, CA.

Endrenyi, J. et.al (2001). “The present status of maintenance strategies and the impact of maintenance on reliability.” *IEEE Transactions on Power systems*, Vol.16, No.4, pp.638-646.

Endrenyi, J., Anders, G. J. and Leite da Silva, A. M. (1998). “Probabilistic evaluation of the effect of maintenance on reliability-An application.” *IEEE Trans. Power Systems*, Vol. 13, No. 2, pp. 576-583.

Endrenyi, J., Anders, G. J., Bertling, L. and Kalinowski, B. (2004). “Comparision of two methods for evaluating the effects of maintenance on component and system reliability.”
International Conference on Probabilistic Methods Applied to Power Systems, September 2004, pp.307-312.

Evans, S., Watson, S., Remark, J. and Hengge, C. (2002). “Review of steam generator chemical cleaning experiences from 1998 – 2002.” *4th CNS international steam generator conference* , Toronto, Ontario, Canada. May 2002.

Frangopol, D. M., Kallen, M.-J., and van Noortwijk, J. M. (2004). “Probabilistic models for life-cycle performance of deteriorating structures: review and future directions." *Progress in Structural Engineering and Materials*, 6, 197-212.

Gertsbakh, I. (2000). “Reliability Theory: with applications to preventive maintenance.” *Springer*, New York.

Goodman, J. R. and Stewart, A. H. (1990). “Life cycle economics of Wood pole utility structures.” *IEEE Transactions on Power Delivery*, Vol. 5, No. 2, pp.1040-1046.

Grubbs, F.E. (1948). “On estimating precision of measuring instruments and product variability.” *Journal of the American Statistical Association*, 43, pp. 243-264.

Gustavsen, B. and Rolfseng, L. (2004). “Asset management of wood pole utility structures.” *International Conference on Probabilistic Methods Applied to Power Systems*, September 2004, pp.975-979.

Harris, J. E., Gorman, J. A. and Turner, A. P. L., CANTIA – “A probabilistic method for assessing steam generator tube inspections.” *AECB Research Project No. 2.353.2*, March 1997.

Hong, H. P. (1999). “Application of stochastic process to pitting corrosion.” *Corrosion*, Vol. 55, No. 1, pp 10-16.

Hong, H. P., Allouche, E. N. and Trivedi, M. (2006). "Optimal scheduling of replacement and rehabilitation of water distribution systems." *Journal of Infrastructure Systems*, Vol. 12, No 3, pp 184-191.

Hosking, J.R.M. and Wallis, H.R., (1987). "Parameter and quantile estimation for the generalized Pareto distribution." *Technometrics* 29: 339-349.

Hoyland, A. and Rausand, M. (1994). "System Reliability Theory: Models and statistical methods." *John Wiley & sons, Inc*. Toronto.

Hougaard, P. (2000). *Analysis of Multivariate Survival Data*. Springer.

IEEE Task Force (J. Endrenyi, Chair). (2001). "The present status of maintenance strategies and the impact of maintenance on reliability." *IEEE Trans. Power Systems*, Vol. 16, No 4, pp. 638-646.

International Atomic Energy Agency (IAEA). (1997). "Assessment and management of ageing of major nuclear power plant components important to safety: Steam generators." *IAEC-TECDOC-981. IAEA*, Vienna, Austria.

Jaech, J.L. (1985). "Statistical analysis of measurement errors." *John Wiley & Sons*, New York.

Jardine, A. K. S. (1973). "Maintenance, replacement and reliability." *London; Pitman Publishing.*

Jardine, A. K. S., Joseph, T. and Banjevic, D. (1999). "Optimizing condition-based maintenance decisions for equipment subject to vibration monitoring." *Journal of Quality in Maintenance*, Vol. 5, No. 3, pp.192-202.

Kalbfleisch, J. D and Prentice, R.L. (2002). "The Statistical Analysis of Failure Time Data." *Wiley*, New Jersey.

Kaplan, E. L. and Meier, P. (1958). "Nonparametric estimation from Incomplete Observations." *Journal of the American Statistical Association*, Vol. 53, No. 282, pp.457-481.

Keyfitz, N. (1985). "Applied Mathematical Demography." *Springer-Verlag*, New York, NY.

Kong, J. S. & Frangopol, D. M. (2003). "Evaluation of expected Life-Cycle maintenance cost of deteriorating structures", *Journal of Structural Engineering*, Vol. 129, No. 5, pp.682-691.

Lawless, J. F. (1987). "Regression Methods for Poisson Process Data." *Journal of the American Statistical Association*, Vol. 82, No. 399., pp. 808-815.

Lawless, J.F. (2003). "Statistical models and methods for lifetime data." *John Wiley & Sons*, New York, NY.

Li, H., Bhuyan, G. S. and Tarampi, D. (2004). "Life prediction of aging wood poles and subsequent inspection practice-a case study." *International Journal for Computation and Mathematics in Electrical and Electronic Engineering*, Vol. 23, No. 1, pp. 15-20.

Lindquist, T., Bertling, L. and Eriksson, R., (2004), "A feasibility study for probabilistic modeling of aging circuit breakers for maintenance optimization", *Probabilistic Methods Applied to Power Systems*, 2004 International Conference on, 12-16 Sept. 2004 Page(s):1020 – 1025.

Makis, V., Jiang, X., Jardine, A. K. S. (1998). "A condition based maintenance model." *IMA Journal of Mathematics Applied in Biostatistics &* Industry, Vol.9, pp.201-210.

Maruska, C. C. (2002). "Steam generator life cycle management – Ontario power generation (OPG) experience." *4th CNS international steam generator conference* , Toronto, Ontario, Canada. May 5-8, 2002.

Meeker, W. Q and Escobar, L. A. (1998). "Statistical methods for reliability data." *John Wiley & Sons,* New York, NY.

Mettas, A. and Zhao, W. (2005). "Modelling and anlaysis of repairable systems with general repair", Annual Reliability and Maintainability Symposium, Proceedings, 2005, pp 176-182.

Mobley, R. K. (2002). "An Introduction to Predictive Maintenance." *Elsevier Science,* USA.

Mola, E. E., Mellein, B., Rodriguez de schiapparelli, M., Vicente, J. L., Salvarezza, R. C., and Arvia, A. J., (1990), "Stochastic approach for pitting corrosion modeling 1. The case of quasi-hemispherical pits", *J. Electrochem. Soc*., Vol. 137, No. 5, May 1990, pp. 1384-1390.

Morrell, J.J. (1996). "Wood Pole Maintenance Manual." *Forest Research Laboratory*, Oregon State University, Corvallis, Oregon.

Morrision, T., Mangat, N. S., Carroll, L.B. and Riznic, J. (2002). "Statistical estimation of flaw size measurement errors for steam generator inspection tools." *Proceedings of the 4th CNS International Steam Generator Conference*, Toronto, Canada. May 2002.

Morton, K., (1999). "Asset management in the electric supply industry." *Power Engineering Journal*, Vol. 13, No. 5, pp.233-240.

Moubray, J. (1997). "Reliability Centered Maintenance." *Industrial Press Inc*, New York.

Nakagawa, T. and Osaki, S. (1975). "The Discrete Weibull Distribution." *IEEE Transactions on Reliability*, Vol. R-24, No. 5, pp.300-301.

Natti, S., Jirutitijaroen, P. and Singh, C., (2004), "Circuit breaker and transformer inspection and maintenance: probabilistic models", *Probabilistic Methods Applied to Power Systems*, 2004 International Conference on, 12-16 Sept. 2004 Page(s):1003-1008.

Nelson, W. (1982). "Applied Life Data Analysis." *Wiley*, New York.

Newbill, M. (1993). "Bonneville Power Administrations wood pole management program." *Proceedings of IEEE 6th International Conference on Transmission and Distribution Construction and Live-Line Maintenance*, ESMO-93, 12-17 September 1993, pp. 185-198.

Obrutsky, L., Watson, N., Fogal, C., Cantin, M., Cecco, V., Lakhan, R. and Sullivan, S. (2002). "Fast single pass eddy current array probe for steam generator inspection." *Proceedings of the 4th CNS International Steam Generator Conference*, Toronto, Canada. May 2002.

Olin, B. D. and Meeker, W. Q. (1996). "Application of statistical methods to nondestructive evaluation." *Technometrics*, Vol.38, No.2, pp. 95-112, May 1996.

Padma, S., Veena S. N., Rufus A. L., Sathyaseelan V. S., Velmurugan S. and Narasimhan S. V. (2001). "Corrosion of carbon steel and monel-400 in EDTA based steam generator cleaning formulations." *Materials and Corrosion*, Vol.52, pp. 771-780.

Pham, H. and Wang, H. (1996). Invited Review – "Imperfect Maintenance", *European Journal of Operational Research*, Vol. 94, pp. 425-438.

Provan, J. W. and Rodriguez, E. S. (1989). "Part 1: Development of a markov description of pitting corrosion." *Corrosion*, Vol. 45, No. 3, pp. 178-192.

Ross, S. M. (2000). "Introduction to Probability Models." *Academic Press,* 7th edition.

Salem, O., AbouRizk, S. and Ariaratnam, S. (2003). "Risk-based Life-cycle costing of Infrastructure Rehabilitation and construction alternatives." *Journal of Infrastructure Systems*, Vol. 9, No 1, pp. 6-15.

Semmler, J., Guzonas, D. A., Rousseau, S. C., Snaglewsk, A. P. and Chenier, M. P. (1998). "Development of an on-line process for steam generator chemical cleaning." *3rd CNS international steam generator conference* , Toronto, Ontario, Canada. June, 1998.

Shibata, T. (1996). "Statistical and stochastic approaches to localized corrosion", *Corrosion*, Vol. 52, No. 11, pp. 813-830.

Smilowitz, K. and Madanat, S. (2000). "Optimal Inspection and Maintenance Policies for Infrastructure Networks." *Computer-aided civil and infrastructure engineering*, Vol.15, pp.5-13.

Smith, R. L. (2004). "Statistics of extremes, with applications in environment, insurance, and finance." *Extreme Values in Finance, Telecommunications, and the Environment- Eds Finkenstadt, B. and Rootzen, H.,* Chapman & Hall/CRC, Florida.

Stein, W. E. and Dattero, R. (1984). "A New Discrete Weibull Distribution." *IEEE Transactions on Reliability*, Vol. R-33, No. 2, pp.196-197.

Sweeting, T. (1995). "Statistical models for nondestructive evaluation." *International Statisitcal Review*, Vol.63, No.2, pp 199-214, Aug 1995.

Tapping, R. L. (2006). "Steam Generator Aging in CANDUs: 30 years of operation and R&D, *5th CNS International Steam Generator Conference*, Toronto, November 2006.

Tapping, R.L., Nickerson, J., Spekkens, P. and Maruska, C. (2000). Technical Note – "CANDU steam generator life management." *Nuclear Engineering and Design*, Vol. 197, pp. 213-223.

Tekin, O. (2005). "Comparison of parameter estimation methods for the three parameter generalized pareto distribution." *Turkish journal of agriculture and forestry*, Vol. 29, No. 6, pp 419-428.

Turnbull, B. W. (1976). "The empirical distribution function with arbitrary grouped, censored, and truncated data." *Journal of the Royal Statistical Society*, Vol. 38, pp.290-295.

U.S.-Canada Power System Outage Task Force. (2004). "August 14th Blackout: Causes and Recommendations." April 2004.

Van Noortwijk, J. M. (2003). "Explicit formulas for the variance of discounted life cycle cost", *Reliability Engineering and System Safety*, 80(2), 185-195, 2003.

Van Noortwijk, J. M. and Klatter, H. E. (2004). "The use of lifetime distributions in bridge maintenance and replacement modelling." *Computers and Structures*, Vol. 82, pp. 1091-1099.

Vatn, J., Hokstad, P., Bodsberg, L. (1996). "An overall model for maintenance optimization", Reliability Engineering and system safety, Vol.51, pp.241-257.

Vaupel, J. W. (1986). "How change in age specific mortality affects life expectancy." Population Studies, Vol. 40, No. 1, pp. 147-157.

Wernsing, R. and Dickens, R. (2004). "Asset management-computerized maintenance management system." *Power Systems Conference and Exposition*, IEEE PES, 10-13 Oct. 2004, pp.1444 – 1445.

Wu, B., Scully, J. R., Hudson, J. L. and Mikhailov, A. S. (1997). "Cooperative stochastic behavior in localized corrosion 1. Model." *J. Electrochem. Soc*., Vol. 144, No. 5, May 1997, pp. 1614-1620.

Yang, S-I., Frangopol, D. M., Kawakami, Y. and Neves, L. C. (2006). "The use of lifetime functions in the optimization of interventions on existing bridges considering maintenance and failure costs." *Reliability Engineering and System Safety*, Vol. 91, pp. 698-705.

Yuan, X.-X, Pandey, M. D. and Bickel, G. A. (2006). "A probabilistic degradation model for the estimation of the remaining life distribution of feeders." *27th Annual Conference of the Canadian Nuclear Society and 30th Canadian Nuclear Society - Nuclear Energy A World of Service to Humanity*, 2006, 10p.

Zhang, Y. and Jamshidian, M. (2003). "The gamma frailty poisson model for the nonparametric estimation of panel count data", *Biometrics*, Vol.59, pp. 1099-1106.